Molecular pharmacology of a Novel NR2B-selective NMDA Receptor Antagonist

Bradford, Andrea Marie

Molecular Pharmacology of a Novel NR2B-selective NMDA Receptor Antagonist

PhD Thesis

Andrea Marie Bradford

School of Biological & Biomedical Sciences

University of Durham

Supervisor: Dr Paul Chazot

October 2006

Abstract

The NMDA receptor is a heteromeric ligand-gated ion channel in the central nervous system (CNS). There are three families of NMDA receptor subunits with various combinations of NR1, NR2A-D and NR3A-B subunits producing unique receptors with distinctive pharmacological and biochemical properties. Pharmacological and functional properties of the NMDA receptor are highly dependent on the composition of the receptor complex. The NMDA receptor is the focus of drug development for therapy and prevention of numerous neurological and psychiatric disorders.

The focus of this thesis was to investigate NMDA receptor subtype selectivity of NMDA antagonists, in particular, RGH-896, a novel NR2B-selective antagonist. The study has utilised radioligand binding competition binding assays with RGH-896 in native, recombinant and immunopurified NMDA receptor preparations. In addition, ligand autoradiography has been employed to quantify and delineate the regional distribution of [^{3}H] RGH-896 binding sites in rodent and human brain tissue.

This study provides the first evidence that [^{3}H] RGH-896 binds to a distinct binding site which displays a significantly lower affinity for spermidine compared to the [^{3}H] Ro 25,6981 binding site. In addition, the low sensitivity of [^{3}H] MK-801 for unlabelled RGH-896 compared to prototypical NR2B ligand ifenprodil is further evidence for the difference in binding sites. Novel immunopurification studies using [^{3}H] RGH-896, in contrast to [^{3}H] CP 101,606, binds to NR2B-containing receptors irrespective of NMDA receptor subunit combinations. Ligand autoradiography in human brain has shown a surprising overall preservation of NR2B receptors in dementia with Lewy bodies (DLB) patients compared to age matched controls in the anterior cingulate cortex (ACC). However, this study has revealed the first evidence of an upregulation of NR2B receptors in ACC of DLB cases related to severity of auditory, but not visual hallucinations.

Candidates Declaration

Acknowledgements

I would like to thank several people that have helped me complete this project at Durham University, including technical staff and members of other labs.

I am grateful to all the members of our lab including Fiona Shenton, Sawsan Abuhamdah, Rebecca Sheahan and Heather Chaffey, who have helped and supported me throughout this PhD.

I would like to thank Dr Margaret Piggott (MRC Neurochemical Pathology, Newcastle General Hospital, Newcastle-upon-Tyne) for her assistance, technical expertise and experience, to accomplish the human autoradiography.

Lastly, I have the greatest appreciation for my supervisor, Dr Paul Chazot, for his continuous assistance in the lab and his knowledge in the field of NMDA receptors and their functional implications in the brain.

Table of Contents

Chapter 1

1. Introduction

Chapter 2

2. Pharmacological Characterisation of NMDA NR2B-Selective Antagonists

Chapter 3

3. The Production of anti- NR2A Antibody for Subsequent Immuno-purification and Pharmacological Characterisation of Recombinant NR1/NR2A & NR1/NR2A/NR2B Subtypes Expressed in HEK 293 Cells

Chapter 4

4. Ligand Autoradiographical Analysis of Rodent and Human Brain Tissue using a Novel NR2B-selective Antagonist RGH-896, Focusing on the Anterior Cingulate Cortex

List of Figures

List of Tables

Abbreviations

ACC	Anterior cingulate cortex
AD	Alzheimer's disease
AMPA	α-amino-3-hydroxy-5-methyl-4-isoxazole propionic acid
ANOVA	Analysis of Variance
APS	Ammonium Persulfate
B_{max}	Maximum number of receptors occupied per milligram of protein
BA	Brodmann's Area
BSA	Bovine Serum Albumin
cDNA	Complementary DNA
CNS	Central Nervous System
CP101,606	[(*R**,*R**)-4-hydroxy-(4-hydroxyphenyl)-β-methyl-4-phenyl-1-piperidine-ethanol]
CSF	Cerebrospinal Fluid
CNQX	6-cyano-7-nitroquinoxaline-2,3-dione
CUSPAD	Columbia University Scale for Psychopathology in Alzheimer's disease
DLB	Dementia Lewy Bodies
DMEM/F12	Dulbecco's Modified Eagle Medium/Nutrient Mixture F12-Ham
DMSO	Dimethyl Sulphoxide
DNA	Deoxyribonucleic Acid
DNQX	6,7-dinitro-quinoxaline-2,3-dione

DTT	Dithiolthreitol
E-Coli	*Escherichia Coli*
pEC_{50}	Log concentration producing 50% of maximal response
EDTA	Ethylenediaminetetraacetic Acid
EGTA	Ethylene glycol-bis(2-amino-ethylether)-N,N,N',N'-tetra-acetic acid
FCS	Fetal Calf Serum
GABA	γ-aminobutyric Acid
HD	Huntington's disease
HEK293	Human Embryonic Kidney 293 Cells
HEPES	N-[2-Hydroxyethyl]piperazine-N'-[2-ethane-sulfonic acid]
HRP	Horseradish Peroxidase
htt	Huntingtin
pIC_{50}	Log concentration of unlabelled drug at which 50% of the radioligand is displaced
IgG	Immunoglobulin G
IP_3	Inositol (1,4,5) tris-phosphate
K_D	Dissociation Constant
kDa	Kilodalton
K_I	Inhibition Constant
LB	Lewy bodies
L-DOPA	1-3,4-dihydroxyphenylalanine
LTD	Long Term Depression
LTP	Long Term Potentiation
MBS	3-Maleimidobenzoic Acid N-hydroxysuccinimide Ester
MCAO	Medial cerebral artery occlusion

MK-801	(+)-5-methyl-10,11-dihydro-*5H*-dibenzo[*a,d*]cyclohepten-5,10-imine
MMSE	Mini-Mental State Examination
MPTP	1-methyl-4-phenyl-1,2,3,6-tetrahydropyridine
mRNA	messenger ribonucleic acid
NBQX	2,3-dihydroxy-6-nitro-7-sulfamoyl-benzo(*F*)quinoxaline
NMDA	N-methyl-D-aspartate
PBS	Phosphate Buffered Saline
PD	Parkinson's disease
PCP	Phencyclidine
PNQX	1,4,7,8,9,10-hexahydro-9-methyl-6-nitropyrido[3,4-*f*]-quinoxaline-2,3-dione
Ro 25,6981	[(*R:(*),S(*)*)-α-(4-hydroxyphenyl)-β-methyl-4-(phenylmethyl)-1-piperidinepropanol [(+/-)-Ro 25,6981]
SD	Standard Deviation
SEM	Standard Error of the Mean
SDS	Sodium Dodecyl Sulphate
TBS	Tris Buffered Saline
Tris	Tris(hydroxmethyl)methylamine

Chapter 1

1. Introduction

1.1 Neurological Disorders and Implications on Society

Over the past decade, many research groups (industrial and academic), have provided major advances in understanding the role of neurological disorders that pose a threat to today's society. As each laboratory has a particular focus, information can be gathered to provide society with a vital indication of neurological disorders that are present in society and how to cope with them. There are neurological disorders which are common in the general public, where some symptoms are more distinguishable than others. Neurological disorders can be difficult to diagnose as many symptoms can overlap. For example, a patient with Parkinsons Disease will show tremor at rest, muscle rigidity hypokinesia and often dementia. First-line treatment with L-DOPA would control the symptoms in the short term, but would cause drug-induced dyskinesias, in longer term treatment. It is therefore critical that more research is conducted to try and pinpoint a particular defect for each disorder in order to treat each individual with appropriate medication. Here is an overview of how the central nervous system works and the implications when certain aspects of the system fail, showing the problematic effects it can have on society. This research reported here focuses on the glutamatergic system, in particular the NMDA receptor and its involvement in psychosis.

1.2 Central Nervous System

The central nervous system (CNS) can be thought of as an information input, processing, storage, retrieval, and output system. Internal stimuli from the body and external stimuli from the environment provide information sent via sensory nerves to the CNS, where it is routed to appropriate brain centres for processing into awareness of sensations and perceptions, for storage in memory, and for the elicitation of relevant motor responses.

The brain is made up of billions of neurons which are functional cells receiving information from other neuronal cells via dendrites and cell bodies which conduct nerve impulses, or action potentials, normally in a direction away from the cell body, where the nucleus of the cell is contained, to other neurons along the axon (Figure 1.1). The point where the axon terminal (presynaptic) comes into contact with other neurons or cells (postsynaptic) is called the synapse with the space in between known as the synaptic cleft. At this point synaptic transmission can occur, by the release of neurotransmitter from the presynaptic terminal to initiate a response on the postsynaptic membrane. As well as neurons, there are glial cells present in the brain which contribute to brain function by supporting neuronal functions. The most numerous glia in the brain are astrocytes which support neurons and regulate the extracellular ionic and chemical environment of the brain.

The CNS comprises a long cylindrical structure, the spinal cord and its anterior expansion, the brain. The brain is suspended in cerebrospinal fluid (CSF) which also fills spaces called ventricles inside the brain. This dense fluid protects the brain and spinal cord from shock and supplies neurons within the brain with respiratory gases and nutrients and removes waste matter. The human brain is the source of the

conscious and cognitive mind. The mind comprises a set of cognitive processes related to perception, interpretation, imagination and memories, of which a person may or may not be aware. Beyond cognitive functions, the brain regulates autonomic processes related to essential body functions such as respiration and heartbeat.

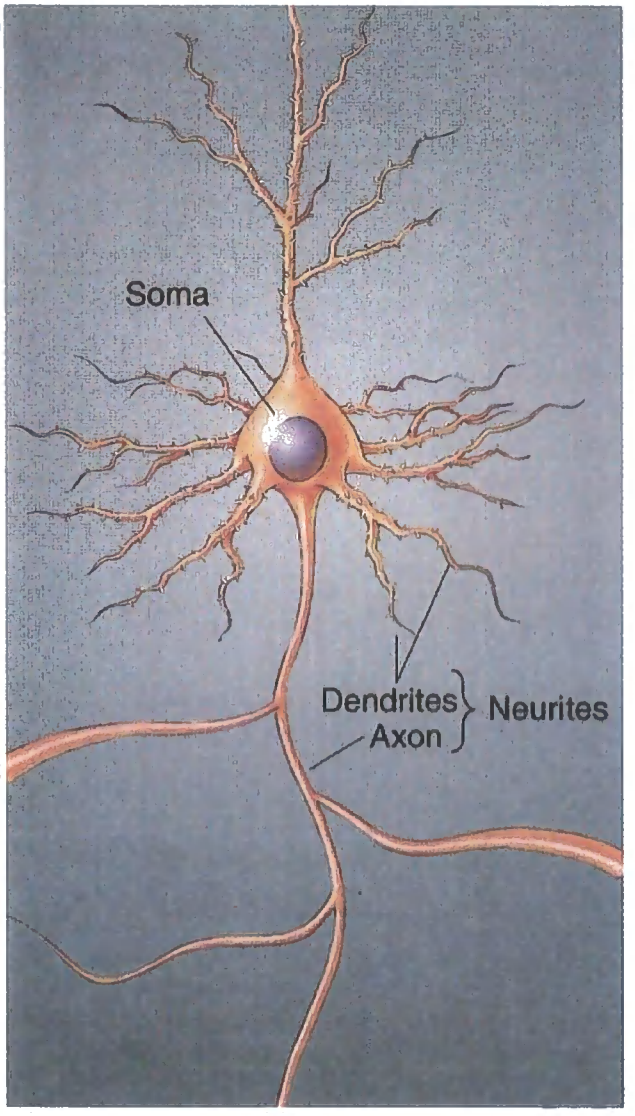

Figure 1.1: The basic parts of a neuron (Bear *et al.*, 1996).

1.3 Anatomy of the Brain

There are three parts of the brain that are common to all mammals, the cerebrum, the cerebellum and the brain stem (Figure 1.2). The cerebrum consists of two cerebral hemispheres which are separated by a prominent central fissure and connected via the corpus callosum. The outer surface of the cerebrum is the cerebral cortex. Lying behind the cerebrum is the cerebellum, which is derived from the Latin "little brain". The brain stem forms a stalk from which the cerebral hemispheres and cerebellum sprout. The spinal cord is attached to the brain stem and is the major pathway of information from the skin, joints and muscles of the body to the brain and vice versa.

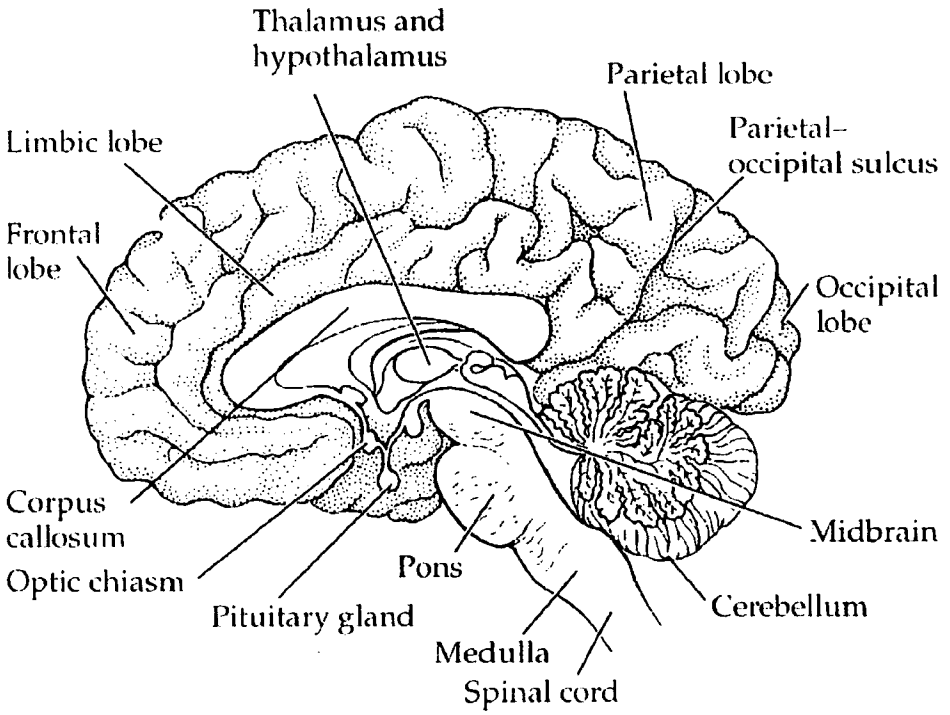

Figure 1.2: A medial view of human brain showing anatomical and structural organisation (Feldman *et al.*, 1997).

1.4 Functions of the Brain

Broadly speaking the brain has three regions, the forebrain, midbrain and the hindbrain. The forebrain is the foundation of perceptions, conscious awareness, cognition and voluntary action. The cortical neurons of the cerebral cortex receive sensory information from perceptions of the outside world, and command voluntary movements. The thalamus forms an important relay centre, connecting other regions of the brain, assisting in the integration of sensory information. The thalamus conveys information to appropriate areas of the cerebrum. Pain and pleasure seem to be perceived by the thalamus. The hypothalamus role is in controlling regions of the autonomic nervous system, where it consists of two centres, one for sympathetic nervous system, and the other for parasympathetic nervous system. Another role of the hypothalamus is to monitor the composition of blood, in particular plasma solute concentration, hence it is very rich in supply of blood vessels.

The midbrain acts as an important link between the hindbrain and the forebrain. Midbrain functions include routing, selecting, mapping and sorting information, including information perceived from the environment and information that is remembered and processed throughout the cerebral cortex.

The hindbrain differentiates into the cerebellum, pons and medulla where it is an important pathway for the passage of information from the forebrain to the spinal cord and vice versa. The cerebellum is an important movement control centre where it receives massive axonal inputs from the spinal cord and the pons. The signals from the pons relay information from the cerebral cortex, specifying the goals of intended movements. The medulla contains important centres of autonomic system. These centres control reflex activities, heart rate & blood pressure. Other activities

controlled by the medulla include swallowing, coughing, and the production of saliva.

1.5 Neurotransmission

In regular neurotransmission, an action potential from one cell can result in action potentials being produced in another cell, thus allowing communication between them. Once molecules of neurotransmitter are released from a cell as the result of the firing of an action potential, they bind to specific receptors on the surface of the postsynaptic cell. In all cases in which these receptors have been cloned and characterised in detail, it has been shown that there are numerous subtypes of receptor for any given neurotransmitter. As well as being present on the surfaces of postsynaptic neurons, neurotransmitter receptors are found on presynaptic neurons. In general, presynaptic neuron receptors act to inhibit further release of neurotransmitter. Neurotransmitter receptors can be divided into two types: G-protein-coupled receptors (metabotropic) or ligand-gated ion channel receptors (ionotropic).

The integral role of neurotransmitters on the normal functioning of the brain makes it clear to see how an imbalance in any one of these chemicals could very possibly have serious clinical implications for an individual. Biological dysfunction of synaptic transmission of various neurotransmitters often leads to such imbalances and is the ultimate source of conditions such as schizophrenia (glutamate) (Olney and Farber, 1995), Parkinson's disease (dopamine) (Cotzias *et al.*, 1969), and Alzheimer's disease (acetylcholine) (D'Amato *et al.*, 1987; Selkoe, 1991). Henry Dale (reviewed in Tansey, 1991) classified neurons into exclusive groups by neurotransmitter release (e.g. cholinergic, glutaminergic, GABAergic). Several substances have been

identified as neurotransmitters. Acetylcholine can act as an excitatory or an inhibitory neurotransmitter. Alzheimer's disease is associated with a decrease in acetylcholine-secreting neurons (D'Amato *et al.,* 1987; Selkoe, 1991). Myasthenia gravis, that is a weakness of skeletal muscles, is a result of a reduction in acetylcholine receptors (Vincent *et al.,* 2001). Serotonin (5-HT) is generally an inhibitory neurotransmitter which is involved with mood, anxiety, and sleep induction. Levels of serotonin are elevated in schizophrenia, hence the symptoms of delusions, hallucinations and withdrawal (Tamminga, 1998b). Dopamine is generally an excitatory neurotransmitter of the CNS. Parkinson's disease results from the destruction of dopamine-secreting neurons (Cotzias *et al.,* 1969), but drugs used to increase dopamine production can cause side effects as the therapeutic index is small. Amino acid neurotransmitters in the CNS, are glutamate and γ-aminobutyric acid (GABA). Glutamate is the main excitatory transmitter whereas GABA is the main inhibitory transmitter in the CNS. Glycine is also an inhibitory transmitter mainly in the spinal cord. Clinically, compounds targeted to the glutamate receptor may prevent neurological disorders where there is neural degeneration from overexcitation, for example, in stroke (Szydlowska *et al.,* 2007). On the other hand, compounds targeting GABA neurons by increasing GABA function can be used to treat epilepsy (Benetello, 1995). Changes in glutamatergic transmission have also been invoked to explain pathologic mechanisms involved in stroke (Choi and Rothman, 1990), epilepsy (Sloviter, 1991), Parkinson's disease (Turski *et al.,* 1991), Huntington's disease (Schwarcz *et al.,* 1983) and Alzheimer's disease (Ulas *et al.*, 1992).

1.6 L-Glutamate as a Neurotransmitter

When GABA was recognised to show inhibitory effects on neurons (Bazemore *et al.*, 1956), work by the Curtis *et al.*, (1959) showed that glutamate produced a strong excitatory effect. The full acceptance of the transmitter role of L-glutamate was not achieved for a further twenty years (Watkins and Evans, 1981; Foster and Fagg, 1984; Watkins, 1986). The major conclusions reached during the 1980s were that L-glutamate was the predominant excitatory neurotransmitter in the CNS; it mediates its actions via multiple receptors and malfunction of glutamate mediated receptors is likely to be involved in certain CNS disorders (Watkins, 1988; Collingridge and Watkins, 1994). L-glutamate is the principal and ubiquitous excitatory transmitter in the CNS where its concentrations are higher than elsewhere in the body. Glutamate from CNS neurons can originate from either glucose, via the Krebs's cycle, or glutamine, which is synthesised from glial cells and taken up by neurons (Storm-Mathisen *et al.*, 1986). Glutamate is stored in synaptic vesicles (Naito and Ueda, 1983) and upon depolarisation of the nerve terminal is released by calcium-dependent exocytosis. The action of glutamate is terminated mainly by carrier mediated reuptake into the nerve terminals and neighboring glial cells. The glutamate taken up into glial cells is converted by glutamine synthetase into glutamine, which is then transported into neighbouring nerve terminals, where it serves as a precursor for glutamate. L-glutamate acts through a variety of ionotropic (ligand-gated ion channels) and metabotropic (G-protein coupled) receptors. There are four main subtypes of glutamate receptors: i) metabotropic receptors, ii) α-amino-3-hydroxy-5-methyl-4-isoxazole propionic acid (AMPA), iii) kainate, and iv) N-methyl-D-aspartate (NMDA).

1.7 Metabotropic Glutamate Receptors (mGluRs)

The metabotropic glutamate receptors are diameric G-protein coupled receptors (GPCRs), linked to intracellular second messenger systems. These second messenger systems can initiate IP_3 production and release intracellular calcium, or can inhibit adenylyl cyclase. They are located both pre- and postsynaptically, as well as on non-neuronal cells. This receptor family provides a mechanism by which activation by glutamate can regulate a number of important neuronal and glial functions that are not typically modulated by ligand gated ion channels (Conn, 2003). They are unusual in that they show no sequence homology with other GPCRs, and in having a large extracellular N-terminal tail, which contains the glutamate binding site, in contrast to most amine receptors, where the agonist binding site is buried amongst the transmembrane domains. The mGluRs consist of at least eight different subtypes ($mGluR_1$-$mGluR_8$), which have been classified into three groups based on sequence homology, pharmacological profile and coupling to intracellular transduction pathways (Pin and Duvoisin, 1995; Conn and Pin, 1997). Group I mGluRs consist of $mGlu_1$ and $mGlu_5$; Group II consist of $mGlu_2$ and $mGlu_3$; and Group III consist of $mGlu_4$, $mGlu_6$, $mGlu_7$ and $mGlu_8$.

1.8 α-amino-3-hydroxy-5-methyl-4-isoxazolepropionic acid (AMPA)

AMPA receptors, an ionotropic glutamate receptor family were cloned and expressed in recombinant systems in the late 1980s (Hollmann *et al.*, 1989). The subunit constituents of AMPA receptors are termed $GluR_{1-7}$ which is based upon their

sequence homology. AMPA receptor subunits are approximately 900 amino acids in length, and show around 65-75% sequence homology between subunits and appear to exist in a pentameric structure (see review by Hollmann and Heinemann, 1994; Ferrer-Montiel and Montal, 1996), although further studies have suggested that they may exist with a tetrameric structure (Mano and Teichberg, 1998; Rosemund *et al.*, 1998). Each subunit of the AMPA receptor consist of three transmembrane domains (M1, M3 and M4) and one reentrant loop within the membrane (M2) (Wo and Oswald, 1994; Bennett and Dingledine, 1995). The M2 reentrant loop is thought to form the channel pore of the receptor, determining the permeability of heteromeric receptors to Ca^{2+}. AMPA receptors have two 150 amino acid sequences (S1 and S2) which are separated by the M1-M3 membrane domains and appear to represent the agonist recognition sites (see review by Keinänen *et al.*, 1997). AMPA receptors were originally defined using quisqualate as an agonist before AMPA was shown to be the preferred ligand (Bleakman and Lodge, 1998). Many AMPA receptor agonists, including AMPA, have been derived from classic structure activity studies using ibotenic acid, quisqualic acid and wallardiine (Stensbol *et al.*, 2002). AMPA receptor agonists can vary considerably in the amount of receptor desensitization that they can induce. Initially, AMPA competitive antagonists included 6-cyano-7-nitroquinoxaline-2,3-dione (CNQX) and 6,7-dinitro-quinoxaline-2,3-dione (DNQX) showed potent competitive antagonism of quisqualate and kainite induced [^{3}H] GABA release from cultured mouse cortical neurons with weaker effects on NMDA responses (Drejer and Honore, 1988). However, later studies demonstrated that these compounds showed unsurmountable antagonism of responses to NMDA in the baby rat (2-7 days old) hemisected spinal cord. This showed the effect was mediated via an action at the strychnine-insensitive glycine receptor, thus lacking selectivity (Birch *et*

al., 1988). From these structures, other competitive antagonists were developed which included 2,3-dihydroxy-6-nitro-7-sulfamoyl-benzo(*F*)quinoxaline (NBQX) (Sheardown *et al*, 1990) and 1,4,7,8,9,10-hexahydro-9-methyl-6-nitropyrido[3,4-*f*]-quinoxaline-2,3-dione (PNQX) (Ohmori *et al.*, 1994). Sheardown *et al* (1990) demonstrated NBQX to be neuroprotective in global ischaemia in the gerbil and subsequently in global ischaemia in the rat (Buchan *et al.*, 1991; Le Peillet *et al.*, 1992). AMPA receptor distribution in the CNS has been widely studied using various techniques including radioligand binding of [^{3}H] AMPA (Monaghan *et al.*, 1984), single cell RT-PCR (Bochet *et al.*, 1994; Jonas *et al.*, 1994; Geiger *et al.*, 1995), *in situ* hybridisation histochemistry (Keinänen *et al.*, 1990; Verdoorn *et al.*, 1991) and immunocytochemistry using AMPA receptor subunit antibodies (Petralia and Wenthold, 1992).

1.9 Kainate Receptors

An alternative ionotropic glutamate receptor family is the kainate receptors that respond to both glutamate, which is their physiological ligand, or kainate which is a drug first isolated from *red alga Digenea simplex.* Kainate receptor pharmacology and pathophysiology are far less defined than for AMPA receptors. The subunits comprising kainate receptors are termed GluR5-GluR7 and KA1-KA2 and were cloned showing high affinity binding for [^{3}H] kainate (Werner *et al.*, 1991; Herb *et al.*, 1992; Kamboj *et al.*, 1994). KA1 and KA2 share around 70% sequence homology but less than 40% homology with the AMPA receptor subunits GluR1-4. KA1 and KA2 subunits are widely distributed in the mammalian CNS (Bettler *et al.*, 1990;

Egebjerg *et al.*, 1991; Lomeli *et al.*, 1992; Wisden and Seeburg, 1993) including the cerebellum, hippocampus and the spinal cord. Kainate receptors have classically been implicated in epileptogenesis where an intraperitoneal injection of kainate is used as a model for temporal lobe seizures.

1.10 N-methyl-D-aspartate (NMDA) Receptor

The NMDA receptor is a heteromeric ligand-gated ion channel in the CNS. NMDA receptors have a high density postsynaptically, although they are present presynaptically. Chemical crosslinking studies and size exclusion chromatography have estimated a size of native NMDA receptors to be ~730kDa (Brose *et al.*, 1993) given the size of NR1 (~120kDa) and NR2 (~160-180kDa), results indicate a pentameric stoichiometry, with a subunit assembly that show different physiological and pharmacological properties and are differentially distributed throughout the CNS (Seeburg, 1993; Hollmann and Heinemann, 1994; McBain and Mayer, 1994; Danysz *et al.*, 1995). Debate is still ongoing whether the receptors have a tetrameric or pentameric structure, as a number of research groups, including Wenthold *et al.*, 1992; Sutcliffe *et al.*, 1996, Premkumar and Auerbach, 1997 & Hawkins *et al.*, 1999 reported it as a pentameric structure. More recently, Laube *et al.*, (1998) demonstrated that NMDA receptors show tetrameric assemblies. Each subunit consists of a large extracellular amino terminal domain, three transmembrane hydrophobic regions, M1, M3 & M4, which transverse the membrane, and an intracellular carboxy terminal. The M2 transmembrane domain forms a reentrant loop in the membrane, forming the channel pore (Figure 1.3). There are three families of NMDA receptor subunits with various combinations of NR1, NR2A-D and NR3A-B

subunits producing unique receptors with distinctive pharmacological and biochemical properties. The NR1 subunit exists as eight distinct isoforms which arise via the insertion or deletion of three short exon cassettes in the N-terminal (N1) and C-terminal (C1, C2) domains of the subunit protein (Hollmann *et al.*, 1993). These are designated NR1-1a, NR1-1b to NR1-4a, and NR1-4b that are generated by differential messenger ribonucleic acid (mRNA). The NR2 subunits are 40-70% homologous to one another, but are only 18% homologous to NR1. The NR3A-B subunit family was described by Das *et al.*, 1998 and Chatterton *et al.*, 2002. NR3 subunits do not appear to form functional NMDA receptors when expressed together with either NR1 or NR2 subunits alone (i.e. NR1/NR3 or NR2/NR3 containing receptors), while it has been reported that NR3 subunits expressed in *Xenopus* oocytes along with NR1 form excitatory glycine receptors that are unaffected by glutamate or NMDA (Chatterton *et al.*, 2002), although controversial as other laboratories have been unable to reproduce these findings. When expressed in combination with both NR1 and NR2 subunits, NR3 subunits suppress NMDA channel unitary conductance and Ca^{2+} permeability relative to NR1/NR2 containing receptors (Ciabarra *et al.*, 1995; Nishi *et al.*, 2001; Matsuda *et al.*, 2002; Sasaki *et al.*, 2002). The NMDA receptor subunits focused on in this thesis are NR1/NR2B and NR1/NR2A/NR2B combinations. Therapeutic significance of non-selective antagonists and blockers of the NMDA receptor has been limited by the extensive side effects, including psychotomimetic symptoms and effects on learning and memory. Specific antagonists of the NR2B subunit may have the ability to show better potential as therapeutic reagents due to their high affinity and improved selectivity. Consequently, it should be possible to develop drugs that are selective or specific to particular combinations of subunits.

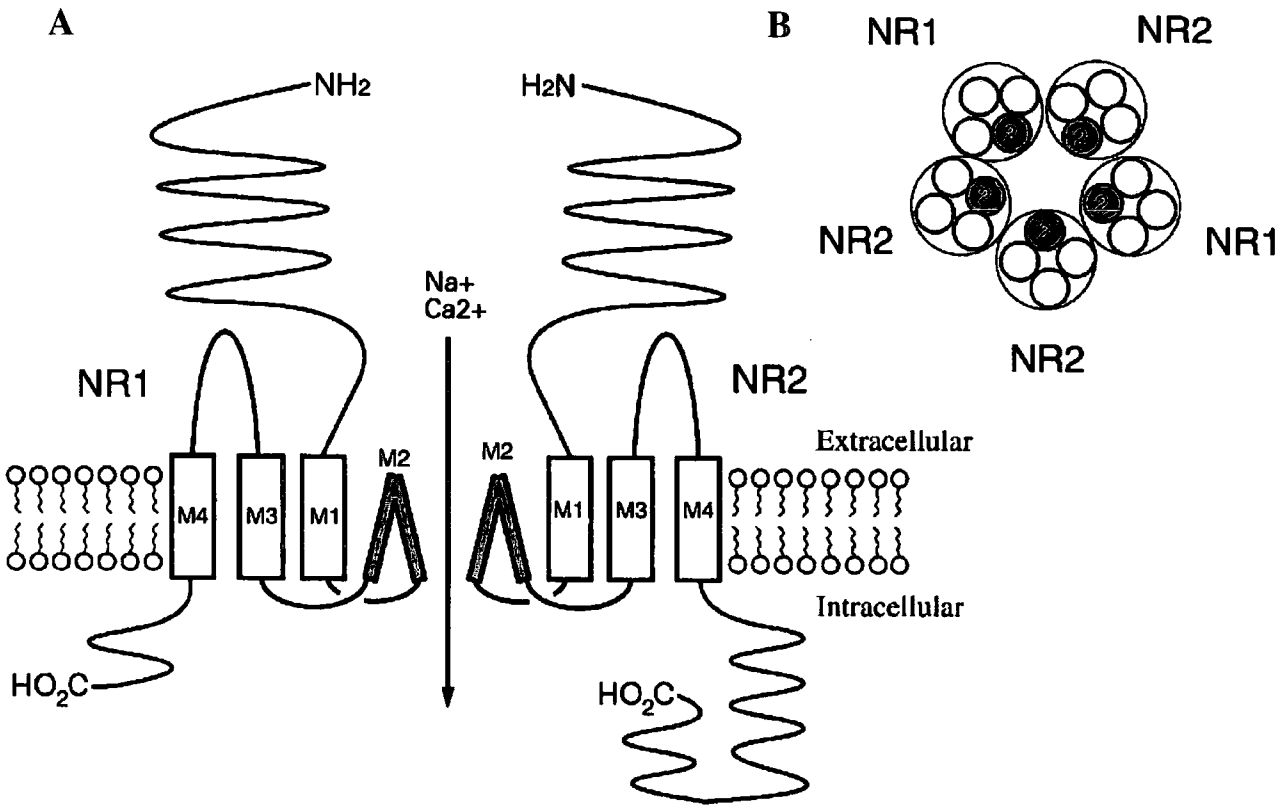

Figure 1.3: (**A**) The NMDA receptor showing the large extracellular amino domain, three transmembrane domains (M1, M3 & M4) and the reentrant loop (M2) and the intracellular carboxy domain. (**B**) The structures of the channel pore where the reentrant loop (M2) forms the opening of the NMDA receptor (Williams, 1997).

1.10.1 NMDA Functional Properties

Functional NMDA receptor complexes are formed with an obligatory NR1 subunit with at least one NR2 subunit, which can be a combination of NR1, NR2A-D and/or NR3A-B subunits. Pharmacological and functional properties of the NMDA receptor are highly dependent on the composition of the receptor complex due to the distribution of the various NMDA receptor populations in the CNS. For example, NR1/NR2C compounds would primarily target the cerebellum (Wenzel *et al.*, 1997), whereas NR1/NR2B antagonists would predominantly target the hippocampus, cerebral cortex, striatum and the olfactory bulbs (Luo *et al.*, 1997; Charton *et al.*, 1999).

NMDA receptors are activated by glutamate and co-agonist glycine, where the binding site for glycine is located on the NR1 subunit (Kuryatov *et al.*, 1994; Wafford *et al.*, 1995; Hirai *et al.*, 1996; Kew *et al.*, 2000) and the binding site for glutamate is located on the NR2 subunit (Laube *et al.*, 1997; Anson *et al.*, 1998). The glutamate binding site is understood to act like a venus fly trap (Madden, 2002) where regions S1 and S2 changes conformation following activation (Figure 1.4). At resting membrane potential, the NMDA receptor is blocked in a voltage-dependent manner by Mg^{2+}, meaning activation occurs following depolarisation of the postsynaptic membrane. The most frequently used agonist at the glutamate recognition site of NMDA receptor is NMDA itself which is a synthetic analogue of L-glutamate (Watkins, 1962), where it shows slight selectivity between receptor subtypes. Other selective agonists include aspartate, quinolinate and homocysteate. Co-agonist for the glycine binding domain is primarily glycine, but other co-agonists include D-serine and D-cycloserine.

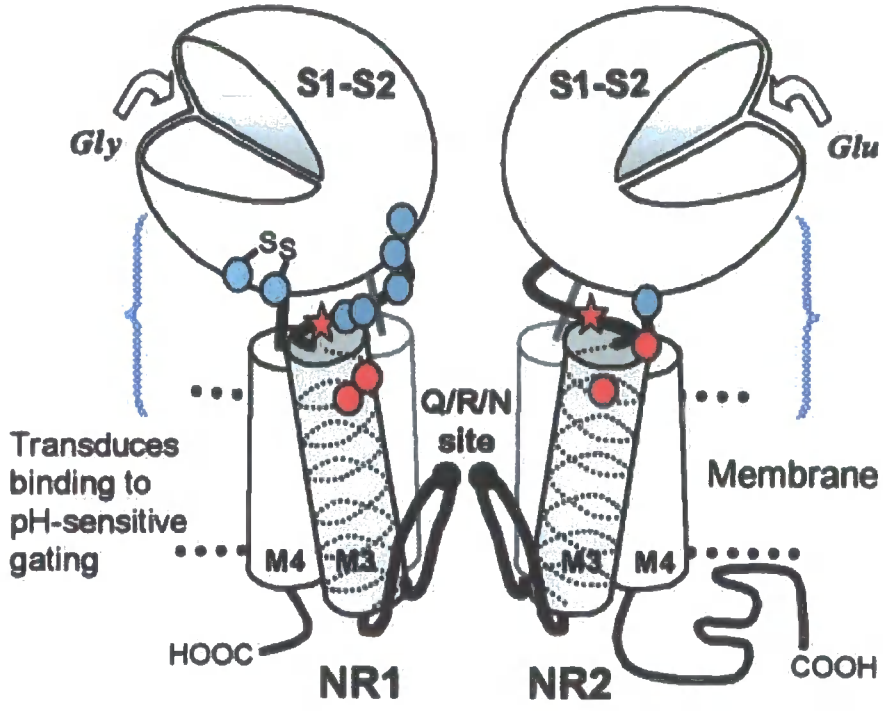

Figure 1.4: Co-localisation of residues influencing proton sensitivity of NMDA receptor (Low *et al.*, 2003).

1.10.2 NMDA Modulatory Binding Sites

There are numerous sites on the NMDA receptor that can act to inhibit, activate or enhance the function of the receptor including the polyamine site, zinc binding domain, as well as reduction/oxidation and pH sensor sites (Kemp and McKernan, 2002). NMDA receptors are coupled to high conductance cationic channels permeable to K^+, Na^+ and Ca^{2+} (McBain and Mayer, 1994) (Figure 1.5). The property of high Ca^{2+} permeability render NMDA receptors suitable for their role in mediating

synaptic plasticity, which underlie learning processes and development (Collingridge and Singer, 1990; Danysz *et al.,* 1995). The zinc modulatory site on the extracellular surface of the receptor inhibits NMDA receptor function in a voltage-dependent manner. Endogenous polyamines, spermidine and spermine, appear to modulate NMDA receptor function by various mechanisms. Sacaan and Johnson (1989) postulated that polyamines enhanced the binding of glycine to NMDA receptors in sub-saturating concentrations showing glycine-dependent stimulation. In saturating concentrations (<200nM) of glycine, polyamines stimulate receptor opening, showing glycine-independent stimulation (Williams *et al.*, 1990; Lynch *et al.,* 1995), whereas, in higher concentrations (>200nM) of glycine, polyamines block NMDA receptors in a voltage-dependent manner (Rock and MacDonald, 1992a&b) and hence decrease the affinity of the receptor for glutamate (Williams *et al.*, 1995).

1.10.3 Synaptic Plasticity

Synaptic plasticity is the ability of the connection, or synapse, between two neurons to change in strength. There are several underlying mechanisms that co-operate to achieve synaptic plasticity, including changes in the amount of neurotransmitter released into a synapse and changes in how effectively cells respond to those neurotransmitters (Gaiarsa *et al.*, 2002). Since memories are postulated to be represented by vastly interconnected networks of synapses in the brain, synaptic plasticity is one of the important neurochemical foundations of learning and memory. NMDA receptors appear to play a pivotal role in long term depression (LTD), long term potentiation (LTP) and developmental plasticity. LTP is a long-lasting

enhancement of the effectiveness of synaptic transmission that is induced by brief, high-frequency afferent stimulation. Prolonged low-frequency stimulation can produce a related phenomenon termed LTD, which involves a reduction in synaptic efficacy. LTP has been found in various brain areas (see Tsumoto, 1992) but was first demonstrated by Bliss and Lømo (1973) in the hippocampus. The NMDA receptor has been accepted as a critical step in the initiation of LTP following Ca^{2+} entry into the postsynaptic cell, where the receptor must be in the appropriate state for LTP to be induced. Disruption of the NMDA receptor, in particular the NR1 subunit led to early postnatal death of transgenic mice (Forrest *et al.*, 1994). Moreover, mice that overexpress NR2B subunit exhibit enhanced hippocampal LTP, prolonged NMDA receptor currents and improved memory (Tang *et al.*, 1999). LTP, LTD and spatial learning are important mechanisms of synaptic plasticity as these require the activation of NMDA receptors in the hippocampus.

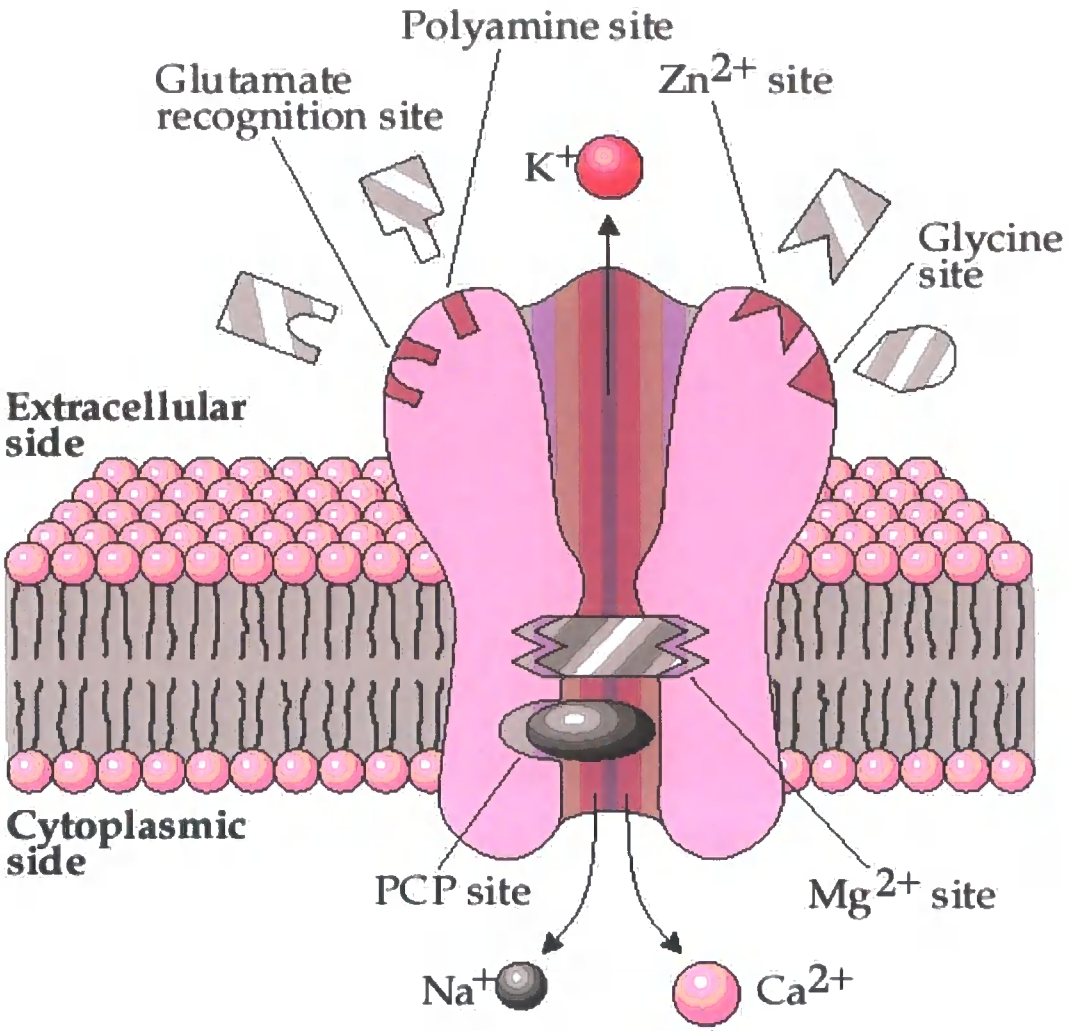

Figure 1.5: The NMDA receptor showing the binding of both glutamate and glycine together with modulatory sites including Mg^{2+} site, polyamine site, redox reagent site, H^{+} sites & the PCP binding site (Feldman and Quenzer, 1984).

1.10.4 NMDA Receptor Distribution in the CNS

1.10.4.1 Expression of NMDA Receptors

The expression of NMDA receptors in the developing and adult brain has been identified using *in situ* hybridisation. Messenger ribonucleic acid (mRNA) encoding the NR1 subunit is distributed throughout pre- and postnatal development (Watanabe *et al.*, 1993; Takai *et al.*, 2003). In developing rats, NR1 mRNA levels in the cortex and hippocampus increase nearly three fold from postnatal day 3 to day 15 and approximately doubled from day 15 to day 67 (Franklin *et al.*, 1993; Riva *et al.*, 1994; Nowicka and Kaczmarek, 1996). In contrast, cerebellum and brain stem showed no change in NR1 mRNA levels between postnatal days 3 and 15 but levels also doubled from day 15 to day 67 (Franklin *et al.*, 1993). Similar findings were also found by a different group, although they found that expression levels in the hippocampus peaked at postnatal day 10 and declined from then on (Pujic *et al.*, 1993). The highest levels of mRNA encoding NR1 in the adult rodent brain are found in the olfactory bulb, and the lowest levels are seen in the spinal cord. Intermediate levels are found in the frontal cortex, hippocampus and cerebellum (Franklin *et al.*, 1993; Akazawa *et al.*, 1994). Similar findings of the expression levels have also been reported when using antibodies to NR1 subunits (Petralia *et al.*, 1994; Benke *et al.*, 1995; Thompson *et al.*, 2000, 2002).

The modulatory subunits, NR2A-D, are differentially expressed (Watanabe *et al.*, 1993; Takai *et al.*, 2003) in the CNS. From *in situ* hybridisation analyses (Monyer *et al.*, 1992; Watanabe *et al.*, 1994; Wenzel *et al.*, 1997; Rafiki *et al.*, 1998; Goebel and

Poosch, 1999), the distribution of the mRNA levels of the NR2A-D show specific developmental regulation throughout the brain. The NR2A subunit is expressed postnatally in the brain. NR2B subunits are widely expressed throughout the entire embryonic brain and from the early stage of development, but expression is restricted to the forebrain postnatally (Mori and Mishina, 1995; Wenzel *et al.*, 1997). The NR2C subunit appears postnatally and is prominent in the cerebellum. The NR2D subunit is mainly present in the diencephalon and the brainstem at embryonic and neonatal stages (Watanabe *et al.*, 1993; Takai *et al.*, 2003). The NR3 subunit is abundant within the late prenatal and early postnatal brain development (Sun *et al.*, 1998). Highest levels of NR3A are expressed in the neocortex, thalamus, amygdala and subiculum (Ciabarra *et al.*, 1995; Sucher *et al.*, 1995; Wong *et al.*, 2002). NR3 subunits show restricted spatio-temporal distributions with NR3A being predominantly expressed during development, although expression in certain neuronal populations persists in adults, and NR3B restricted to somatic motoneurones of the brainstem and spinal cord (Nishi *et al.*, 2001; Chaffey and Chazot, unpublished).

In situ hybridisation does not clearly define expression of the resultant protein subunits in the CNS. Immunocytochemical localisation studies have shown NR1 protein levels to be prominent in all brain areas, which is consistent with mRNA expression (Brose *et al.*, 1993). NR2A protein is found throughout the brain but highest levels are detected in the hippocampus, cerebral cortex, thalamus, cerebellum and striatum (Wenzel *et al.*, 1995; Luo *et al.*, 1997; Thompson *et al.*, 2000). The NR2B subunit is predominantly found in the hippocampus, cerebral cortex, striatum and the olfactory bulbs (Luo *et al.*, 1997; Charton *et al.*, 1999). In accordance with mRNA levels, NR2C protein is almost exclusively expressed in the cerebellum

(Wenzel *et al.*, 1997). NR2D subunits are restricted to the spinal cord, brainstem regions, striatum, thalamic regions and the olfactory bulbs (Dunah *et al.*, 1998).

1.10.4.2 Biochemical Evidence for NMDA Receptor Subtypes

Functional NMDA receptor complexes require an obligatory NR1 subunit with at least one NR2 subunit; a combination of NR1, NR2A-D and/or NR3A-B subunits (Figure 1.5). The first group to demonstrate that NR1 and NR2 subunits do coexist in adult and developing brain, by immunoprecipitation using NMDA receptor subunit-specific antibodies was Sheng *et al* (1994). This study investigated the actual composition of the NMDA receptors in the rat neocortex where the subunits are present as heteromeric complexes of considerable heterogeneity. These studies implied, but did not demonstrate that NR1, NR2A and NR2B subunits coexisted within a receptor complex. Further studies using a combination of immunoaffinity chromatography and immunoprecipitation, have shown directly the co-association of NR1, NR2A and NR2B subunits in an NMDA receptor subpopulation of adult mammalian brain (Chazot and Stephenson, 1997b). Pharmacological and functional properties of the NMDA receptor are highly dependent on the composition of the receptor complex.

1.10.5 Drug Targets of the NMDA Receptor

The NMDA receptor is the focus of drug development for therapy and prevention of numerous neurological and psychiatric disorders. Excessive activation of NMDA

receptors produces an increase of glutamate causing excitotoxicity of the CNS which is implicated in various neurological conditions including ischemic neuronal cell death and epilepsy (Choi and Rothman, 1990; Dingledine *et al.*, 1990). Abnormal expression, function or regulation of NMDA receptors may be involved in psychoses and some neurodegenerative disorders (Choi, 1988; Carlsson and Carlsson, 1990). Pathologically, glutamate acting as an excitotoxin can be involved in extending the damage of an acute cerebral injury such as stroke or initiating neurodegeneration in chronic illness such as epilepsy or Huntington's chorea (Whetsell and Shapira, 1993). Agents that block the NMDA receptor, for example, ketamine, have been shown to alleviate pain in human clinical trials. However, the small therapeutic window relative to side effects, such as, hallucinations, dysphoria, and loss of co-ordination, make these compounds unattractive for chronic pain therapy (Hocking and Cousins, 2003). Therefore, beneficial treatments of such cases need to target the NMDA receptor to block or reduce NMDA receptor activity, or potentiate the activity of the receptor.

1.10.5.1 Non-selective NMDA Antagonists

Therapeutic significance of nonselective antagonists and blockers of the NMDA receptor has been limited by the extensive side effects, including psychotomimetic symptoms and effects on learning and memory. For example, NMDA receptor antagonists that functionally inhibit NMDA receptors can work in three ways. Firstly via the phencyclidine (PCP) site of the receptor situated in the channel pore. Alternatively, by competitive antagonism binding to the primary transmitter site, or by binding to the strychnine-insensitive glycine site (Glycine $_B$ site). [^{3}H] MK-801 binds to the activated state of the NMDA receptor complex; it has been used as a

functional assay *in vitro* to investigate modulation by ion channel blockers (Wong *et al.*, 1988), glutamate and glycine recognition site ligands (Foster and Wong, 1987; Foster *et al.*, 1992) and polyamines (Williams *et al.*, 1989). These non-selective NMDA receptor antagonists all show inadequate selectivity and therefore cause many unwanted side effects. Consequently, due to the diversity of the NMDA receptor subtypes, there is encouragement to develop more selective compounds to a particular receptor subtype which lack the side effects of the nonselective antagonists.

1.10.5.2 Selective NMDA Antagonists

Researchers are still developing new ligands that block or reduce the activity of NMDA receptors for therapeutic benefit as neuroprotective agents, anticonvulsants and analgesics. It is thought that inappropriate activation of NMDA receptors are involved with a number of neurodegenerative and psychiatric disorders (see Section 1.10.6). Non-competitive antagonists, ifenprodil and haloperidol are subtype selective NMDA receptor antagonists specific to the NR2B-containing receptor (Williams, 1993; Williams *et al.*, 1994; Lynch *et al.*, 1995; Ilyin *et al.*, 1996; Lynch and Gallagher, 1996; Coughenour and Cordon, 1997). Ifenprodil was originally known as a α_1-adrengeric antagonist, but its NMDA activity was discovered in the late 1980s showing that ifenprodil was an NMDA antagonist with a novel pharmacological profile (Carter *et al.*, 1988; Reynolds and Miller, 1989). Ifenprodil blocks several other types of receptors and channels including voltage dependent Ca^{2+} channels (Adeagbo, 1984; Biton *et al.*, 1995) and σ-sites (Contreras *et al.*, 1990), showing it is not ideal due to its lack of overall receptor selectivity. Haloperidol is a dopaminergic antagonist which has an 8-10-fold higher affinity for NMDA receptors

containing the NR2B subunit compared to other NMDA receptors thus showing the same subunit specificity as ifenprodil (Ilyin *et al.*, 1996; Lynch and Gallagher, 1996). Two compounds which are structurally similar to ifenprodil and haloperidol are CP 101,606 [(*R**, *R**)-4-hydroxy-(4-hydroxyphenyl)-β-methyl-4-phenyl-1-piperidine-ethanol] and Ro 25,6981 [(*R:(*),S(*)*)-α-(4-hydroxyphenyl)-β-methyl-4-(phenylmethyl)-1-piperidinepropanol [(+/-)-Ro 25-6981]] (Figure 1.6), have been developed as high affinity NR2B subunit specific antagonists (Chenard *et al.*, 1995; Brimecombe *et al.*, 1998; Mutel *et al.*, 1998; Tamiz *et al.*, 1998). These all bind to a similar recognition site, termed the ifenprodil site (Figure 1.7) and are selective for the NR2B subunit-containing receptors. CP 101,606 and Ro 25,6981 are phenylethanolamines and act by an interaction with one of the polyamine recognition sites of the receptor complex by increasing the sensitivity of the receptor to negative modulation by protons (Kew and Kemp, 1998; Mott *et al.*, 1998). Ro 25,6981 shows no affinity for the non-competitive binding sites of phencyclidine (PCP) and (+)-5-methyl-10,11-dihydro-*5H*-dibenzo[*a,d*]cyclohepten-5,10-imine (MK-801) (Fischer *et al.*, 1997; Mutel *et al.*, 1998; Lynch *et al.*, 2001). Ro 25,6981 binds NR1/NR2B and NR1/NR2A/NR2B subtype receptors with similar high affinities, indicating Ro 25,6981 to be selective for all NR2B-containing subtype receptors (Hawkins *et al.*, 1999). CP 101,606 shows further selectivity as it can distinguish between NR1/NR2A, NR1/NR2B and NR1/NR2A/NR2B subtype receptors showing high selectivity for NR1/NR2B as has been shown in single channel recording (Brimcombe *et al.*, 1997) and in cytotoxicity studies (Boeckmann and Aizenman, 1996).

Ro 25,6981 and CP 101,606 are routinely used as reference compounds in research of NR2B-selective NMDA receptor antagonists. There are many new NR2B-selective NMDA receptor antagonists in development from major pharmaceutical companies

based on the functional groups required for binding in the structure of ifenprodil, for example, the compound investigated in this thesis, RGH-896 (Figure 1.8). Throughout this thesis, one of the testing hypothesis is that RGH-896 will resemble Ro 25,6981 closer than CP 101,606 for its NMDA subtype selectivity.

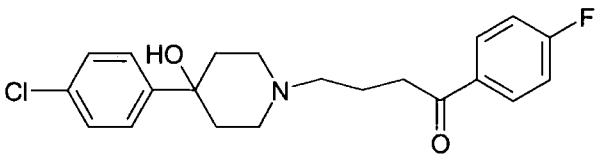

Haloperidol

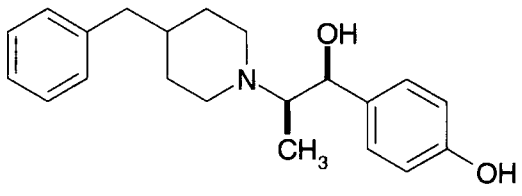

Ifenprodil

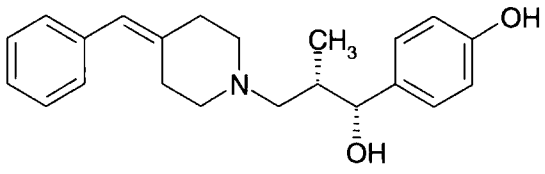

Ro 25,6981

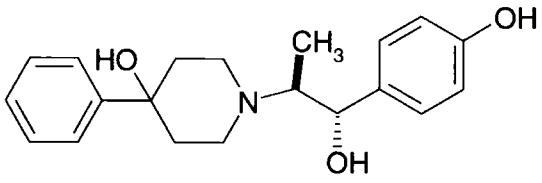

CP 101,606

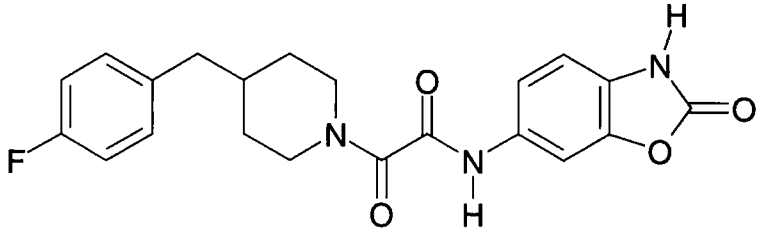

RGH-896

Figure 1.6: Chemical Structure of NMDA Antagonists

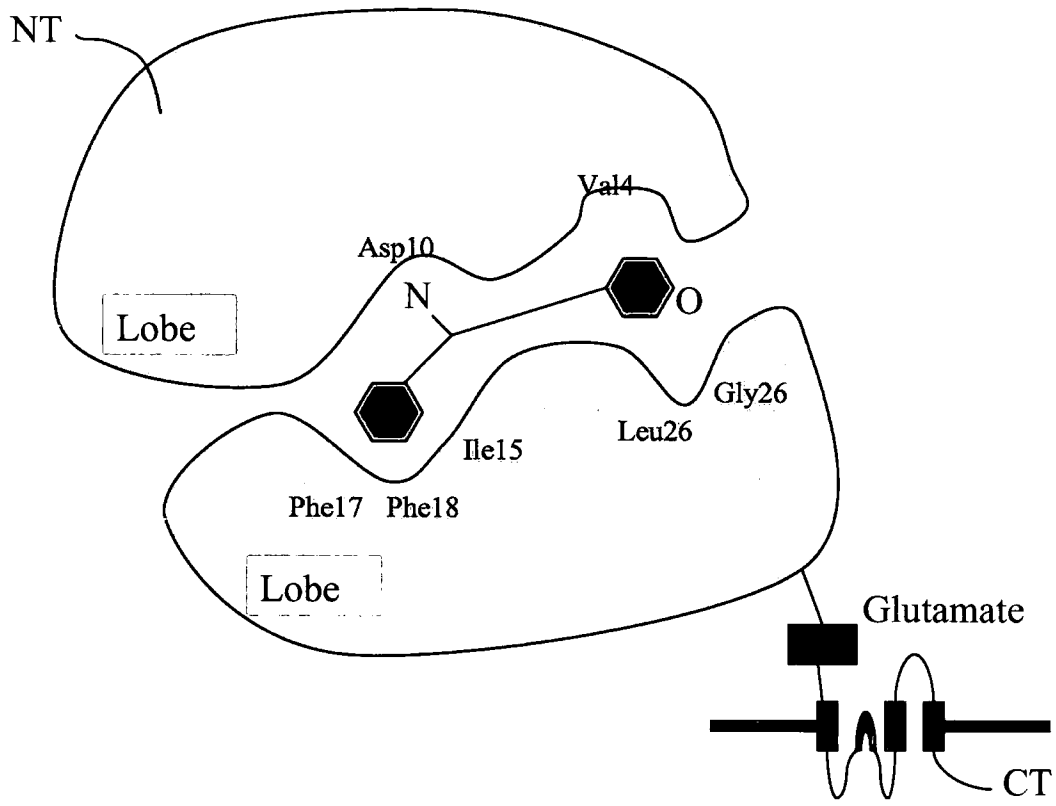

Figure 1.7: The ifenprodil binding domain showing a hydrophobic ring for the phenyl ring, an electrostatic pocket for the central basic nitrogen, a hydrophobic and H-bond acceptor pocket for the phenol group (Chazot, 2004)

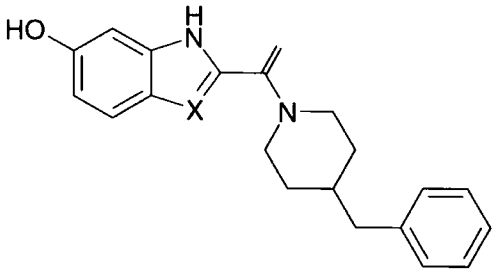

Gedeon Richter (X = N or CH)

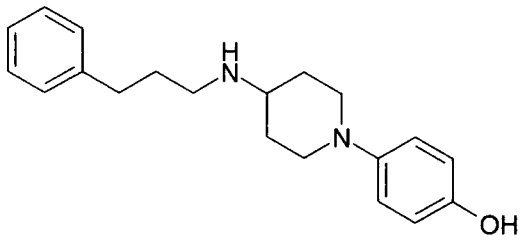

Roche

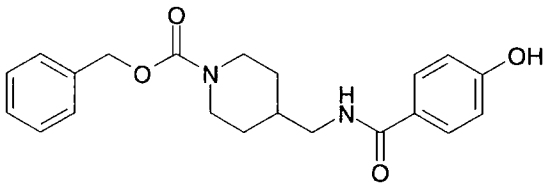

Merck & Co

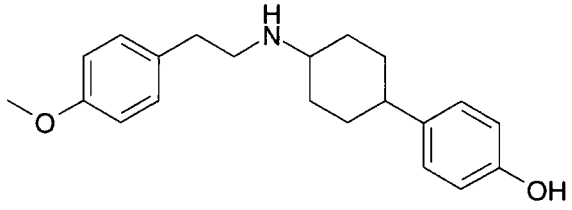

Warner-Lambert

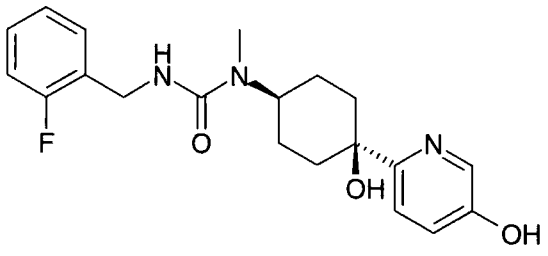

Pfizer

Figure 1.8: Chemical structure of NR2B-selective NMDA antagonists in development from major pharmaceutical companies (McCauley, 2005).

1.10.6 Therapeutic Targets for NR2B subunit-selective NMDA Antagonists

NR2B subunit-selective NMDA antagonism may have therapeutic applications for many CNS disorders. These antagonists show better potential as therapeutic reagents due to their high affinity and improved selectivity. The NR2B selective compound ifenprodil has shown to have neuroprotective effects in animal models of stroke without the unwanted side effects associated with non-selective NMDA antagonists (Gotti *et al.*, 1988). This study showed that ifenprodil was able to reduce infarction volume in a dose-dependent manner, when administered after middle cerebral artery occlusion in the cat (Gotti *et al.*, 1988). More recently, CP 101,606 and Ro 25,6981 have shown neuroprotective effects in animal models, producing minimal side effects at maximally neuroprotective doses (Kemp *et al.*, 1999). Consequently, there are potential therapeutic targets for NR2B subunit-selective antagonists which are discussed in detail below.

1.10.6.1 Pain

Pain is a disabling accompaniment of many medical conditions; consequently pain control is of great importance. NMDA receptors have been reported to have an involvement with the induction and maintenance of central sensitisation during pain states. NMDA receptors are important in the plasticity of the synaptic processes of the nervous system, such as sensitisation of the nociceptive pathways (Sandkuhler, 2000). In the 1980s, two groups recognised that NMDA antagonists inhibited the hyperexcitability of spinal cord nociceptive neurons induced by C-fibre stimulation

(Davies and Lodge, 1987; Dickenson and Sullivan, 1987). In animal studies, NR2B-selective antagonists are antinociceptive at doses below those that impair motor coordination and show stimulant activity (Boyce *et al.*, 1999; Chizh *et al.*, 2001). A study by Wei *et al* (2001) utilised mice overexpressing NR2B receptors in the forebrain and demonstrated enhanced pain behaviour compared with control animals, suggesting a potential cortical site of action of NR2B receptor antagonists. The NR2B subunit-containing receptors are thought to play an important role in pain states; hence NR2B-selective antagonists targeting the dorsal horn of the spinal cord (Boyce *et al.*, 1999) or the anterior cingulate cortex (Wei *et al.*, 2001) may be useful for the treatment of chronic pain. The restricted distribution of the NR2B receptors makes them promising candidates as targets of side effect free analgesic drugs (Gurwitz and Weizman, 2002).

1.10.6.2 Huntington's Disease

Huntington's Disease (HD) is an autosomal dominantly inherited neurodegenerative disorder characterised by progressive brain deterioration, which commences in adulthood with progressive degeneration and death. It is characterised by extrapyramidal movement disorder, cognitive function and behavioural changes (Kremer *et al.*, 1992). NMDA receptor-mediated excitotoxicity has been suggested to be involved in the pathogenesis of HD. HD results from the expansion of polyglutamine repeat in the protein designated *huntingtin* (*htt*), in the N-terminus of the receptor. HD is mainly affected by the neurodegeneration of striatal medium-sized spiny projection neurons, where expression of the NR2B subunit-containing receptor is increased relative to other NR2 containing subunits (Li *et al.*, 2003). Furthermore,

the earliest changes associated with neuronal expression of mutant *htt* are increased NMDA receptor-mediated current, disrupted calcium homeostasis and enhanced vulnerability to NMDA-mediated excitotoxicity (Li *et al.*, 2004). This creates the prospect that a selective interaction of mutant *htt* with NR1/NR2B-subtype NMDA receptor may explain the selective susceptibility of medium-sized spiny projection neurons in HD. Therefore, an interaction between *htt* and NR2B-containing NMDA receptors in the early neurodegeneration of HD, support the use of NR2B-selective antagonists in the presymptomatic or early stages of the disease.

1.10.6.3 Stroke

An ischemic stroke occurs when a blood clot blocks a blood vessel or artery, or when a blood vessel breaks, interrupting blood flow to an area of the brain causing a chain reaction called the "ischemic cascade". The only currently approved stroke therapy, tissue plasminogen activator, is a thrombolytic that targets the thrombus within the blood vessel. In the ischemic brain there is an excessive amount of glutamate in the extracellular space (Szatkowski and Attwell, 1994; Rossi *et al.*, 2000) which is thought to induce hyperactivation of NMDA receptors causing an influx of Ca^{2+} into neurons and ultimately leading to cell death (Rothman and Olney, 1986; Choi and Rothman, 1990). NMDA receptor antagonists, in particular, glycine-binding site antagonists are been tested in animal models of stroke to inhibit hyperactivation of NMDA receptors. By targeting the glycine site on the NMDA receptor, the risk of unwanted adverse effects seen with non-selective NMDA receptor antagonists and channel blockers are reduced. Medial cerebral artery occlusions (MCAOs) are a pathological hallmark of stroke patients. A recent study using electrocoagulation of a unilateral middle cerebral artery distal to the olfactory tract using spontaneously

hypertensive rats, demonstrated a glycine-binding site antagonist SM-31900 showed significant neuroprotective effects even when administered one hour following MCAO (Ohtani *et al.*, 2002, 2003). Other investigators targeting the glycine binding site have reported a reduction in infarct volume when treatment is initiated 10 minutes (Takaoka *et al.*, 1997), 30 minutes (Takano *et al.*, 1997), one hour (Tanaka *et al.*, 1995) or six hours (Bordi *et al.*, 1997; Reggiani *et al.*, 2001) after MCAO. The use of glycine-binding site antagonists may prove beneficial in the treatment of stroke in the future.

1.10.6.4 Parkinson's Disease

In Parkinson's disease (PD), degeneration of the dopaminergic nigrostriatal pathway leads to enhanced transmission at NMDA receptors containing NR2B subunits. Accordingly, pharmacological dopamine replacement with chronic 1-3,4-dihydroxyphenylalanine (L-DOPA) treatment represents the most effective therapeutic option (Lang and Lozano, 1998). However, although L-DOPA is effective therapeutically, it also possesses a narrow therapeutic index, disabling adverse complications can occur including motor fluctuations and dyskinesias (Obeso *et al.*, 2000). NMDA receptor antagonists have been shown to potentiate the actions of L-DOPA in rats, and the low affinity NMDA antagonist amantadine has been shown to improve L-DOPA-induced dyskinesias in humans (Del Dotto *et al.*, 2001; Marino *et al.*, 2003). NMDA receptor antagonists have also been shown to potentiate the actions of dopamine receptor agonists in animal models of PD suggesting these compounds may be beneficial for the treatment of PD (Klockgether and Turski, 1990). Ifenprodil showed efficacy in reserpine-treated rat model of PD, as well as in 1-methyl-4-phenyl-1,2,3,6-tetrahydropyridine (MPTP)-treated marmosets (Nash *et al.*, 1999;

Nash *et al.*, 2000); however, a small clinical trial in which ifenprodil was used as an add-on therapy with L-DOPA in PD pateients failed to demonstrate significant therapeutic benefit (Montastruc *et al.*, 1992). Ro 25,6981 and CP 101,606 have been characterised *in vivo* where Ro 25,6981 has potentiated the action of dopamine receptor agonists in lesioned rats (Löschmann *et al.*, 2004). Steece-Collier (2000) studied the antiparkinsonian effects of CP 101,606 in rodents and non-human primates. In rats, CP 101,606 decreased haloperidol catalepsy, whereas in MPTP-treated monkeys, the selective antagonist reduced parkinsonian motor symptoms by ~20%. Another study using MPTP-lesioned parkinsonian monkeys treated with levadopa were given an NMDA antagonist LY235959 and this significantly attenuated dyskinesias (Papa and Chase, 1996). More recently, intracerebral pharmacological studies in a rat model of PD suggests an overactivity of NR2B-containing NMDA receptors within the striatum is responsible for mediating parkinsonism (Nash and Brotchie, 2002). As a result, these preclinical data, taken together with results from clinical studies of NMDA receptor antagonists, suggest that NR2B-selective antagonists hold therapeutic utility as antiparkinsonian agents.

1.10.6.5 Alzheimer's Disease

Alzheimer's disease (AD) is a progressive neurodegenerative disease characterised by mental deterioration with diffuse neuronal loss. Amyloid-β peptide is elevated in the brains of patients with AD and is believed to be causative in the disease process. Recent findings have demonstrated that non-toxic amounts of secreted amyloid-β peptide reduce synaptic plasticity and glutamatergic transmission (Kamenetz *et al.*, 2003). NMDA receptors play a pivotal role in the synaptic mechanisms of learning

and memory (Bliss and Collingridge, 1993). Memory is one of the earliest cognitive functions to be affected during the normal aging process (Albert and Funkenstein, 1992). There are declines in expression of NMDA receptors with increasing age in humans (Piggott *et al.*, 1992), monkeys (Wenk *et al.*, 1991), dogs (Magnusson *et al.*, 2000), rats (Tamaru *et al.*, 1991) and mice (Magnusson, 2001). Changes in both NMDA receptor binding and mRNA expression of the ε2 (NR2B) subunit in the prefrontal cortical regions in mice have been shown to be related to working memory deficits (Bai *et al.*, 2002). A further study by Bai *et al* (2004) in macaque monkeys revealed a significant decrease in mRNA expression of NR2B subunit in the prefrontal cortex and the caudate nucleus. Studies have reported that glutamate induced-excitotoxicity interferes with normal neurotransmission and glutamate receptor activation in disorders including Alzheimer's disease (AD) (Choi, 1988). Furthermore, Koh *et al.*, 1990 and Mattson *et al.*, 1999, have described how glutamate receptors can interact with amyloid precursor protein or β-amyloid, which can lead to beneficial or damaging effects on neurons. In a transgenic animal model, overexpression of the NR2B subunit in the forebrain had proved to enhance activation of NMDA receptors and therefore an enhancement in learning and memory (Tang *et al.*, 1999) in various behavioural tasks. These observations suggest the NMDA receptor could play a significant role in the neurobiology of AD.

1.10.6.6 Dementia with Lewy Bodies

Dementia with Lewy Bodies (DLB) is the second most frequent neurodegenerative dementing disorders after Alzheimer's disease (Byrne *et al.*, 1989; McKeith *et al.*, 1996). DLB is clinically characterised by progressive dementia, which is frequently

accompanied by parkinsonism and psychiatric symptoms (Luis *et al.,* 1999). DLB is pathologically characterised by the presence of cytoplasmic inclusions of α-synuclein, a cytoplasmic protein associated with synaptic vesicles, in the cerebral cortex and in the nuclei of the brain stem. Lewy bodies (LB) occur as thin filaments in the form of eosinophilic inclusions, seen mostly in the cerebral cortex, particularly in the cingular gyrus, in parahippocampal gyrus, in temporal neocortex, in amygdala and also in the nuclei of the brain stem, mainly in the substantia nigra and in locus coeruleus (McKeith *et al.*, 1995). It is believed that patients with LB in the brain stem are connected with movement disorders, in the limbic system with psychosis and in the cortex with depression. Psychosis can be the most disturbing feature of DLB, where patients with DLB often have complex hallucinations (McKeith *et al.*, 1996) and depressive symptoms (Harding *et al.*, 2002). A clinical study has been conducted to compare neurotransmitter amino acid levels in the cerebrospinal fluid and the cerebrospinal/plasma ratios using an ion-exchange chromatographic method. It was found that there were no alterations in concentrations of glutamate, aspartate and GABA in the cerebrospinal fluid of DLB patients compared to a control group (Molina *et al*, 2005).

1.10.6.7 Psychosis

The word *psychosis* was first used by Ernst von Feuchtersleben in 1845 as an alternative to insanity and mania. Psychosis is a condition in which a person is not in contact with reality unlike most normal people. Although the general term is psychosis, this condition can take many forms, differing in symptoms and diagnosis. These psychotic conditions are associated with abnormalities in the central nervous

system (CNS). The most common psychotic disorders of the CNS include schizophrenia and bipolar affective disorder. Others include mania, delusional (paranoid) disorders and psychotic depression. Occasionally, it can be difficult to diagnosis psychotic conditions, as most patients have a mixture of symptoms. Psychosis is characterised by delusions, hallucinations, incoherent communication, illogical thinking and disorganised behaviour.

1.10.6.7.1 Schizophrenia

In 1908, Eugen Bleuler introduced the term 'schizophrenia', defining the expression as 'when someone cannot tell the difference between what is real and what is imaginary'. The clinical features of the heterogeneous disorder schizophrenia usually appear in late adolescence or early adulthood, where Kreapelin (1919) found that 3.5% of cases of dementia praecox began before the age of 10, with a further 2.7% arising between the ages of 10 and 15. Bleuler (1911) suggested that about 5% of cases of schizophrenia had their onset prior to the age of 15. Schizophrenic symptoms can be divided into positive, negative and cognitive symptoms. Delusions (paranoia, false beliefs), hallucinations (visual and auditory), and thought disturbances are classified as positive symptoms where these are additional to normal life experience, whereas negative features which lack normal experience include depression, withdrawal from social contacts, incapability to feel pleasure (anhedonia) and flattening of emotional responses. Cognitive defects involve deficits in attention and memory. Schizophrenia is thought to be a neurodevelopmental disorder rather than a neurodegenerative disorder, as Harrison (1997) reported that schizophrenia affects the cerebral cortex in the first few months of prenatal development. Post

mortem analysis of schizophrenic brains show evidence of misplaced cortical neurons with abnormal morphology, suggestive of defective cell migration during early development.

1.10.6.7.1.1 Area of the Brain Affected by Schizophrenia

There are many sections of the brain that can be affected in schizophrenia, for example, abnormal function in the basal ganglia is thought to contribute to paranoia and hallucinations (Heckers *et al.*, 1991). A schizophrenic having difficulty in planning and organisation will have defects in the frontal lobe of the brain which is critical to problem solving and higher level reasoning (Fuster, 1999). Agitation is brought about by the limbic system of the brain which controls emotion (Stevens, 1973; Chiodo and Bunney, 1983). Impaired hippocampal formation mediates learning and memory difficulties. Visual disturbances are caused by damage to the occipital lobe whereas the auditory system is responsible for auditory hallucinations. As mentioned there are many affected brain regions that are associated with the pathophysiology of schizophrenia, all linked by either excitatory, inhibitory or dopaminergic connections (Figure 1.9). Excitatory cortical efferent pathways project to subcortical regions in the brain containing dopamine cell bodies or terminal, while dopaminergic pathways modulate cortical excitatory neurons, hence, NMDA blockade produces dopaminergic hyperactivity (Lewis and Liebermann, 2000). The anterior cingulate cortex (ACC) is implicated to play a key role in the pathogenesis of schizophrenia. Schizophrenia usually involves abnormalities in brain functions related to ACC including emotion, affect (Hempel *et al.*, 2003) and cognition (Carter *et al.*, 2001; Salgado-Pineda *et al.*, 2003) (Figure 1.9).

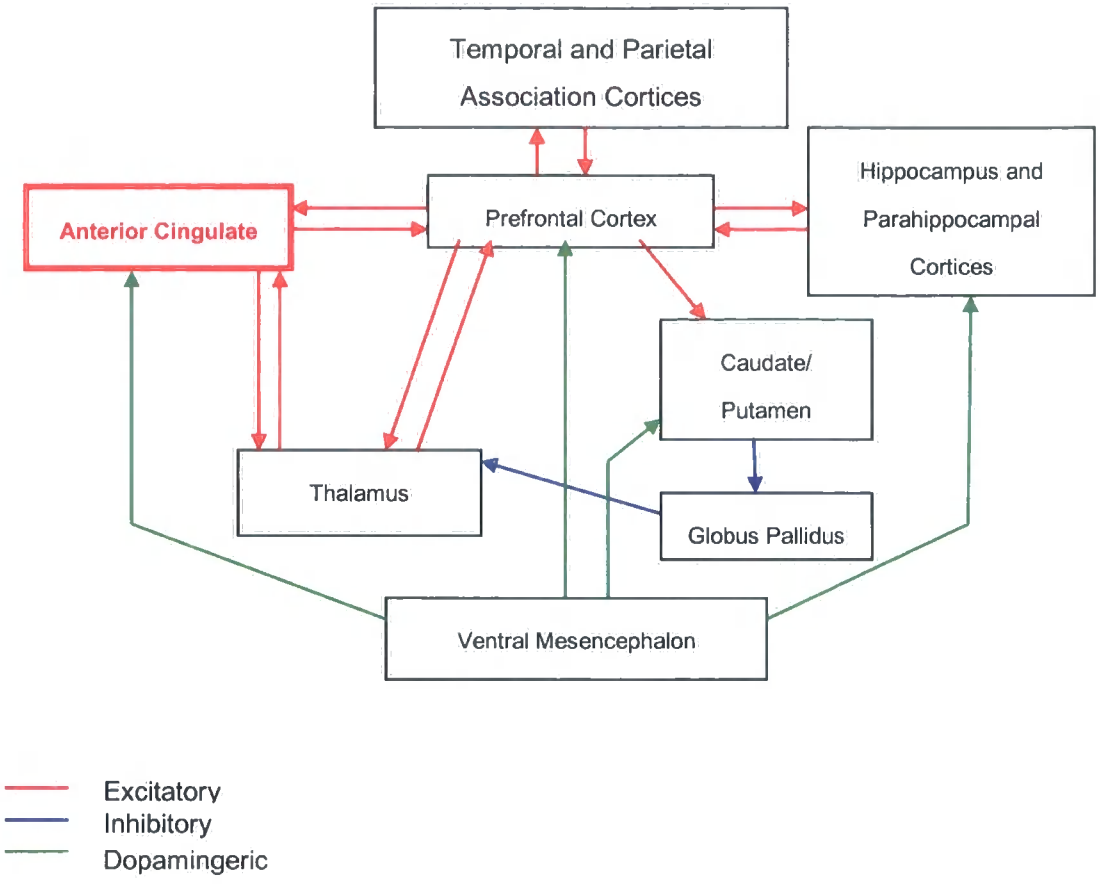

Figure 1.9: Affected brain regions in schizophrenia showing the various connecting pathways involved between brain areas (Lewis and Liebermann, 2000)

.1.10.6.7.1.2 Dopamine Hypothesis of Schizophrenia

The dopamine hypothesis of schizophrenia was proposed by Carlsson and Lindqvist (1963) where it was stated the over activity of dopamine in the mesencephalic projections to the limbic striatum was involved. Schizophrenic symptoms can be prompted by the administration of amphetamine (Angrist *et al.*, 1974) which releases dopamine in the brain, producing primarily positive symptoms of schizophrenia. Drug therapy acting on dopamine type D_2- receptors is beneficial for controlling the positive symptoms of the disease, but not the negative or cognitive defects. Dopamine treatment of schizophrenia can either block postsynaptic dopamine receptors or inhibit the release of dopamine from the presynaptic cleft. The dopamine theory is still unable to explain the multiple characteristics of schizophrenia.

1.10.6.7.1.3 Glutamate Hypothesis of Schizophrenia

Glutamate is the principal excitatory neurotransmitter in the brain. Glutamate hypofunction in the CNS could be due to inadequate glutamate release, over activity of glutamate transporters removing glutamate from the synaptic cleft or defective receptors. The initial report of the glutamate hypothesis of schizophrenia was the observation of low levels of glutamate in cerebrospinal fluid samples from schizophrenic patients (Kim *et al.*, 1980). Further evidence that glutamate dysfunction is involved in the pathogenesis of schizophrenia involves phencyclidine (PCP) and its congener ketamine (Javitt and Zukin, 1991; Krystal *et al.*, 1994). They have been shown to induce psychosis in humans that closely resembles schizophrenia, and are representative of not only the positive symptoms and cognitive defects of the disease,

but also the negative symptoms (Adler *et al.*, 1999). PCP was originally introduced into science as a surgical anaesthetic, but was soon withdrawn due to patients reporting psychotic events including hallucinations, disoriented speech and behaviour. Following the withdrawal of PCP, ketamine was introduced as a dissociative anaesthetic but the extrapyramidal side effects were suppressed with the administration of benzodiazepines or prevented with barbiturates. PCP is a non-competitive N-methyl-D-aspartate (NMDA) receptor antagonist, as are ketamine and MK-801 (dizocilpine). These bind within the channel pore of the receptor in its activated state and block the transmission of glutamate, hence causing hypofunction of glutamate activity. Following growing evidence of the psychotomimetic effects produced by this class of NMDA receptor antagonists, PCP-induced psychosis is widely been used as an *in vivo* experimental model of schizophrenia (Jarvitt and Zukin, 1991).

It is hypothesised that schizophrenia affects many brain regions in early development including the midbrain, nucleus accumbens, thalamus, temporo-limbic and prefrontal cortices (Selemon and Goldman-Rakic, 1999). Connecting tracts, including corticostriatal, thalamocortical and corticocortical association fibre all utilise glutamate as a neurotransmitter (Huntley *et al.*, 1994). Defects in glutamate transmission in these connecting tracts produced some clinical findings of schizophrenia (Weinberger, 1993). Recently, abnormalities in glutamatergic transmission have been reported in the anterior cingulate cortex (Brodmann's area 24) which is localised within a gyrus on the medial surface of each hemisphere, bordering on the corpus callosum (Zavitsanou *et al.*, 2002)

Since glutamatergic and dopaminergic systems are closely related in the forebrain (Kotter, 1994), it is unclear whether glutamate hypofunction is the primary defect in schizophrenia or a secondary change due to excessive activation of dopamine receptors. Increased dopamingeric activity can inhibit glutamatergic function and can result in a hypoglutamatergic state in schizophrenia (Kotter, 1994).

1.11 Aims of the Study

The focus of this study is to characterise a novel putative NR2B subtype selective compound RGH-896, currently in Phase II clinical trials. A series of radioligand binding experiments will be performed in rodent adult forebrain and NR1/NR2B transfected HEK 293 cells, to determine the affinity of RGH-896 for the NR2B subtype NMDA receptor complex in comparison to other established prototypical NR2B-selective antagonists. In order to directly measure the affinity of RGH-896 for NR1/NR2A/NR2B subtype, an immunopurification strategy was employed. To conduct this assay, a specific anti-peptide antibody against the NMDA NR2A subunit will be developed in order to produce an anti-NR2A antibody column. This column will be utilised to immunopurifying NR1/NR2A/NR2B receptors expressed in HEK 293 cells in order to determine the affinity of RGH-896 for this subtype. By conducting these studies, the testing hypothesis will establish the subtype selectivity of RGH-896 in comparison to Ro 25,6981 (binds to all NR2B containing receptor subtypes) or CP 101,606 (binds to only NR2B containing receptor subtypes), to determine if RGH-896 displays a pharmacological profile closer to Ro 25,6981 than CP 101,606.

Rodent and human autoradiography studies will be used to determine anatomical distribution of NR2B subtype using the pharmacological defined radioligand [^{3}H] RGH-896. The involvement of NR2B subtype in human DLB will be probed focusing on the anterior cingulate cortex (ACC) and a range of psychotic symptoms. Here the hypothesis to test is the levels of anterior cingulate cortex NR2B receptors correlates with the psychotic symptoms displayed by DLB suffers.

Chapter 2

Pharmacological Characterisation of NMDA NR2B-Selective Antagonists

2.1 Introduction

The NMDA receptor is the focus of drug development for therapy and prevention of numerous neurological and psychiatric disorders. Beneficial treatments of such cases can target the NMDA receptor to block or reduce NMDA receptor activity, or potentiate the activity of the receptor. The therapeutic usefulness of non-selective NMDA antagonists and NMDA channel blockers is limited due to extensive adverse effects, including psychotomimetic symptoms (Krystal, 1994) and effects on learning and memory (Malhotra *et al.*, 1996). Due to the diversity of the NMDA receptor, there is encouragement to develop selective compounds which lack the side effects of the non-selective antagonists, where researchers are developing new ligands that block or reduce the activity of NMDA receptors. The NR2B subunit is a valid target for treatment of many CNS pathologies (Chazot, 2004), and thus is the focus of NMDA receptor antagonism using novel NR2B-selective compounds. The structures of many novel antagonists are based upon the basic structure of ifenprodil, a non-selective NMDA receptor antagonist (Carter *et al.*, 1988; Reynolds and Miller, 1989). Two compounds which are structurally similar to ifenprodil are CP 101,606 and Ro 25,6981 which have been developed as high affinity NR2B subunit specific

antagonists (Chenard *et al.*, 1995; Brimecombe *et al.*, 1998; Mutel *et al.*, 1998; Tamiz *et al.*, 1998). CP 101,606 and Ro 25,6981 bind to a similar recognition site, termed the ifenprodil site and are selective for the NR2B subunit-containing receptors. Using radioligand binding techniques, Ro 25,6981 binds NR1/NR2B and NR1/NR2B/NR2A subtype receptors with similar high affinities, indicating Ro 25,6981 to be selective for all NR2B-containing subtype receptors (Hawkins *et al.*, 1999). CP 101,606 shows further selectivity as it can distinguish between NR1/NR2A, NR1/NR2B and NR1/NR2A/NR2B subtype receptors showing high selectivity for NR1/NR2B as has been shown in single channel recording (Brimcombe *et al.*, 1997) and in cytotoxicity studies (Boeckman and Aizenman, 1996). Ro 25,6981 and CP 101,606 are routinely used as reference compounds in research of NR2B-selective NMDA receptor antagonists. There are many novel NR2B-selective NMDA receptor antagonists being developed for their potential as therapeutic reagents as a result of their high affinity and improved selectivity.

Radioligand binding studies help to determine whether a drug will produce therapeutic effects or adverse effects at the various receptor subtypes in the brain. This type of study is one method of mapping the distribution of a particular receptor in different areas in the CNS. The basis of radioligand binding studies is to show binding of the radioligand (L) to the receptor complex (R) to form a radioligand-receptor complex (RL). The radioligand-receptor complex is more commonly described as the 'bound' ligand, whereas the unbound radioligand is referred to the 'free' radioligand. To perform radioligand binding, the reaction must reach steady-state equilibrium based on the law of mass action, where: -

Receptor (R) + Radioligand (L) $\rightleftharpoons$ Radioligand-Receptor Complex (RL)

When performing radioligand binding, it is necessary to account for non-specific binding, where the radioligand binds to receptors other than the one of interest. Consequently, it is essential to measure both total and non-specific binding, in order to determine specific binding to the receptor of interest. Non-specific binding is assessed using the presence of a high concentration of an unlabelled compound that binds essentially to all receptors of interest.

RGH-896 is a highly selective compound for the NR2B subunit developed by Gedeon Richter, Hungary. When comparing RGH-896 with CI-1041 (a selective NR2B antagonist) and MK-801 (a non-selective antagonist) for functional affinity, both RGH-896 and CI-1041 inhibited NMDA-evoked $[Ca^{2+}]_i$-elevation in a concentration dependent manner in cells expressing the subunit combination hNR1/hNR2B where maximal inhibition achieved for RGH-896 and CI-1041 was 83.6% and 85.4% respectively, and MK-801 showed full inhibition (personal communication with Gedeon Richter).

The aim of this chapter is to characterise the pharmacological profile of a prototypical NR2B-selective antagonist ifenprodil and a novel NR2B-selective compound, RGH-896 using a series of radioligand binding assays with native and recombinant NMDA receptors.

2.2 Methods

2.2.1 Membrane Preparation

Following concussion and decapitation, adult male Sprague-Dawley rat brain (250-300g) was removed from the skull. Forebrain tissue was dissected from the whole brain by removal of the cerebellum, medulla and spinal cord. Using cold homogenisation buffer (50mM Tris-HCl, pH 7.4, containing 5mM EDTA, 5mM EGTA, 320mM sucrose), forebrain tissue was homogenised in a Dounce glass/glass homogeniser. Homogenised forebrain tissue was equally placed into JA20 tubes prior to centrifugation at 2,200rpm, 4°C for 10 minutes. The supernatant was carefully removed and retained on ice. The remaining pellet was resuspended in cold homogenisation buffer and the later two steps were repeated. The supernatants were pooled together and centrifuged at 15,000rpm, 4°C for 30 minutes. This supernatant was discarded and the resuspended pellet was gently homogenised to a smooth mixture with additional homogenisation buffer required for the assay. The forebrain preparation was aliquoted into 1ml fractions and frozen at -20°C. The protein concentration of the forebrain membrane preparation was determined by a Lowry assay (Lowry *et al.*, 1951).

2.2.2 Lowry Assay

Protein concentration of the forebrain membrane preparation was determined using the method of Lowry *et al* (1951). A series of standards were set-up (three repeats for

each concentration) using a standard protein, bovine serum albumin (BSA), at a range of concentrations from 0-100μg/mL from a stock of 1mg/mL. In parallel, a series of various concentrations of protein to be assayed, in this case, forebrain membrane preparations were set-up (three repeats for each concentration). Reagent A (2% (w/v) sodium carbonate, 0.1M sodium hydroxide, 0.5% (w/v) lauryl sulfate (SDS)), reagent B (2% (w/v) sodium potassium tartrate) and reagent C (1% (w/v) copper sulphate) were assembled in the ratio of 100:1:1 respectively to form reagent D. 0.5mL of reagent D was added to each tube and vortexed before incubating at room temperature for 10 minutes. An addition of 50μL of Folin solution (Folin & Ciocalteu's phenol reagent: water (1:1)) was added and vortexed prior to incubation at room temperature for 30 minutes. To stop the reaction, 0.5mL of water was added to each tube and mixed well. The absorbance of each tube was determined where the optical density (O.D.) at λ = 750nM, using a spectrophotometer, in a 1mL plastic cuvette. Each concentration analysed produced an average from three tubes. From a standard curve, of absorbance against concentration, the protein concentration of the samples assayed in μg/mL can be estimated.

2.2.3 Radioligand Binding

Well washed adult male rat Sprague-Dawley forebrain membranes (100μg protein) (section 2.2.1) or transfected HEK 293 cell homogenates (100μg protein) were incubated (three repeats for each concentration), with radioligand, assay buffer (25mM sodium phosphate buffer, pH 7.4), and compound of interest in a total volume of 200μL, for 2 hours at room temperature. Non-specific activity was defined in each

assay. The assay was terminated and bound radioligand was collected by rapid filtration through Whatman GF/B filters, pre-soaked in 10mM sodium phosphate buffer, pH 7.4. The filters were washed (3 x 3mL) using ice-cold 10mM sodium phosphate buffer, pH 7.4, using a Brandel cell harvester. Filters were transferred into scintillation vials with Ecoscint A liquid scintillation cocktail fluid (1mL) and incubated overnight at room temperature. Bound radioactivity was quantified using Packard Tri-Carb 1600TR scintillation spectrophotometer with a counting time of 3 minutes per vial. The data was analysed using GraphPad Prism version 4.0.

2.2.3.1 [^{3}H] RGH-896 Saturation Binding Assay

For [^{3}H] RGH-896 saturation experiments, well washed forebrain membranes (1mg/mL) (section 2.2.1) (100μL) were incubated in 25mM sodium phosphate buffer pH 7.4, in the presence of a range of concentrations of [^{3}H] RGH-896 (0.5–80nM, 20μL) to a final volume of 200μL. All concentration points included three repeats for each concentration were incubated for 2 hours at room temperature. Non-specific binding was defined using Ro 25,6981 (10^{-5}M). The assay was terminated by rapid filtration (section 2.2.3).

2.2.3.2 [^{3}H] Ro 25,6981 Competition Binding Assay

[^{3}H] Ro 25,6981 competition binding assays were performed with ifenprodil (10^{-9}M – 10^{-3}M) using both forebrain and NR1/NR2B or NR1/NR2A/NR2B transfected HEK

293 cell homogenates, defining non-specific binding with ifenprodil (10^{-4}M) or RGH-896 (10^{-5}M).

[^{3}H] Ro 25,6981 and [^{3}H] MK-801 competition binding assay (in the presence of 10μM glutamate) were performed to further characterise the pharmacological profile of unlabelled RGH-896. Non-specific binding of [^{3}H] Ro 25,6981 was defined using RGH-896 (10^{-5}M), whereas non-specific binding of [^{3}H] MK-801 was defined using ketamine (10^{-3}M). The protocol was carried out as described in section 2.2.3.

2.2.3.3 [^{3}H] RGH-896 Competition Binding Assay

[^{3}H] RGH-896 competition binding assays were performed with Ro 25,6981 (10^{-11}M – 10^{-5}M) and spermidine (10^{-5}M – 10^{-2}M) defining non-specific binding with Ro 25,6981 (10^{-5}M) as described in section 2.2.3.

2.2.4 Analysis of Radioligand Binding Assay Data

2.2.4.1 Analysis for Competition Binding Studies

Results from the competition studies were analysed by non-linear least square regression using GraphPad Prism version 4.0 for either a one-site and a two-site binding model. The competition results were analysed by a sigmoidal dose response curve with a variable slope. To analyse one-site or two-site binding, the F-test was used to assess whether the one-site or the two-site competition model best fit the data, where $p<0.05$ was significant. The IC_{50} values for competition curves fitted to a one-site competition model were calculated from the following equation, where:-

$$y = \frac{A+(B-A)}{1+10^{(x-\log IC_{50})}}$$

A and B = the minimum and maximum percentage specific binding respectively

Y = specific binding at a fixed concentration of displacing drug

X = $\log_{10}$ concentration of the displacer

IC_{50} = concentration of the displacer which inhibits 50% of the specific binding of the radioligand.

The IC_{50} values for competition curves fitted to a two-site competition model were calculated from,

$$Y = \frac{A+(B-A)}{\left(\frac{Fraction1}{1+10^{(x-\log IC_{50}1)}}\right)+\left(\frac{1-Fraction1}{1+10^{(x-\log IC_{50}2)}}\right)}$$

Where; A, B, X and Y are as above, (1) and (2) = the high and low affinity sites for the one-site and two-site binding models, the apparent inhibition constants (K_i) were calculated using the Cheng and Prusoff equation (Cheng and Prusoff, 1973),

$$K_I = \frac{IC_{50}}{\left(1+\left(\frac{L}{K_D}\right)\right)}$$

Where:-

IC_{50} = concentration of radioligand giving 50% of the specific binding

[L] = [^{3}H] concentration

K_D = dissociation constant from saturation binding of the radioligand in forebrain membranes.

2.2.4.2 Data Analysis for Saturation Binding Studies

Results from saturation studies were analysed by non-linear least square regression using GraphPad Prism version 4.0. The saturation data were analysed by either the one-site or two-site binding hyperbola. The F-test was used to assess whether the one-site or the two-site model fit the data best where $p<0.05$ was significant.

The K_D values for saturation curves fitted to a one-site hyperbola were calculated from the following equation,

$$Y = \frac{B_{max} X}{K_D + X}$$

Where:-

Y = specific bound [^{3}H] RGH-896

X = concentration of [^{3}H] RGH-896

B_{max} = maximum number of binding sites

Saturation data was fit to the line by linear regression using GraphPad Prism for the Rosenthal transformations,

$$F(x) = ax + b$$

Where:-

F(x) = specific bound [^{3}H] RGH-896/[^{3}H] RGH-896 free

A = slope – ($1/K_D$)

x = specific bound [^{3}H] RGH-896

b = X-axis intercept (B_{max}/K_D).

2.3 Results

In order to minimise the adverse effects of NMDA receptor antagonists, it is necessary for compounds in development to be subtype selective antagonists specific to the NR2B-containing receptor. Here, we pharmacologically characterise a novel putative NR2B-selective antagonist, RGH-896. Competition binding studies determine the inhibition constant (K_i) of unlabelled compounds for receptors of interest. By measuring the K_i of various compounds, it is possible to define the pharmacology and subtype-selectivity of a range of unlabelled compounds.

2.3.1 [^{3}H] RGH-896 Competition Binding to Forebrain Membranes

Previous studies have utilised spermidine to define specific binding to NR2B-containing receptors (Hawkins *et al.*, 1999; Chazot *et al.*, 2002) in ligand autoradiography studies (see also Chapter 3). The effect of spermidine on [^{3}H] Ro 25,6981 and [^{3}H] RGH-896 binding to adult rat forebrain was investigated, defining non-specific binding using Ro 25,6981 (10^{-5}M). Results are shown in Figure 2.1. Analysis of these data using a one site competition model, shows spermidine displayed an apparent pIC_{50} of 2.16 ± 0.9 for [^{3}H] RGH-896 binding (K_i value of 5.34mM), and an apparent pIC_{50} of 3.13 ± 0.1 for [^{3}H] Ro 25,6981 binding (K_i value of 382μM).

Well washed forebrain homogenates were used and assayed in competition studies using Ro 25,6981 (10^{-11}M – 10^{-5}M) binding, defining non-specific value of [^{3}H]

RGH-896 with Ro 25,6981 (10^{-5}M). Results are shown in Figure 2.2. These data were best-fit to a one-site competition model producing a pIC_{50} of 7.8 ± 0.2 (K_i value of 11.7nM)

2.3.2 [^{3}H] RGH-896 Saturation Binding to Forebrain Membranes

Saturation binding studies were performed to determine the equilibrium dissociation constant (K_D) and the maximum number of binding sites (B_{max}) of [^{3}H] RGH-896 in well washed forebrain membranes. Saturation binding studies used [^{3}H] RGH-896 (0.5nM–80nM), and defined non-specific binding with Ro 25,6981 (10^{-5}M). Results shown in Figure 2.3 were best fitted to a one-site binding hyperbola with the corresponding Rosenthal transformation. Analysis of the saturation data using non-linear least square regression showed that [^{3}H] RGH-896 bound with a K_D of 6.5 ± 4.6 nM, and a B_{max} of 738.1 ± 45.2 fmoles/mg of protein (two repeats of the same forebrain preparation). In comparison [^{3}H] MK-801, which will bind to all NMDA receptors, displays a B_{max} of 1.8 pmoles/mg protein (Chazot *et al.*, 1993). Thus, illustrating RGH-896 is selective for a subpopulation of NMDA complexes, that is those containing NR2B subunit (41%). whereas MK-801 will bind to all major NMDA receptors (Chazot and Stephenson, 1997b).

2.3.3 [^{3}H] Ro 25,6981 Competition Binding to Forebrain Membranes

In parallel, well-washed forebrain membranes and NR1/NR2B transfected HEK 293 cell homogenates were assayed in competition studies using ifenprodil (10^{-9}M – 10^{-3}M), defining non-specific binding of [^{3}H] Ro 25,6981 with ifenprodil (10^{-3}M). Results are shown in Figure 2.4. Competition data were analysed using a sigmoidal model with a variable slope, where the F-test determines whether the one-site or the two-site competition best fit the data. These data were best-fit to a two-site competition model, comprising high- and low-affinity binding sites in the ratio 88:12 (high:low %, SD = 7), which yielded a pIC_{50}site1 of 7.14 ± 0.1 and pIC_{50}site2 of 3.89 ± 1.2 for forebrain membranes (K_i for the high affinity site 1 of 37nM). Analysis of NR1/NR2B expressed in HEK 293 cell homogenates were best-fit to a two-site competition model (n_H = -0.65 ± 0.1), comprising high- and low-affinity binding sites in the ratio 86:14 (high:low %, SD = 5), which displayed a pIC_{50}site1 of 6.88 ± 0.1 and pIC_{50}site2 of 4.44 ± 0.9 (K_i for the high affinity site of 66nM).

Competition binding studies were carried out in rat forebrain membranes using ifenprodil (10^{-9}M - 10^{-3}M), defining non-specific binding of [^{3}H] Ro 25, 6981 with RGH-896 (10^{-5}M) and [^{3}H] MK-801 with ketamine (10^{-3}M), respectively. Using [^{3}H] Ro 25,6981, these data were best-fit to a two-site competition model, containing high- and low-affinity binding sites in the ratio 41:59 (high:low %, SD = 29), which yielded a pIC_{50}site1 of 6.45 ± 0.7 and pIC_{50}site 2 of 5.05 ± 0.4 (K_i value for high affinity site of 180nM). Using [^{3}H] MK-801, data were best-fit to a two-site competition model (n_H = -0.36 ± 0.1), containing high- and low-affinity binding sites in the ratio 25:75 (high:low %, SD = 11), which displayed a pIC_{50}site1 of 6.93 ± 0.2 and pIC_{50}site2 of 4.3 ± 0.1 (K_i value for high affinity site of 150 nM) (Figure 2.5).

In the next series of experiments, competition curves were generated for unlabelled RGH-896 binding using adult rat forebrain membranes and NR1/NR2B transfected HEK 293 cell homogenates, defining non-specific of [^{3}H] Ro 25,6981 with RGH-896 (10^{-5}M) and [^{3}H] MK-801 with ketamine (10^{-3}M), respectively. In adult rat forebrain membranes, using [^{3}H] Ro 25,6981, data were best-fit to a two-site competition model (n_H = -0.91 ± 0.2), containing high- and low-affinity binding sites in the ratio 86:14 (high:low %, SD = 4), which yielded a pIC_{50}site1 of 7.82 ± 0.1 and pIC_{50}site2 of 5.45 ± 0.6 (K_i for the high affinity site of 7.8nM). In contrast, RGH 896 elicited minimal displacement of [^{3}H] MK-801 (pIC_{50} < 5.0) (Figure 2.6).

In NR1/NR2B transfected cell homogenates, using [^{3}H] Ro 25,6981, the data were best-fit to a two-site competition model (n_H = -0.56 ± 0.3), comprising high- and low-affinity binding sites in the ratio 13:87 (high:low %, SD = 5), which yielded a pIC_{50}site1 of 7.74 ± 1.5 and pIC_{50}site2 of 5.79 ± 0.3 (K_i value for high affinity site of 9.5nM). In contrast, RGH 896 elicited minimal displacement of [^{3}H] MK-801 (pIC_{50} < 5.0) (Figure 2.7).

2.3.4 [^{3}H] Ro 25,6981 Competition Binding to Compare NR1/NR2B- and NR1/NR2A/NR2B- subtype Receptors

Competition binding curves were generated using unlabelled RGH-896 and either NR1/NR2B or NR1/NR2A/NR2B co-transfected subunit combinations in HEK 293 cells, defining non-specific of [^{3}H] Ro 25,6981 with RGH-896 (10^{-5}M).

The competition curves for unlabelled RGH-896 binding using NR1/NR2B transfected HEK 293 cell homogenates were best-fit to a two-site competition model

(n_H = -0.83 ± 0.3), comprising high- and low-affinity binding sites in the ratio 18:82 (high:low %, SD = 19), which yielded a pIC_{50}site1 of 7.56 ± 1.3 and pIC_{50}site2 of 5.70 ± 0.3 p (K_i value for the high affinity site of 13.9nM). Data for unlabelled RGH-896 binding using NR1/NR2A/NR2B transfected HEK 293 cell homogenates produced competition curves which were best-fit to a two-site competition model (n_H= -0.52 ± 0.2), comprising high- and low-affinity binding sites in the ratio 46:54 (high:low %, SD = 20), which yielded a pIC_{50}site1 of 7.67 ± 0.6 and pIC_{50}site2 of 5.74 ± 0.6 (K_i value for the high affinity site of 11.1nM) (Figure 2.8).

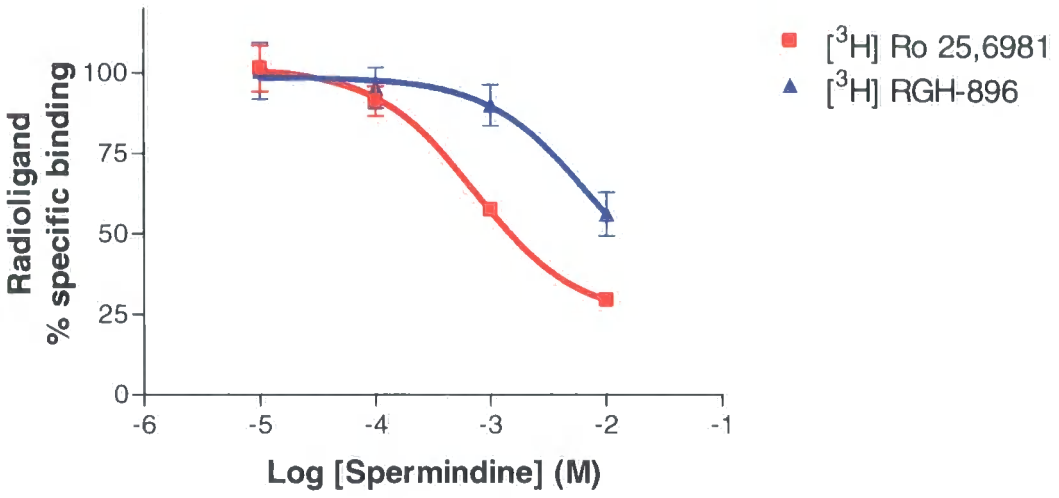

Figure 2.1: The effect of spermidine on [^{3}H] Ro 25, 6981 and [^{3}H] RGH-896 binding to adult rat forebrain membranes was investigated, defining non specific binding using Ro 25, 6981 (10^{-5}M). Results shown are mean ± standard deviation for four repeats of the same forebrain preparation.

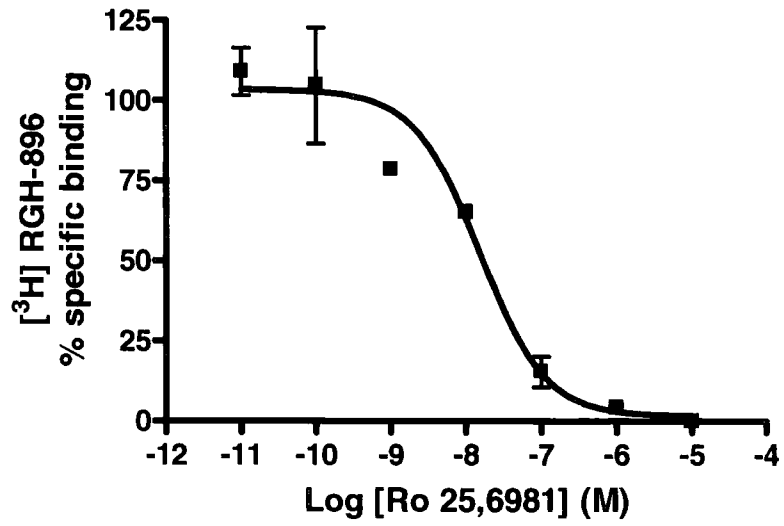

Figure 2.2: Well washed adult rat forebrain membranes were used and assayed in competition binding studies using Ro 25,6981 (10^{-11}M - 10^{-5}M), defining non-specific binding with Ro 25,6981 (10^{-5}M). These data were best-fit to a one-site competition model with an overall pIC_{50} of 7.8 ± 0.2 (K_i = 11.7 nM). Results shown are mean ± standard deviation for two repeats of the same forebrain preparation.

A

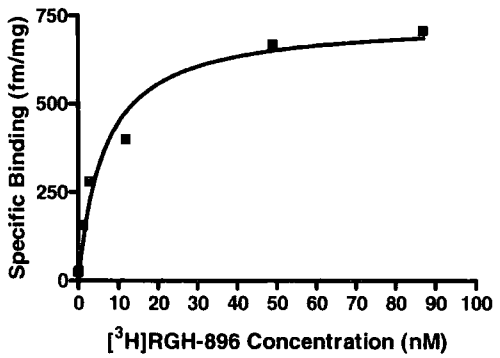

B

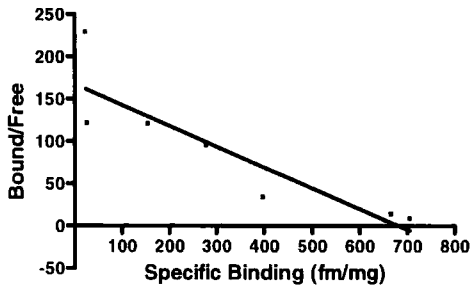

Figure 2.3: Well washed forebrain membranes were used and assayed in saturation binding studies preformed using [^{3}H] RGH-896 (0.5nM-80nM), defining non-specific binding with Ro 25, 6981 (10^{-5}M). Representative results shown are best-fit to a one-site binding hyperbola. Analysis of the saturation binding data using non-linear least square regression and hyperbola fit showed that [^{3}H] RGH-896 bound with a K_D of 6.5 ± 4.6nM and a B_{max} is 738.1 ± 45.2 fmoles/mg of protein.

A: Saturation binding curve of [^{3}H] RGH-896 binding, defining non-specific binding with Ro 25,6981 (10^{-5}M)

B: Rosenthal transformation of the saturation data

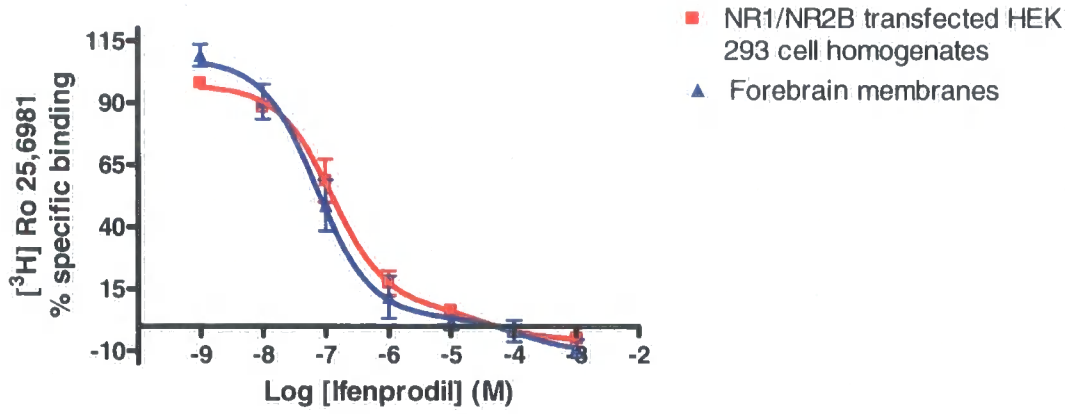

Figure 2.4: Pharmacological comparison of adult rat forebrain membranes and NR1/NR2B transfected HEK 293 cell homogenates using parallel ifenprodil competition binding studies, defining non-specific binding with Ro 25,6981 (10^{-5}M). Results shown are mean ± standard deviation for 2-5 repeats of the same forebrain preparation.

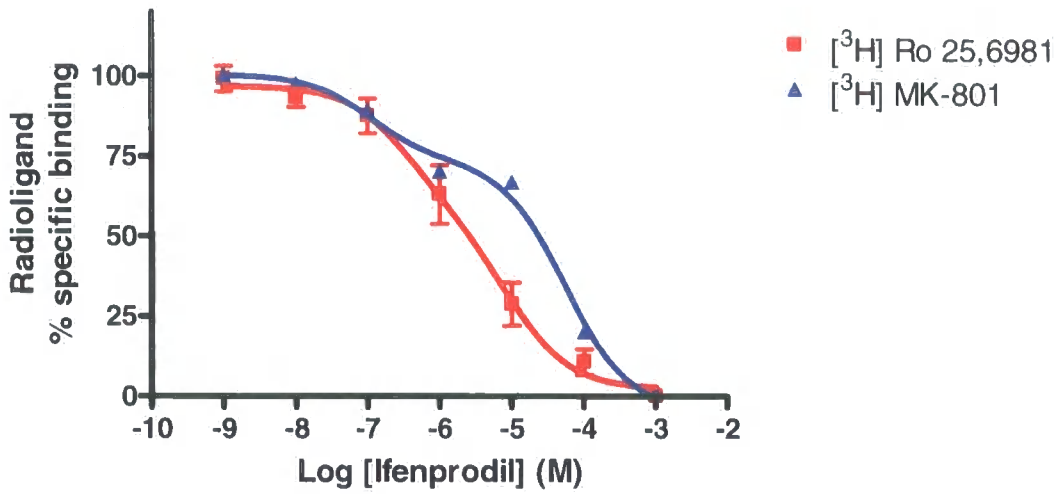

Figure 2.5: Well washed adult rat forebrain membranes were used and assayed in competition binding studies using ifenprodil (10^{-9}M - 10^{-3}M), defining non-specific binding of [^{3}H] Ro 25, 6981 with RGH-896 (10^{-5}M), and [^{3}H] MK-801 with ketamine (10^{-3}M), respectively. Results shown are mean ± standard deviation for five repeats of the same forebrain preparation.

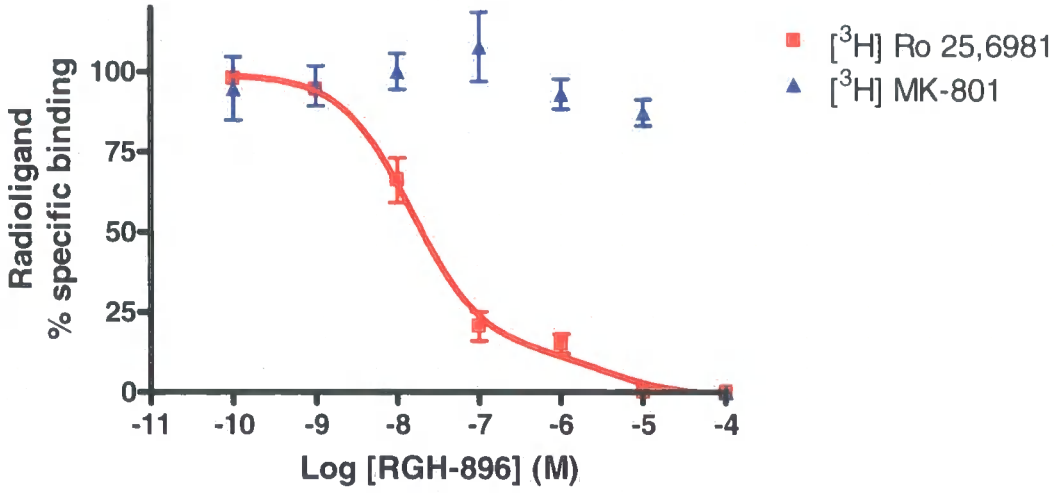

Figure 2.6: Well washed adult rat forebrain membranes were assayed in competition binding studies using RGH-896 (10^{-10}M - 10^{-5}M), defining non-specific of [^{3}H] Ro 25, 6981 with RGH-896 (10^{-5}M), and of [^{3}H] MK-801 with ketamine (10^{-3}M), respectively. Results shown are mean ± standard deviation for three repeats of the same forebrain preparation.

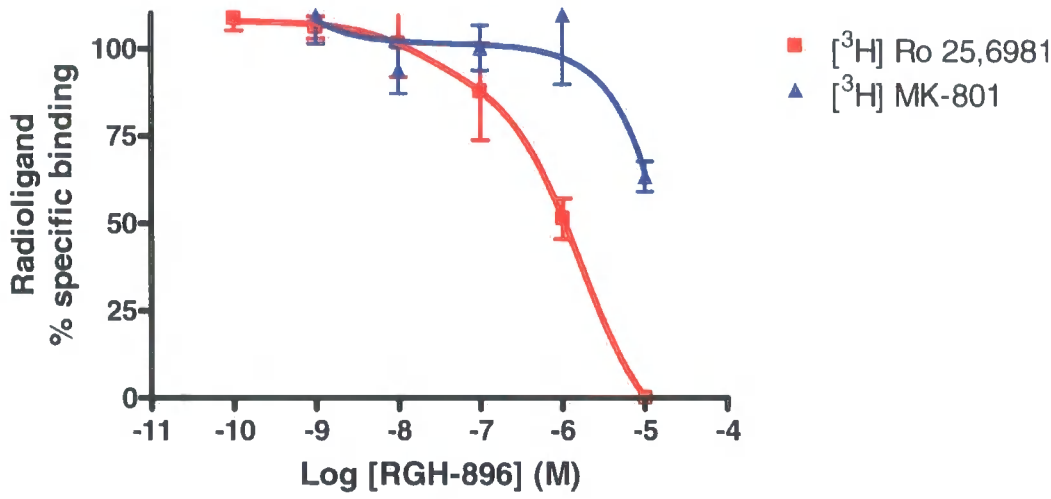

Figure 2.7: Competition curve for RGH-896 binding using NR1/NR2B transfected HEK 293 cell homogenates, defining non-specific binding of [^{3}H] Ro 25,6981 with RGH-896 (10^{-5}M), and [^{3}H] MK-801 with ketamine (10^{-3}M), respectively. Results shown are mean ± standard deviation for four repeats of the same forebrain preparation.

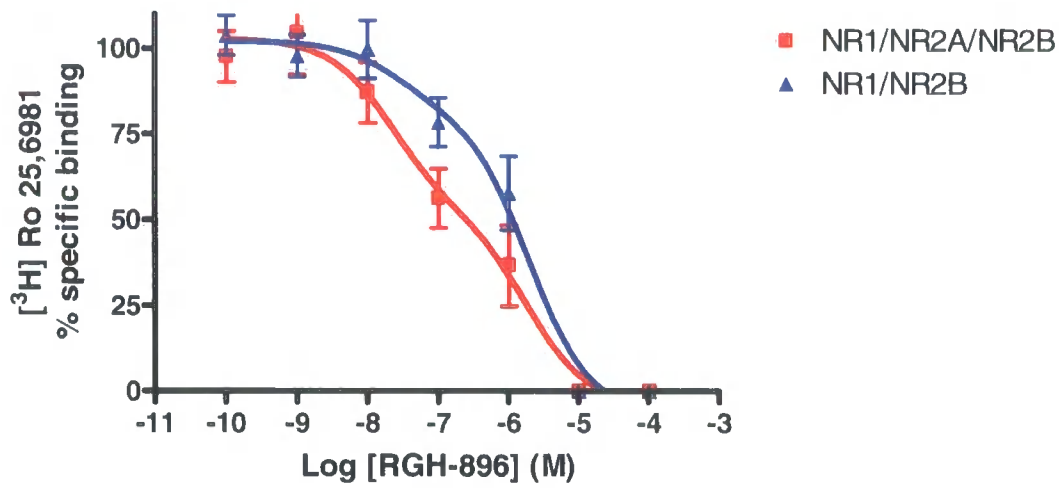

Figure 2.8: Competition curve for RGH-896 binding using NR1/NR2B or NR1/NR2A/NR2B co-transfected HEK 293 cell homogenates, defining non-specific binding of [^{3}H] Ro 25,6981 with RGH-896 (10^{-5}M).

NR1/NR2B: Results shown are mean ± standard deviation for four repeats of the same forebrain preparation. Mean K_i value for high affinity site is 13.9nM

NR1/NR2A/NR2B: Results shown are mean ± standard deviation for four repeats of the same forebrain preparation. Mean K_i value for high affinity site is 11.1nM.

3.4 Discussion

Ifenprodil was originally known as a α_1-adrenergic antagonist, but its NMDA receptor activity was discovered in the late 1980s showing that ifenprodil was a non-competitive NMDA antagonist with a novel pharmacological profile (Carter *et al.*, 1988; Reynolds and Miller, 1989). Ifenprodil displays an approximately 400-fold higher functional affinity for NR1/NR2B than NR1/NR2A containing receptors measured in the frog ooctye system (Williams, 1993) and in transfected HEK 293 cells (Gallagher *et al.*, 1996). Early development of high affinity NR2B subunit specific antagonists produced the phenylethanolamines which included Ro 25, 6981 and CP 101,606 which are structurally similar to ifenprodil (Chenard *et al.*, 1995; Brimecombe *et al.*, 1998; Mutel *et al.*, 1998; Tamiz *et al.*, 1998) (see Chapter 1). A number of high affinity ifenprodil congeners have been developed as potential subtype selective antagonists (reviewed in McCauley, 2005).

These NR2B-subtype selective groups of antagonists have potential as neuroprotectants (Di *et al.*, 1997; Kemp *et al.*, 1999; Gill *et al.*, 2002), anticonvulsants (Barton and White, 2004; Barton *et al.*, 2004), analgesics (Boyce *et al.*, 1999; Chizh *et al.*, 2001), antipsychotics (Grimwood *et al.*, 1999) and in the treatment of many CNS disorders, as they can selectively target subpopulations of NMDA receptors that are involved in specific physiological functions or specific pathologies. Excitotoxicity can result from sustained or excessive activation of NMDA receptors or from normal activation of receptors in defected neurons (Waxman and Lynch, 2005). Several phenylethanolamines, like ifenprodil, are neuroprotective *in vitro* and *in vivo* models of a variety of neurological disorders and many lack the side effects associated with non-subunit-selective NMDA antagonists (Kew and Kemp, 1998). NMDA receptor antagonists have been shown to be effective in different models of *in vitro* and *in vivo*

experimental brain injury. CP 101,606 potently inhibited glutamate-mediated toxicity in hippocampal neurons with 100-fold less effect on cultured cerebellar cells (Menniti *et al.*, 1997). *In vivo,* CP 101,606 has been shown to block 50% of initial pressure rise (4-fold above basal) and totally block the second-phase pressure increase in a rat model of intracranial pressure following head trauma (Gray, 2000).

Animal studies have indicated an important physiological role for NMDA receptors in both the induction and maintenance of neuropathic pain states (Parsons, 2001). *In vivo* studies have indicated NR2B-selective antagonists are antinociceptive properties at doses below those that impair motor coordination and elicit stimulant activity (Boyce *et al.*, 1999; Chizh *et al.*, 2001).

An additional therapeutic area that may benefit from the properties of NR2B selective antagonists is neurodegenerative diseases, for example, Parkinson's disease (PD). Intracerebral pharmacological studies in rat models of PD suggest that overactivity of NR2B-containing NMDA receptors within the striatum is responsible for mediating parkinsonism (Nash and Brotchie, 2002). Hence by selectively targeting the NR2B NMDA receptors within the striatum, NR2B antagonists could exhibit anti-parkinsonian activity, while being absent of the side effects observed with non-selective NMDA antagonists.

There are numerous NR2B selective antagonists tested pre-clinically and in clinical trial that block or reduce the activity of NMDA receptors to have therapeutic benefit for the patient.

Herein, this chapter focuses on the pharmacological properties of a novel NR2B selective ligand RGH-896, which currently represents the most advanced drug candidate in this class, using a series of radioligand binding assays.

A series of initial experiments were performed to validate the assay system to be adopted. Non-specific binding is determined by measuring radioligand binding in the presence of a concentration of unlabelled compound that binds essentially all the receptors. Previous studies have utilised spermidine to define non-specific binding of NR2B receptors (Hawkins *et al.*, 1999; Chazot *et al.*, 2002) particularly in ligand autoradiography experiments (See also Chapter 3 and 4). A series of radioligand binding results using unlabelled spermidine (10^{-5}–10^{-2} M) showed that spermidine displays a significantly lower (42-fold) affinity for the [^{3}H] RGH-896 binding site compared to the [^{3}H] Ro 25,6981 binding site indicating spermidine is overlapping the Ro 25,6981 binding site more than the RGH-896 binding site. This is surprising as spermidine has been routinely used to define non-specific binding with [^{3}H] Ro 25,6981 and [^{3}H] CP-101,606 (Hawkins, 1999; Chazot *et al.*, 2002; Sheahan and Chazot, unpublished). Interestingly, this novel finding indicates [^{3}H] RGH-896 and [^{3}H] Ro 25,6981 are binding to distinct, but overlapping sites.

Subsequent to this initial finding, Ro 25,6981 (10^{-5}M) was selected to define non-specific binding. This was based on two criteria: Ro 25,6981 displaced [^{3}H] RGH-896 with a K_i in close agreement with previous studies (Mutel *et al.*, 1998; Hawkins *et al.*, 1999; Chazot *et al.*, 2002; Sheahan and Chazot, unpublished), and the K_D value for [^{3}H] RGH-896 (K_D = 6.5nM) in adult rat forebrain membranes using Ro 25,6981 (10^{-5}M) to define non-specific binding, was in close agreement with previous unpublished Gedeon Richter preclinical studies (personal communication).

The prototypical compound, ifenprodil was investigated using a series of competition binding experiments. The ifenprodil competition curves (Figures 2.4 and 2.5), were best-fit to a two site curve using both [^{3}H] Ro 25,6981 and [^{3}H] MK-801 in both native and recombinant NR1/NR2B receptor preparations. Ifenprodil shows a similar

affinity binding for NR1/NR2B-subtype subunit (66nM) and forebrain membranes (37nM) when using [^{3}H] Ro 25,6981. This biphasic phenomenon in forebrain shows that ifenprodil can discriminate at least two subpopulations of NMDA receptors that are differentially expressed during development (Williams, 1993). The biphasic observation has also been demonstrated in hippocampal neurons (Legendre and Westbrook, 1991). Ifenprodil displays a high affinity for NR1/NR2B subtype receptors expressed in HEK 293 cell homogenates, whereas receptors containing NR1/NR2A, NR1/NR2C and NR1/NR2D subunits are all relatively insensitive to ifenprodil binding (Priestley *et al.*, 1995; Williams, 1995; Grimwood *et al.*, 1996; Varney *et al.*, 1996; Avenet *et al.*, 1997; Hess *et al.*, 1998). Ifenprodil has been shown to interact with several other types of receptors and channels including voltage dependent Ca^{2+} channels (Adeagbo, 1984; Biton *et al.*, 1995) and σ-sites (Contreras *et al.*, 1990), partially explaining the low-affinity binding site in both native and HEK 293 cells, consequently showing that ifenprodil is not ideal due to its lack of selectivity in both forebrain membranes and HEK 293 cell homogenates. This low affinity site has been detected in HEK 293 cells using other NR2B ligands, and appears not to be due to σ-sites (Chaffey & Chazot, unpublished observations). Researchers have developed novel NR2B-subtype selective antagonists based upon the structure of ifenprodil but without the affinity for many of these other sites (McCauley, 2005).

To broaden our knowledge of the properties of RGH-896, competition studies were designed to look at [^{3}H] MK-801 binding and [^{3}H] Ro 25,6981 binding in both rat forebrain membranes and NR1/NR2B transfected HEK 293 cell homogenates, simultaneously. Using rat forebrain membranes, [^{3}H] Ro 25,6981 is highly sensitive to RGH-896, whereas [^{3}H] MK-801 is insensitive to RGH-896. In comparison,

competition binding studies showed comparable displacement by ifenprodil of [^{3}H] MK-801 and [^{3}H] Ro 25,6981 binding (Figure 2.5). Displacement curves in both cases were best fit to a two site competition model, displaying a high and low affinity binding sites with similar respective affinities. The contrasting allosteric coupling to the MK-801 binding site displayed by ifenprodil and RGH-896 indicate further evidence for a fundamental difference in the binding sites of the NR2B-selective ligand family. Future experiments are required to assess allosteric sensitivity of RGH-896 using shorter sub-equilibrium binding timepoints. Further novel NR2B ligands show similar effects to RGH-896 (Chaffey & Chazot, unpublished), indicating a common property for some members of this class of ligand.

Following on from studies in rat forebrain, RGH-896 was tested in recombinant homogenates using NR1/NR2B and NR1/NR2A/NR2B transfected HEK 293 cells. All data for competition studies using unlabelled RGH-896 were best-fit to a two-site competition model comprising of a high- and a low-affinity binding site. The high-affinity site is presumably binding NR1/NR2B-containing receptors (pIC_{50}site1 = 7.56), whereas the low affinity site (pIC_{50}site2 = 5.70) is likely to be binding non-NR1/NR2B-containing receptors, as discussed previously. This was confirmed using untransfected HEK 293 cell homogenates (not shown). These data together suggest RGH-896 (10^{-6}M) is the appropriate concentration to define specific binding in future experiments. Competition studies displayed an apparent very similar high affinity of RGH-896 for NR1/NR2B receptors (pIC_{50} = 7.56) and NR1/NR2A/NR2B receptors (pIC_{50} = 7.67) in transfected HEK 293 cell homogenates. These data suggest that RGH-896 displays little selectivity for NR1/NR2A/NR2B receptors in comparison to NR1/NR2B receptors. It should be noted that when expressing multiple subunits in HEK 293 cells that a complex mixture of receptor combinations are produced. In

order to **directly** measure the affinity of RGH-896 for NR1/NR2A/NR2B subtype, an immunopurification strategy was employed, which is described in Chapter 3.

In conclusion, the novel findings in this chapter indicates [^{3}H] RGH-896 and [^{3}H] Ro 25,6981 are binding to distinct, but overlapping sites due to [^{3}H] RGH-896 been insensitive to spermidine. The contrasting allosteric coupling to the MK-801 binding site displayed by ifenprodil and RGH-896 indicate further evidence for a fundamental difference in the binding sites of the NR2B-selective ligand family. RGH-896 is similar to Ro 25,6981, as these data suggest that RGH-896 displays little selectivity for NR1/NR2A/NR2B receptors in comparison to NR1/NR2B receptors.

Chapter 3

Immunopurification and Pharmacological Characterisation of Recombinant NR1/NR2A & NR1/NR2A/NR2B Subtypes Expressed in HEK 293 Cells

3.1 Introduction

Antibodies are used routinely in research to probe for specific interactions of proteins due to their unique structure. They consist of two identical domains to form the arms of the 'Y'-structure, where the third domain forms the base of the 'Y'-structure. The two domains that carry the antigen binding sites are known as Fab fragments, and the protein domain that is involved in immune regulation is termed the Fc fragment. The two heavy-chain polypeptides in the 'Y'-structure are identical and are approximately 55kDa. The two light-chain polypeptides are also identical but are around 25kDa in size. One light chain associates with the amino-terminal region of one heavy chain to form an antigen binding domain. The carboxy-terminal region of the two heavy chains fold together to form the Fc domain. The four polypeptide chains are held together by disulfide and noncovalent bonds (Figure 3.1).

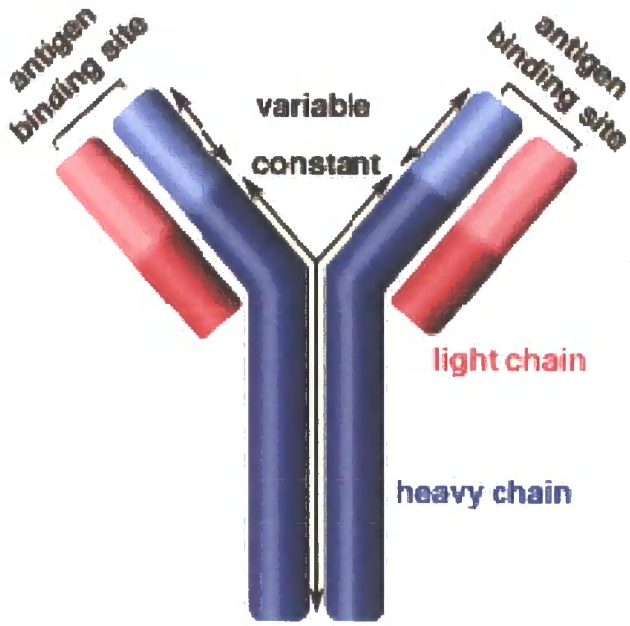

Figure 3.1: Antibody binding domains

Due to their unique structure, antibodies are very useful as selective tools to study the structure and function of biological macromolecules as they recognise a specific antigen unique to its target. By using immunoprecipitation or immunopurification strategies, the subunit composition of native receptors can be delineated and quantified (e.g. Chazot and Stephenson, 1997b).

In situ hybridisation studies have shown NMDA receptor subunit mRNAs have distinct distribution patterns in adult brain as well as during development (Watanabe *et al.*, 1993). Receptor autoradiography studies identified four pharmacologically distinctive native NMDA receptor subtypes where the anatomical distribution matched the distribution of mRNA encoding NR2A-NR2D (Buller *et al.*, 1994). The heterogeneity of the NMDA receptor was first suggested by *in situ* hybridisation which showed mRNA expression of NMDA receptors where the NR1 subunit is expressed throughout the brain, whereas NR2 subunits are co-localised in various brain regions (Wenzel *et al.*, 1995). Colocalisation of receptors is not definitive proof that two subunits actually coexist within the same receptor molecule. Sheng *et al* (1994) were the first group to use an immunoprecipiation technique, to demonstrate using NMDA receptor subunit-specific antibodies, that NR1 and NR2 subunits do coexist in developing and adult brains, although this study did not show the exact composition of the complexes. Many studies implied the co-existence of NR2A and NR2B together with NR1, but it was still not proved until Chazot and Stephenson (1997b) displayed direct co-association of NR1, NR2A and NR2B subunits in an NMDA receptor subpopulation of adult mammalian brain using a double immunopurification/immunoprecipitation strategy.

Further characterisation of the receptor co-existence has looked at studies involving

pharmacological and physiological properties of recombinant NMDA receptors using radioligand binding techniques and single channel recordings. In 1993, Cik *et al*, described the optimal conditions for expression in mammalian HEK 293 cells of NMDA receptor subtypes, in particular, NR1 and NR2A. These optimal conditions looked at a time course for transfection and the ratio of cDNA required to achieve maximal transfection levels. Co-transfection of mammalian cells with pCISNR1, NR2A and NR2B cDNA produces a heterogeneous mix of NR1/NR2A, NR1/NR2B and NR1/NR2A/NR2B subtype receptors (Brimecombe *et al.*, 1997) which are difficult to study individually.

Many functional studies have looked at the selectivity of various NR2B-subtype selective NMDA antagonists versus simple dimeric NMDA receptor subtypes expressed in cell lines. A study by Hawkins *et al* (1999) showed [^{3}H] Ro 25,6981 binds to both NR1/NR2B and NR1/NR2A/NR2B subtype receptors with similar high affinities (K_D = 10.5 ± 1.7nM and 10.9 ± 1.2nM, respectively), suggesting Ro 25,6981 binds to **all** NMDA receptors containing the NR2B subunit. A later study by Chazot *et al* (2002) suggested that [^{3}H] CP-101,606 binds only to NR1/NR2B subtype receptors, but not to NR1/NR2A or NR1/NR2A/NR2B subtype receptors. This indicates that CP 101,606 is affected by the presence of other NR2-type subunits within the complex.

This chapter describes the development and characterisation of a panel of anti-NR2A specific antibodies which will be utilised to produce an anti-NR2A immunoaffinity column, essentially as described by Chazot *et al* (2002). The immunoaffinity column will be validated through solubilisation and immunopurification of NR1/NR2A receptors expressed in HEK 293 cells. In order to investigate the selectivity of the novel NR2B-selective antagonist RGH-896 described in Chapter 2, using a

recombinant approach, pCISNR1, NR2A and NR2B cDNA subunits will be expressed in HEK 293 cells. To isolate the NR1/NR2A/NR2B from NR1/NR2B receptors following triple subunit-transfection, we will utilise an immunopurification strategy with a novel anti-NR2A (1381-1394) immunoaffinity column. Anti-NR2A (1381-1394) correlates to the amino acid sequence, i.e. the peptide from which the antibody is derived. The antibody will then bind to this region of the receptor subunit. To establish the pharmacological properties of this novel compound RGH-896, isolated NR1/NR2A/NR2B will be analysed using a radioligand binding technique to determine directly the affinity of RGH-896 for this NMDA trimeric subtype.

3.2 Methods

3.2.1 Production of anti-NMDAR2A Antibody

3.2.1.1 Peptide Conjugation by means of the Glutaraldehyde Method

This method was adopted to cross-link the anti-NR2A peptide, KRCPSDPYKHSLPSQ (corresponds to amino acids 1381-1394), to the carrier protein by a reaction with the N-terminus of the peptide using thyroglobulin as a carrier protein previously described by Chazot and Stephenson (1997a). Equal amounts (4mg) of thyroglobulin and peptide were dissolved in 2mL 0.1M sodium hydrogen carbonate buffer, containing freshly thawed 0.05% (v/v) gluteraldehyde. The peptide-carrier protein complex was incubated at room temperature in a glass test tube for 16 hours with vigorous shaking. The addition of 200μL 1M glycine ethyl ester, pH 8.0 terminated the reaction and was left to stand at room temperature for 30 minutes. The peptide-carrier protein conjugate was separated from the uncoupled peptide by dialysis against phosphate buffered saline (PBS) (10mM sodium hydrogen phosphate, 1.7mM potassium hydrogen phosphate, 137mM sodium chloride, 107mM potassium chloride, pH 7.4) for 4 hours at 4°C with hourly 500mL buffer changes. The dialysed peptide-protein conjugate was diluted with PBS to a final concentration of 1mg/mL and stored in 100μL aliquots at -20°C until use.

3.2.1.2 Inoculation Procedure

A vial (100μL) of freshly thawed conjugated peptide-protein carrier was added to 200μL of sterile PBS and emulsified with an equal volume (300μL) of Freunds complete, using a wide bore needle and syringe. The preparation was injected intramuscularly into both hind legs of a female New Zealand White rabbit. Initial immunisation was performed with Freunds complete, whereas, subsequent immunisations, at 1 month intervals, were performed with Freunds incomplete. The rabbit was bled from the marginal ear vein 7-10 days following booster injections, where 10-15mL blood was collected. Blood was allowed to stand at room temperature for 2 hours and clot contraction was allowed to occur for 16 hours at 4°C. The cellular material was removed by centrifugation at 12,000 x g for 10 minutes at 4°C. The remaining serum was stored at -20°C in 1mL aliquots.

3.2.1.3 Production of a Peptide Affinity Column

The production of a peptide affinity column is used to imitate the coupling of the peptide to the carrier protein. When using a peptide-carrier protein conjugate to raise an antibody, high non-specific binding can cause a problem. It is therefore essential to carry out affinity purification of the anti-peptide antibodies from the resultant antiserum to remove the anti-carrier protein antibodies.

3.2.1.3.1 Coupling of Peptides to Sepharose Beads via Primary Amine Groups

0.35g of activated CH-sepharose was allowed to swell in 100mL water for 15 minutes at room temperature. The swollen sepharose was then placed on a sintered glass filter and washed with 1mM HCl (100mL) at 4°C. The sepharose was equilibrated with 0.1M sodium hydrogen carbonate pH 8.0, containing 0.3M sodium chloride (25mL), and transferred to a capped tube in 1mL equilibration buffer. 1mL of 5mg/mL peptide dissolved in equilibration buffer was added to the sepharose and incubated for 1 hour at room temperature with gentle mixing. The reaction was terminated by placing the sepharose on a sintered glass filter and washing with equilibration buffer (25mL). The sepharose was returned to a capped tube and all remaining active groups were blocked by incubation with 0.1M Tris-HCl pH 8.0, containing 0.5M sodium chloride (3mL) for 1 hour at room temperature with gentle mixing. The sepharose was washed 4 times each and alternately with 0.1M acetic acid, pH 4.0, containing 0.5M sodium chloride, and 0.1M Tris-HCl pH 8.0, containing 0.5M sodium chloride. The sepharose was then poured into a 25mL column, washed with PBS (20mL) and stored in PBS containing 0.02% (w/v) NaN_3, at 4°C until use.

3.2.1.4 Peptide Affinity Antibody Purification

The peptide column was washed with 100mL Tris Buffered Saline (TBS) (50mM Tris, 0.9% (w/v) sodium chloride, pH 7.4). Serum (3-4mL) was added to the column and was gently shaken at room temperature for 2 hours. The unbound serum was collected and frozen at -20°C for further analysis. The column was washed under

gravity with 50mL TBS. The bound fractions were eluted with 50mM glycine (pH 2.3) and quenched with 2M Tris to neutralise the elutant. The absorbance of the collected fractions were measured at O.D. λ = 280nm using a spectrophotometer. The peak fractions were pooled together before dialysis using TBS over night at 4°C. The collected dialysate was measured at O.D. λ = 280nm. The concentration of the antibody in mg/ml was calculated using the Beer Lambert Law,

$$C = \frac{A}{\epsilon L}$$

where,

C = concentration of antibody

A = absorbance of the antibody at λ = 280nm

ϵ = molar extinction coefficient

L = 1cm path length

The column was regenerated with 50mL TBS and stored in TBS supplemented with 0.02% (w/v) NaN_3 at 4°C until further use.

3.2.2 Screening of the anti-NMDA Antibodies using SDS-PAGE Electrophoresis and Immunoblotting

The technique of immunoblotting was described by Chazot & Stephenson (1997b).

3.2.2.1 Preparation of the Gel

The resolving acrylamide gel (7.5%) was prepared by mixing 3mL running gel buffer (1.5M Tris, 8mM EDTA, pH 8.8 containing 0.4% (w/v) SDS), 3mL 30% acrylamide/Bis-acrylamide solution, 6mL dH_2O, 6μL N,N,N′,N′-Tetramethylethylenediamine (TEMED) & 60μL 10% (w/v) ammonium persulphate (APS). The polyacrylamide solution was immediately poured into a Hoefer™ Dual Gel Caster using 10 x 10 cm plates with 1mm spacers. Approximately 100μL of saturated butanol was added to smooth the top of the gel. Gels were covered with parafilm and were allowed to polymerise for 1-2 hours. Gels were stored into tissue paper soaked with electrode buffer pH 8.8 (50mM Tris, 384mM glycine, 1.8mM EDTA, pH 8.8 containing 0.1% (w/v) SDS,) at 4°C, until use.

3.2.2.2 Chloroform/methanol Preparation of Gel Samples for SDS-PAGE

A given amount of protein sample (100μg) was prepared and made up to a volume of 100μL in an eppendorf. To this, 4 volumes of methanol were added before vortexing and pulsing up to 13,000 rpm at 4°C. Chloroform (1 volume) was added, vortexed and pulsed to 13,000 rpm at 4°C. Distilled water (3 volumes) was added, vortexed and centrifuged for 1 minute at 13,000 rpm at 4°C. The samples were carefully placed on ice and the top layer was removed making sure not to disturb the intermediate phase of the sample. To this, 1 volume of methanol was added, vortexed and centrifuged for 4 minutes at 13,000 rpm at 4°C. The supernanent was removed and the remaining pellet was left to dry for 30 minutes. The dried protein samples

were prepared for SDS-PAGE by resuspending the protein pellet in 5μL sample buffer (30mM sodium hydrogen phosphate, 30% (v/v) glycerol, 0.05% (v/v) bromophenol blue, pH 7.0 containing 7.5% (w/v) SDS), 8μL dH_2O and 2μL (100mM) DTT, giving a final volume of 15μL. The samples were boiled at 95°C for 5 minutes, before pulsing at 6,000 rpm and vortexing to ensure the samples are evenly mixed. The samples were now ready for analysis by SDS-PAGE.

3.2.2.3 SDS-PAGE

The set gel was clamped into a Hoefer™ Mighty Small II vertical slab SE260 unit. The stacking gel was prepared by mixing 2.3mL dH_2O, 0.65mL 30% acrylamide/Bis-acrylamide solution, 1mL stacking gel buffer (0.5M Tris, 8mM EDTA, pH 6.8 containing 0.4% (w/v) SDS,), 5μL TEMED & 80μL APS. The polyacrylamide solution was immediately poured onto the set gel and 10-well comb was inserted into the stacking gel. Once the stacking gel was polymerised, the comb was removed and the wells were washed with water. Electrode buffer was poured into the wells and in the base of the unit. Protein samples (15μL) and pre-stained standards (protein molecular weight range 200-6.5 kDa, Sigma) were loaded into the wells using a Hamilton syringe. Electrophoresis was carried out at a starting current for 30 minutes of 10mA, increasing to 15mA, until the dye-front reached the bottom of the gel.

3.2.2.4 Immunoblotting

Following SDS-PAGE, the proteins from the gel were transferred onto nitrocellulose membrane in a transfer cassette. The cassette was set up on the white side with sponge, 2 pieces of blotting paper, nitrocellulose membrane, gel, and 2 pieces of blotting paper and sponge, which had all been pre-soaked in transfer buffer (25mM Tris, 192mM glycine, 20% (v/v) methanol) and all bubbles had been removed by rolling each layer with a test tube. The sandwiched cassette was placed into a Hoefer™ TE series Transphor transfer tank filled with transfer buffer to transfer the proteins to the nitrocellulose membrane at a voltage of 50V for 2.5 hours at room temperature.

Following the transference of proteins, the nitrocellulose membrane was incubated in 10mL blocking buffer (5% (w/v) dried milk, 0.2% (v/v) Tween 20, in TBS supplemented with 50μL 2M sodium hydroxide per 50ml buffer) for 1 hour at room temperature with gentle shaking. The appropriate affinity-purified primary antibodies were diluted in incubation buffer (2.5% (w/v) dried milk in TBS) to specific concentrations (0.5-2 μg/mL) and incubated overnight at 4°C with gentle shaking. Following incubation, the nitrocellulose was washed 4 x 10mL wash buffer (2.5% (w/v) dried milk, 0.2% (v/v) Tween 20 in TBS) every 10 minutes with gentle shaking at room temperature. The nitrocellulose membrane was incubated with horseradish peroxidase (HRP) labelled secondary antibody (dependent upon the species the primary antibody was raised in) at a dilution of 1:2000 in 10mL incubation buffer at room temperature for 1 hour with gentle shaking. The unbound secondary antibody was removed by a series of 4 x 10mL wash buffer every 10 minutes at room temperature with gentle shaking. After washes, the nitrocellulose membrane was

rinsed with TBS to remove any excess wash buffer. Immunoreactive bands on the nitrocellulose membrane were developed in a developing solution (68mM p-coumaric acid (100µL), 1.25mM luminol (10mL), 30% hydrogen peroxide (6µL)) for 1 minute at room temperature. The drained immunoblot was wrapped in cling film and taped into a developing cassette. Exposure times (1-5 minutes) to Hyperfilm™ differed depending upon the intensity required. The film was developed in Kodak Polymax RT developer and replenisher and fixed in Kodak Polymax RT fixer and replenisher at room temperature.

Following peptide affinity purification of anti-NR1 (17-35 Cys) (**A**), anti-NR2A (1381-1394) (**B**) and anti-NR2B (40-60) (**C**), the specificity and optimum concentration (0.5-1µg/mL) of these antibodies were determined (Figure 3.2) prior to use in immunopurification studies later in this chapter. The lower molecular weight species are likely to be proteolytic fragments.

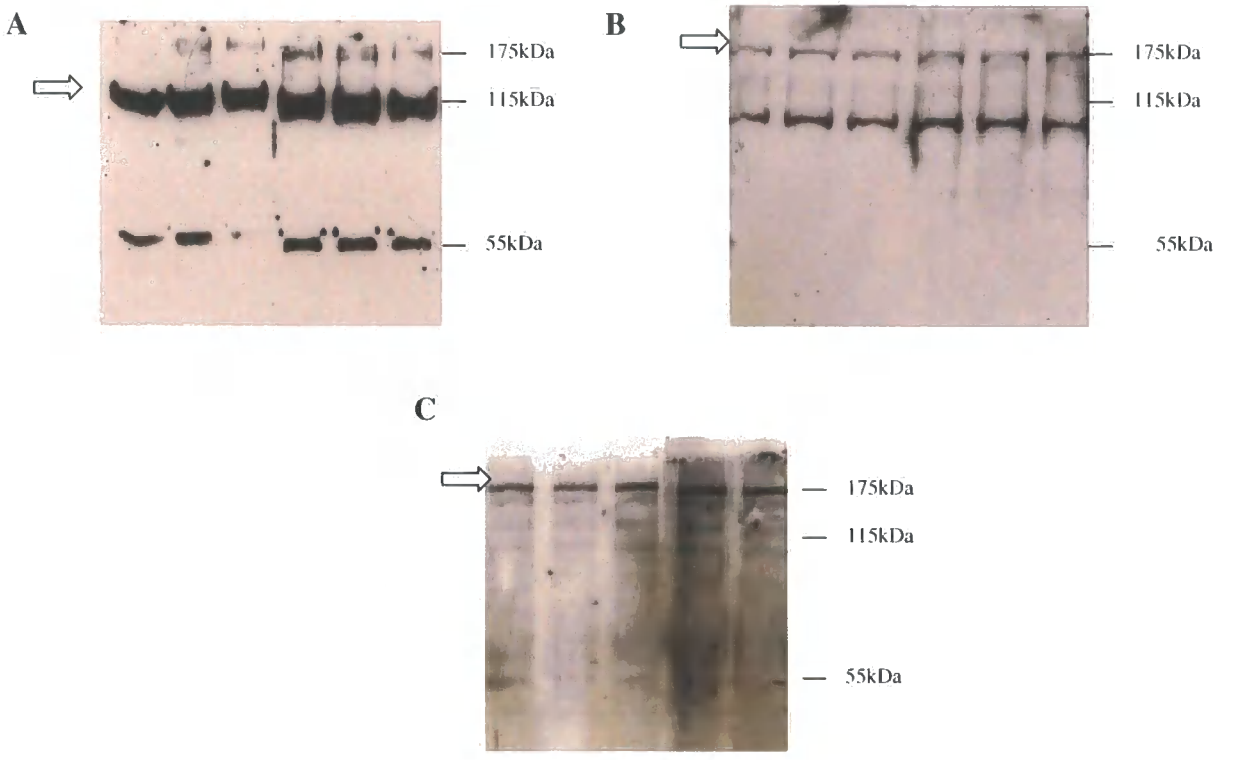

Figure 3.2: Peptide affinity purification of anti-NR1 (17-35 Cys) (**A**), anti-NR2A (1381-1394) (**B**) and anti-NR2B (40-60) (**C**).

3.2.3 cDNA Preparation of Mouse pCISNR1, pCISNR2A and pCISNR2B

3.2.3.1 Transformation of Competent *E-coli* Cells

This method of transformation was performed essentially by Dagert and Ehrlich (1979). A frozen aliquot (100μL) of HB101 competent cells from -80°C stocks were thawed on ice for 5 minutes. The stock cDNA (1μg/μL) was diluted with sterile water to a final concentration of 20ng/μL. The HB101 competent cells (100μL) were gently mixed with plasmid DNA (10μL) and were incubated on ice for 30 minutes. The cell mixture was given a heat shock by placing in a 42°C water bath for 1 minute and returning on ice for a further 2 minutes. To the mixture, 900μL Luria Bertani (LB) Broth media containing ampicillin (50μg/mL), was added to the transformed cells and was incubated on an orbital shaker at 250 x g for 1 hour at 37°C. The cell suspension was plated onto culture plates (47g LB Broth containing ampicillin (50μg/mL) and 1.5% (w/v) solid agar) and was incubated at 37°C for 18-20 hours in an inverted position.

3.2.3.2 Amplification and Purification of Plasmid DNA

3.2.3.2.1 Preparation of Small Scale Culture of Plasmid DNA

LB Broth (10mL) containing ampicillin (50μg/mL) was added to a sterile 50mL centrifuge tube. One colony from the culture plate was isolated using a sterile loop and added to the LB Broth. This small culture was incubated for 18-20 hours in an orbital shaker at 250 x g at 37°C.

3.2.3.2.2 Glycerol Stocks of Transformed Competent *E-coli* Cells

LB Broth (500μL) containing 50% (v/v) sterile glycerol and ampicillin (50μg/mL) was added to 500μL of the small overnight culture. This cell culture mixture was immediately aliquoted to a cryogenic vial and stored at -80°C until further use.

3.2.3.2.3 Preparation of Large Scale Culture of Plasmid DNA

LB Broth (500mL) containing ampicillin (50μg/mL) was inoculated with 3mL of small overnight culture in a sterile 500mL flask. This large scale culture was incubated for 18-20 hours in an orbital shaker at 250 x g at 37°C.

3.2.3.3 Harvesting the Large Scale Culture and Purifying the Plasmid DNA using QIAGEN™ Plasmid Maxi Kit

The large overnight culture was transferred into two ice-cold centrifuge tubes and centrifuged at 6,500 x g for 10 minutes at 4°C. The supernanent was discarded and the pellet was resuspended into ice-cold P1 buffer (10mL). The bacteria containing plasmid was lysed by the addition of P2 buffer (10mL) with gentle inversion and was incubated at room temperature for 5 minutes. The mixture was neutralised with ice-cold P3 buffer (10mL) by gentle inversion and was incubated on ice for 20 minutes. The mixture was centrifuged at 14,000 x g for 30 minutes at 4°C. The clear lysate was removed and placed in a fresh tube. A QIAGEN™ 500 tip was equilibrated with QBT buffer (10mL) and the lysate was gently poured into the column and allowed to

pass through under gravity. The column was washed twice with QC buffer (2 x 3mL), followed by the addition of QF buffer (15mL) to elute the plasmid DNA. Ice-cold isopropanol (0.7 Vol) (10.5mL) was added to the eluted DNA, before centrifugation at 14,000 x g for 30 minutes at 4°C. The remaining pellet was washed with ice-cold ethanol (1mL) and left to air dry for 30 minutes. The purified DNA was dissolved in TE buffer (500μL) (10mM Tris, 1mM EDTA, pH 8.0) and stored at 4°C until the purity and the yield of DNA was determined.

3.2.3.4 Quantification and Determination of the Purity of DNA Yield

The purity and concentration of the plasmid DNA was determined by measuring the optical density (O.D.) at λ=260nm and λ=280nm (Sambrook *et al.*, 1989) against TE Buffer. The ratio of the O.D. at λ=260nm and λ=280nm should be within the range of 1.8-2.0. The plasmid DNA concentration at λ=260nm where the O.D.=1, corresponds to approximately 50μg/mL for double stranded DNA (dsDNA). The plasmid DNA was diluted in TE buffer to a final concentration of 1μg/mL and was aliquoted into 100μL fractions and stored at -20°C until use.

3.2.4 Preparation of DMEM/F12 Medium + L-Glutamine

All procedures were performed using sterile conditions. Dulbecco's Modified Eagle Medium/F12 (DMEM/F12) 1:1 mix, containing HEPES (15mM) and L-glutamine was supplemented with 10 % (v/v) heat inactivated fetal calf serum (FCS), 40mL of 7.5 % (w/v) $NaHCO_3$ and penicillin (500I U/mL) / streptomycin (500 μg/mL) solution (20

mL). The pH of the final volume of the medium was adjusted to pH 7.6 using NaOH (10M). The medium was filter-sterilised using a 0.2μm Nalgene filter unit and stored at 4°C until use.

3.2.5 Subculturing of HEK 293 Cells

HEK 293 cells were grown in 250mL Greiner culture flasks at 37°C in 5% CO_2 in DMEM/F12 medium containing L-glutamine in a Shell Lab CO_2 incubator. The cells were subcultured weekly by the removal of the old medium and a wash with pre-warmed sterile phosphate buffered saline (PBS) (10mL). Following 1 minute incubation in trypsin-EDTA (2mL) at 37°C, DMEM/F12 medium containing L-glutamine (10mL) was added to the cells. The cells were then separated by gentle pipetting. Finally, the cell suspension (2mL) was added to a fresh flask containing 10mL of DMEM/F12 medium containing L-glutamine, which was incubated at 37°C in 5% CO_2.

3.2.6 Preparation of New Stocks of HEK 293 Cells

HEK 293 cell stocks were prepared by the addition of trypsin-EDTA (4mL) to dissociate the cells for 1 minute at 37°C and 20mL of DMEM/F12 medium containing L-glutamine was added. The cells were centrifuged at 200xg for 5 minutes at 4°C. The pellet was resuspended in DMEM/F12 medium containing L-glutamine (4.8mL) supplemented with FCS (0.6mL) and dimethyl sulphoxide (DMSO) (0.6mL). The cell suspension was immediately divided into three cryogenic vials and stored at –80°C for 34 hours and then transferred to liquid nitrogen.

For the preparation of a new culture, a single cryogenic vial of frozen HEK 293 cells was thawed at 37°C. The cells were centrifuged at 200xg for 5 minutes at 4°C and resuspended in DMEMF/12 medium containing L-glutamine (15mL). The cells were added to a tissue culture flask, which was incubated at 37°C in 5 % CO_2 and cultured.

3.2.7 Calcium Phosphate Precipitation-Mediated Transfection of HEK 293 Cells

HEK 293 cells were transfected by the calcium phosphate precipitation method (Chazot *et al*, 1999). Cells were subcultured 24 hours prior to the transfection to a density of ~$4x10^6$ cells per flask (approx 30% confluence). On the day of the procedure the medium was removed 3 hours prior to the transfection and replaced with 10mL of DMEM/F12 medium without L-glutamine (Sigma, UK). The cells were incubated at 37°C in 7.5 % CO_2. For the transfection of the cells tubes A and B were prepared. Tube A contained 440 µL 1:10 TE buffer and 10µL DNA (10µg/µL) and Tube B contained 500µL of 2xHBS buffer pCISNR1/NR2A or pCISNR1/NR2A/NR2B (1:3 or 1:3:3 cDNA ratios, respectively). Calcium chloride (2.5 M) (50 µL) was warmed to 37°C and was slowly added to Tube A and mixed vigorously. The contents of Tube A were added to Tube B at a rate of 1 drop per 5 seconds and the mixture was pipetted up and down until the solution appeared cloudy. The contents of Tube B were added slowly to the medium over HEK 293 cells and the medium was swirled to distribute the precipitate evenly. Following 3 hours incubation at 37°C at 7.5% CO_2, the medium from the cells was removed. 15% (v/v) glycerol in PBS was gently spread over the cells and incubated for 30 seconds at room temperature. The glycerol solution was removed and the cells were rinsed with

DMEM/F12 medium without L-glutamine (~5mL). Fresh DMEM/F12 medium without L-glutamine (10mL) was added to the cells and incubated at 37°C for 48 hours with a 5% CO_2 level. In the case of transfection of functional receptors, ketamine (10^{-3}M) was added to the medium to prevent receptor-mediated cytotoxicity.

3.2.8 Routine Harvesting and Membrane Preparation of HEK 293 Cells

Transfected HEK 293 cells were harvested 48 hours following calcium phosphate precipitation transfection. Homogenisation buffer (50mM Tris, 5mM EDTA, 5mM EGTA, pH7.4) (5mL) was added and the cells were scraped using Greiner cell scrapers and placed into ice-cold centrifuge tubes. The cell suspension was washed by centrifugation for 3 minutes at 3000xg to pellet the cells. The pellet was resuspended in homogenistion buffer (5mL) and homogenised using a dounce glass/glass homogeniser (~20 strokes). The homogenate was re-centrifuged for 30 minutes at 11,000rpm at 4°C. The supernatant was discarded and the cell pellet was then resuspended in ice-cold homogenisation buffer (6mL) and homogenised to a smooth suspension. The cell suspension was assayed for radioligand binding activity or was stored in 100µL aliquots at –20°C until use for immunoblotting.

3.2.9 Generation of anti-NR2A Affinity Column using ImunoPure® rProteinA IgG Plus Orientation Kit

The gel beads (1mL) were gently suspended by gentle stirring with a Pasteur pipette before allowing the storage solution to pass through the column under gravity. The

column was equilibrated with 2.5mL ImmunoPure® Antibody Binding/Wash buffer. The NR2A antibody (1mg/mL) from Bleed 2 was diluted 1:1 with ImmunoPure® Antibody Binding/Wash buffer to make a total volume of 8ml and added to the column, mixing batchwise over night at 4°C. Under gravity, the unbound antibody was allowed to pass through the column and was retained at 4°C to determine binding efficiency. The column was washed 2 x 2.5mL with ImmunoPure® Antibody Binding/Wash buffer. Cross-linking buffer was prepared by reconstituting BupH™ Buffer Pack with sterile distilled water and Disuccinimidyl Suberate (DSS) was dissolved in 500µL Dimethylsulfoxide (DMSO). The dissolved DSS was transferred to a new glass vial with the addition of 750µL cross-linking buffer. Once this solution was mixed, it was immediately pipetted onto the antibody-bound column and incubated batchwise for 1 hour at room temperature. Following incubation, the remaining solution was allowed to pass through the column before washing the gel beads with 2.5mL of cross-linking buffer. The remaining non-reacting NHS-ester (DSS) groups were blocked with the addition of 1mL of ImmunoPure® Blocking Buffer to the column with gentle mixing batchwise for 10 minutes at room temperature. The remaining solution was allowed to pass through the column under gravity prior to the incubation with 2.5mL ImmunoPure® IgG Elution Buffer mixing batchwise for 5 minutes at room temperature. The solution was passed through the column but retained at 4°C to analyse the cross-linking efficiency. The column had a series of wash steps including 1mL of ImmunoPure® IgG Elution Buffer, 2 x 2.5mL ImmunoPure® Antibody Binding/Wash buffer and 3 x 5mL 50mM diethylamine (pH 11.5), to ensure all non-covalent attached antibody was removed from the column. The column was regenerated with PBS and stored in PBS with 0.02% (w/v) sodium azide at 4°C (Figure 3.3).

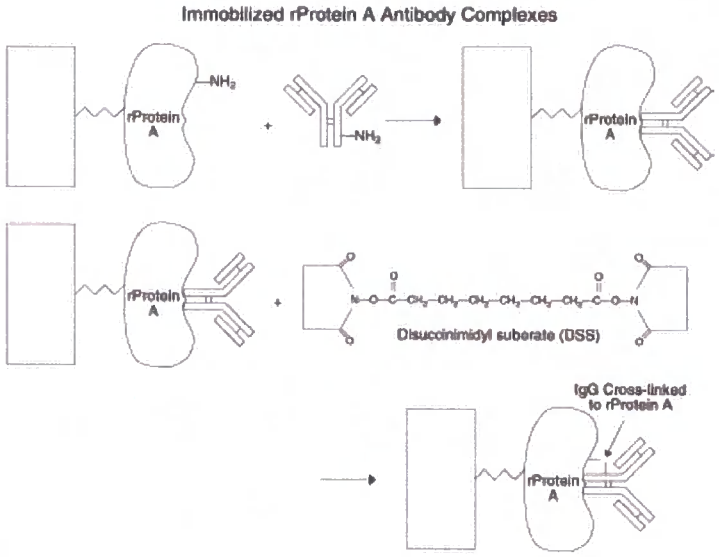

Figure 3.3: Reaction Scheme of ImmunoPure® rProtein A IgG Plus Orientation Kit (Pierce, Rockford, UK)

3.2.10 Isolation of NR1/NR2A and NR1/NR2A/NR2B Subtype Receptor from Transfected HEK 293 Cells

250mL flasks of HEK 293 cells with a confluence of 30-40% were co-transfected with pCISNR1/NR2A or pCISNR1/NR2A/NR2B to a ratio of 1:3 or 1:3:3, respectively, with a total concentration of 10μg cDNA using the calcium phosphate precipitation transfection method. Cells were harvested 48 hours post-transfection. PBS (5mL) was added and the cells were scraped using Greiner cell scrapers and placed into ice-cold centrifuge tubes. The cell suspension was washed by centrifugation for 3 minutes at 3000xg to pellet the cells. The pellet was resuspended in PBS (5mL) and homogenised using a dounce glass/glass homogeniser (~20 strokes). The homogenate was re-centrifuged for 30 minutes at 11,000rpm at 4°C. The solubilisation of the membranes was essentially described by Hawkins *et al* (1999). The supernatant was discarded and the cell pellet was then resuspended in ice-cold solubilisation buffer (0.5M sodium chloride, 50mM Tris, 1% (v/v) Triton X 100, pH 7.4) (3.3mL) to give a final protein concentration of 1.5 mg/mL. Protease cocktail inhibitors (1:100) were added to the cells and were homogenised to a smooth suspension before dividing the volume into two eppendorfs. The eppendorfs were mixed for 30 minutes at 4°C followed by centrifugation at 13,000 rpm for 5 minutes at 4°C. Supernatants were pooled with an aliquot (25μL) taken for further analysis. The pellets were resuspended in solubilisation buffer (3.3mL) and homogenised before taking an aliquot (25μL) for further analysis.

3.2.11 Purification of NR1/NR2A or NR1/NR2A/NR2B Subtype Receptor using an anti-NR2A Antibody Affinity Column

Immunopurification using the new anti-NR2A immunoaffinity column was carried out as described by Chazot *et al* (2002) (Figure 3.4). The solubilised material (from section 3.2.10) was dialysed for 2 x 1½ hours in dialysis buffer (0.45M potassium chloride, 10mM HEPES, 1mM EDTA, 0.1% (v/v) Triton X 100, 0.2% (w/v) sodium deoxycholate, pH 7.6) at 4°C. Meanwhile, the anti-NR2A immunoaffinity column was equilibrated with dialysis buffer (20mL). The dialyste was diluted to 6mL with dialysis buffer, with an aliquot (25µL) taken for further analysis. The solubilised membranes were filtered, applied to the column and re-circulated at a rate of 10mL/hour, overnight at 4°C. The unbound material was collected with an aliquot (25µL) taken for further analysis. The column was washed with dialysis buffer for 2 hours at a rate of 25mL/hour at 4°C. Fractions were eluted at a rate of 10mL/hour with elution buffer (50mM diethylamine, 0.05% (w/v) sodium deoxycholate, pH 11.5) at 4°C and immediately quenched with 2M glycine to a pH<9.0. Aliquots of the elution fractions 1-5 (100µL) were taken for further analysis. The column was regenerated with PBS and stored in PBS with 0.02% (w/v) sodium azide at 4°C.

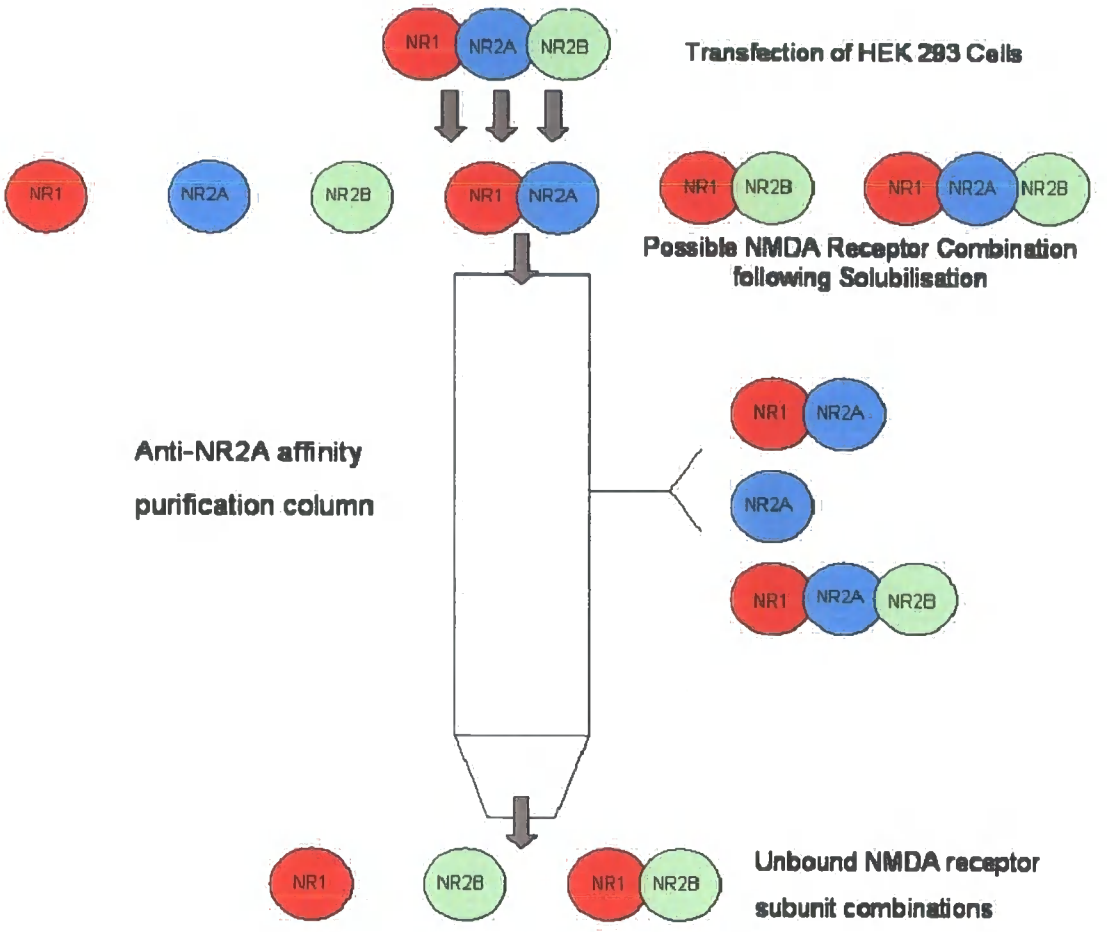

Figure 3.4: Schematic diagram of the possible NMDA receptor subunit combinations following transfection, the bound subunit combinations to the anti-NR2A affinity purification column following solubilisation and unbound NMDA receptor subunit combinations following anti-NR2A affinity purification

3.2.12 Analysis of the Solubilisation and Purification using the anti-NR2A Affinity Column

All of the aliquots retained from the immunopurification of the NMDA receptor subtypes were prepared by chloroform/methanol extraction procedure of protein precipitation (Chazot *et al.*, 1998) (see section 3.2.2.2) for SDS-PAGE (see section 3.2.2.3) and Immunoblotting (see section 3.2.2.4) analyses. The nitrocellulose membrane was probed with anti-NR1, anti-NR2A and anti-NR2B antibodies (1μg/mL) respectively, for validation of all subtype subunits been present in the starting material and the efficiency of the anti-NR2A immunoaffinity column.

3.2.13 Radioligand Saturation Binding Following Immunopurification of pCISNR1/NR2A/NR2B Transfected HEK 293 Cells

Following validation of the immunopurification of NR1/NR2A transfected HEK 293 cell homogenates, triple subunit transfection (NR1/NR2A/NR2B) was analysed. Immunopurified material (peak fractions 2 & 3) (100μL) were incubated, in duplicate, with radioligand assay buffer (25mM sodium phosphate buffer, pH 7.4), [^{3}H] RGH-896 (1.25nM - 60nM) (20μL) to a total volume of 200μL, for 2 hours at 4°C. Non-specific activity was defined using Ro 25,6981 (10^{-5}M) for [^{3}H] RGH-896 binding. The saturation binding assay was terminated and bound radioligand was collected by rapid filtration through Whatman GF/B filters, pre-soaked in 1% (v/v) poly(ethyleneimine) solution. The filters were washed (3 x 3mL) using ice-cold

10mM sodium phosphate buffer, pH 7.4, using a Brandel cell harvester. Filters were transferred into scintillation vials with Ecoscint A liquid scintillation cocktail fluid (1mL) and incubated overnight at room temperature. Bound radioactivity was quantified using Packard Tri-Carb 1600TR scintillation spectrophotometer with a counting time of 3 minutes per vial. The data was anaylsed using GraphPad Prism version 4.0. See section 2.2.4 for analysis of the radioligand binding data.

3.3 Results

3.3.1 Antibody concentration following peptide affinity purification

When using a peptide-carrier protein conjugate to raise an antibody, high non-specific binding can cause a problem. It is therefore essential to carry out affinity purification of the anti-peptide antibodies from the resultant antiserum to remove the anti-carrier protein antibodies. The production of the peptide affinity column ensured the appropriate orientation of peptide coupling to the sepharose beads which mimics the coupling between the peptide and the carrier protein in the immunogen. Following the incubation of the antiserum on the column, the column is washed and the bound antibody is eluted and pH quenched in 1 ml fractions. These fractions are analysed by measuring the OD at λ=280nm. The results of the peptide affinity purification of the anti-NR2A antibody (1381-1394) (Bleed 2) are shown in Figure 3.5. The peak antibody containing fractions (1 and 2) were pooled and dialysed against PBS. The final antibody concentration of the dialysed fractions was 1.1mg/ml. The yield of antibody from each bleed is shown below:

Bleed Number	**Yield of antibody per millilitre of serum (µg/mL)**
1	128
2	468
3	487
4	625

3.3.2. Immunoblotting Analysis of Adult Rat Forebrain Membranes with Bleeds 1, 2, 3 & 4 of the anti- NR2A Antibody

To assess the utility of the new anti-NR2A antibody from all bleeds, western blotting analysis was performed to determine if the antibody recognised the NR2A receptor using an adult rat forebrain membrane preparation. Following SDS-PAGE under reducing conditions, the nitrocellulose was probed with varying concentrations (0.5 and 1μg/mL) of affinity purified anti-NR2A (1381-1394) antibody from bleeds 1, 2, 3 & 4. The resultant immunoblot, shows a specific immunoreactive protein species with a molecular weight of M_r 180000 ± 8000 (mean ± SD, n=4) (Figure 3.6). The 180kDa species is coincident with that previously identified as the NR2A subunit (e.g. Hawkins *et al.*, 1999). In Bleed 3, another immunoreactive band is been detected at a molecular weight of M_r 120000, which may reflect a calpain proteolytic fragment. The size of the fragment matched that of fragments that can be generated should NR2 be cleaved at putative consensus sites located in the long intracellular C-terminal domain (Bi *et al.*, 1998). Affinity-purified anti-NR1 (17-38Cys) and anti-NR2B (40-60) were assessed in an identical fashion; these labelled immunoreactive species of M_r 120,000 and M_r 180,000, respectively (section 3.2.2.4), consistent with previous results (e.g. Chazot *et al.*, 1997a&b, 2002).

3.3.3 Immunoblotting Analysis of Transfected HEK 293 Cell Homogenates using the anti-NR2A (1381-1394) Antibody

Transfection protocol was optimised, and fresh cDNA preparations generated. The original stock and freshly prepared preparations of pCISNR2A cDNA were assessed by transfection into HEK 293 cells. Following harvesting, the cells were subjected to

SDS-PAGE and immunoblotting. To analyse the transfection success, the nitrocellulose was probed with the new batch of anti-NR2A (1381-1394) antibody (1μg/mL) (Figure 3.7). The resultant immunoblot showed a distinct co-incident immunoreactive band (M_r 180000) with both the original and freshly prepared preparations of pCISNR2A cDNA expressed in HEK 293 cells. Importantly, no detectable immunoreactive bands were present from cells which have subjected to transfection without cDNA present (control) HEK 293 cells (Figure 3.7, Lane 1).

3.3.4 Immunoblotting Analysis of the Specificity of the anti-NR2A (1381-1394) Antibody

To examine the specificity of the new anti-NR2A (1381-1394) antibody, SDS-PAGE under reducing conditions was performed with control transfected HEK 293 cells, NR2A transfected HEK 293 cells, NR2B transfected HEK 293 cells and forebrain membranes. The immunoblot was probed with affinity-purified anti-NR2A receptor antibody at a final concentration of 1μg/mL in the presence and absence of the respective peptide (500μg/mL).

The resultant immunoblot probed with anti-NR2A (1381-1394) receptor antibody shows no immmunoreactive band with control transfected cells and NR2B transfected HEK 293 cells, whereas there is a distinct immunoreactive band (M_r 180000) with NR2A transfected HEK 293 cells. All bands were abolished by prior incubation of the anti-NR2A receptor antibody with NR2A peptide (1381-1394) overnight at 4°C. Anti-NR2A (1381-1394) antibody displayed no immunocross-reactivity with other NMDA receptor subunits (not shown) when used against HEK 293 cells transfected, for

example, with pCISNR2B cDNA (Figure 3.8).

3.3.5 Production and Validation of anti-NR2A (1381-1394) Immunoaffinity Column

The antibody prior and post affinity column application was assayed for immunoreactivity. The binding efficiency of the anti-NR2A (1381-1394) antibody to the column was very high (94.1%) column compared to that of Hawkins *et al* (1999), where only 67 ± 18% of the anti-NR2A antibody immunnoreactivity was retained. To further analyse the efficiency of the column, the various steps and washes undertaken while producing the column were subjected to immunoblotting. The immunoreactive protein bands that are detectable in Lane 1 and Lane 2 (M_r 50000) are the heavy chain of purified antibody that was applied to the column before coupling to the sepharose beads and the unbound antibody material after coupling to the sepharose beads, respectively (Figure 3.9). Interestingly, there was no antibody elution detected which has previously been a significant problem with earlier methodologies (Chazot and Stephenson, 1997a). To validate the efficiency of the anti-NR2A immunoaffinity column, HEK 293 cells were transfected with pCISNR1/NR2A, harvested and solubilised (see section 3.2.10) before isolation by immunopurification (see section 3.2.11). The aliquoted fractions were subjected to immunoblotting and probed with the anti-NR2A (1381-1394) antibody (1μg/mL) (Figure 3.10). Elution fractions 2 and 3 were pooled and were used as a positive control for the anti-NR2A (1381-1394) antibody in subsequent experiments. A single immunoreactive species (Mr 180,000) was detected in the eluted fractions.

3.3.6 Saturation Binding Analysis using NR1/NR2A/NR2B Immunopurified Homogenates

Trimeric NR1/NR2A/NR2B immunopurified material was assayed in saturation binding studies using [^{3}H] RGH-896 (1.25nM–60nM), defining non-specific binding with Ro 25,6981 (10^{-5}M) as determined in Chapter 2. Results shown in Figure 3.11 were best fitted to a one-site binding hyperbola. Analysis of the saturation data using non-linear least square regression showed that [^{3}H] RGH-896 bound with a K_D of 7.2 ± 8.1 nM, and a B_{max} of 257 ± 67 fmoles/mg of protein (two repeats of the same forebrain preparation).

3.3.7 SDS-PAGE and Immunoblotting Analysis of NR1/NR2A/NR2B Immunopurified Homogenates

The presence of NR1, NR2A and NR2B subunits in immunopurified material was assessed by immunoblotting analysis. Incubation with anti-NR1, anti-NR2A and anti-NR2B antibody (1μg/mL) produced immunoreactive protein bands of M_r 120000 for anti-NR1 antibody, M_r 180000 for anti-NR2A and M_r 180000 for NR2B, respectively, in anti-NR2A antibody immunopurified pooled fractions.

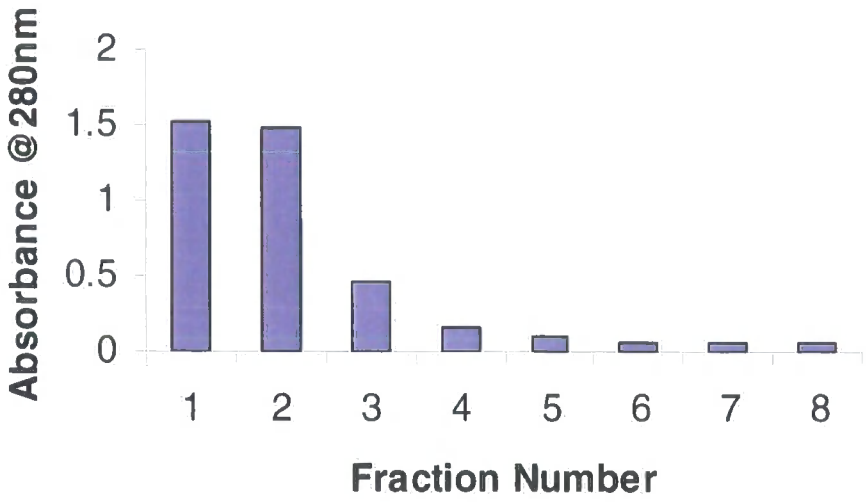

Figure 3.5: Absorbance measurements of the peptide affinity purification of anti-NR2A (1381-1394) antibody.

This graph shows the elution profile, following peptide affinity purification of anti-NR2A receptor antibody. Fractions 1 and 2 were pooled together prior to dialysis. This is a representative experiment in which 1.1mg of total antibody was purified. This purification profile was observed for all bleeds.

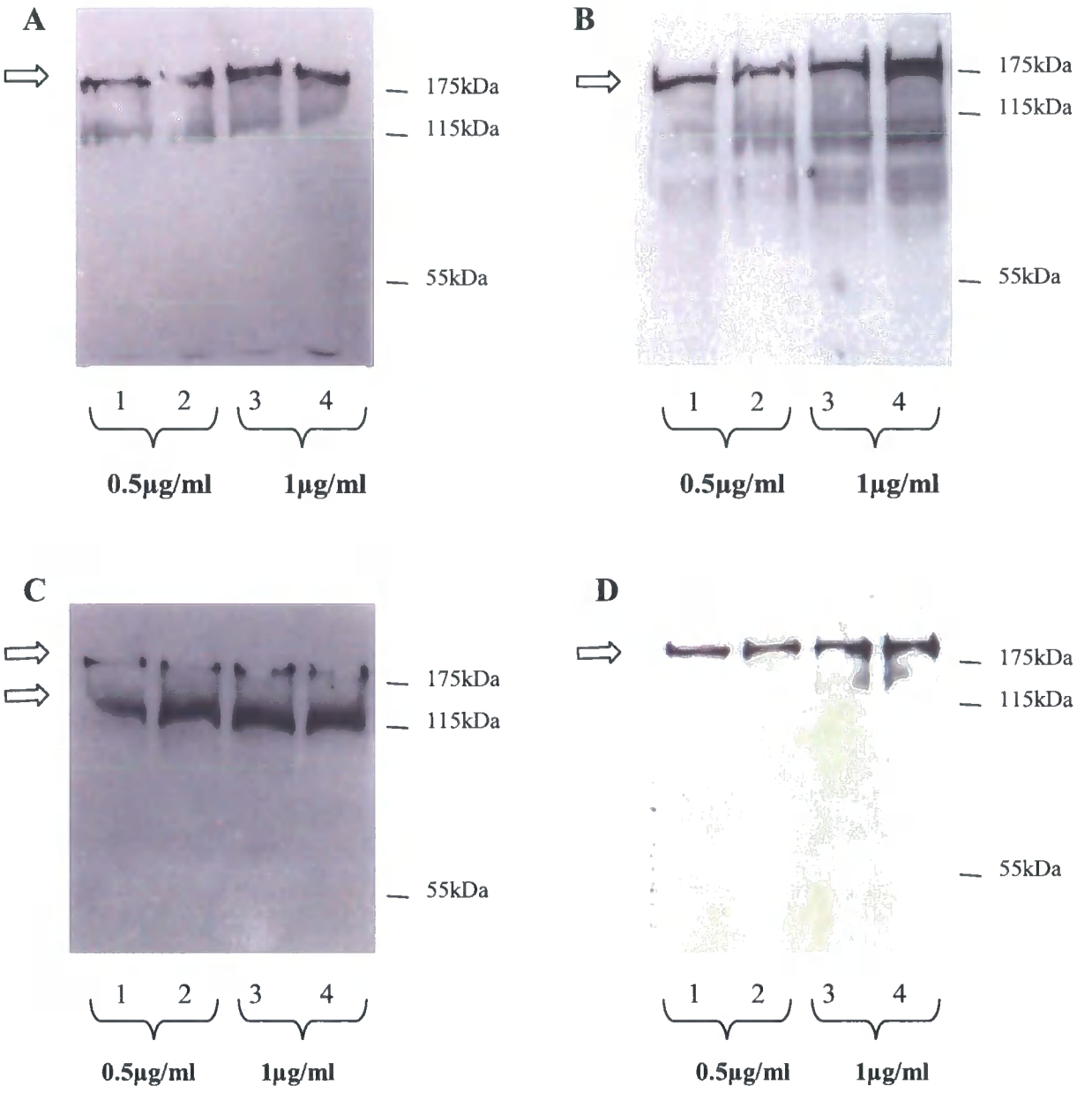

Figure 3.6: Representative immunoblot of adult rat forebrain membranes probed with Bleed 1 (A), Bleed 2 (B), Bleed 3 (C) and Bleed 4 (D) of the anti-NR2A receptor antibody at the specified concentrations. All bleeds gave an immunoreactive protein band of M_r 180000 and occasionally a smaller proteolytic species of M_r 120000 (**A** + **C**).

Lanes 1-4 Adult rat forebrain membranes (100µg protein)

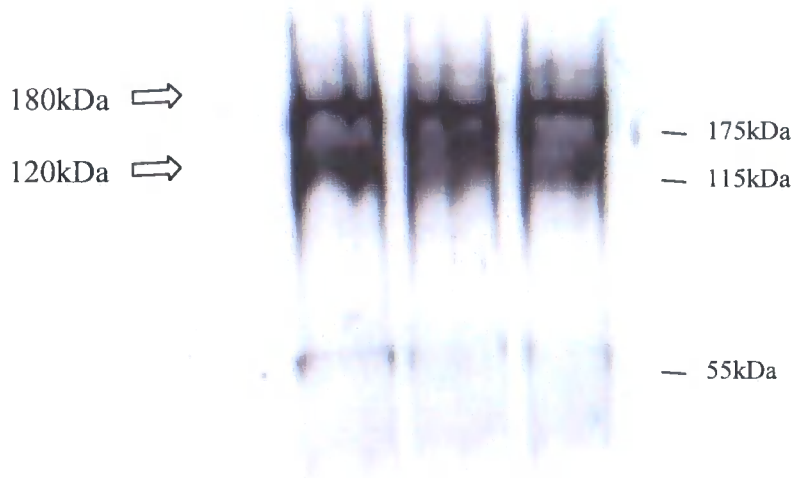

Figure 3.7: Immunoblot showing successful cDNA preparation by transfection of control, NR2A (original cDNA stock) and NR2A (freshly prepared cDNA stock from MaxiPrep)

Lane 1	Control transfected cells (100μL)
Lane 2	Original NR2A cDNA stock (100μL)
Lane 3 and 4	Freshly prepared NR2A cDNA stock (100μL)

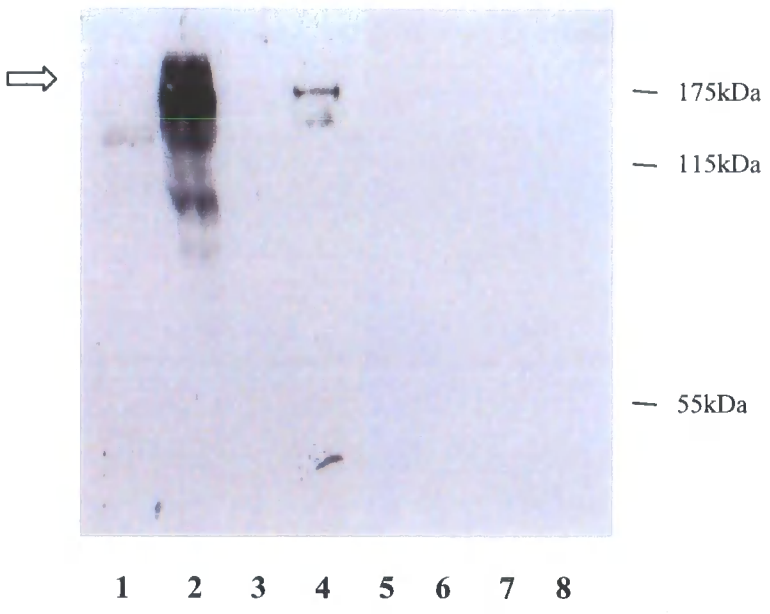

Figure 3.8: Immunoblot showing the specificity of the anti-NR2A antibody probed with affinity-purified anti-NR2A receptor antibody at a final concentration of 1µg/mL in the absence (Lanes 1-4) and presence (Lanes 5-8) of the respective peptide (1µg/mL).

Lane 1 & 5 Control transfected HEK 293 cells (100µL)
Lane 2 & 6 NR2A transfected HEK 293 cells (100µL)
Lane 3 & 7 NR2B transfected HEK 293 cells (100µL)
Lane 4 & 8 Adult rat forebrain membranes (100µg)

Figure 3.9: Immunoblot of the fractions from the production of the anti-NR2A immunoaffinity column illustrating the heavy chain of antibody at 55kDa.

Lane 1	Pure anti-NR2A antibody @ 0.55mg/ml (10.7µL)
Lane 2	Unbound antibody solution (10µL)
Lane 3	Cross-linking solution (10µL)
Lane 4	Blocking Buffer (10µL)
Lane 5	Elution Buffer (100µL)
Lane 6	Wash with Elution Buffer (100µL)
Lane 7	Diethylamine wash 1 (100µL)
Lane 8	Diethylamine wash 2 (100µL)
Lane 9	Diethylamine wash 3 (100µL)

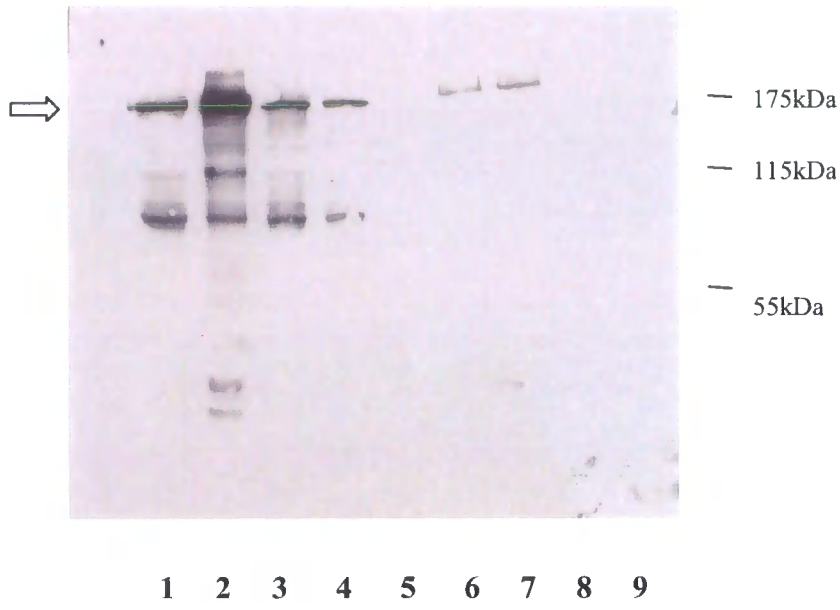

Figure 3.10: Immunoblot showing validation of anti-NR2A (1381-1394) immunoaffinity column. The immunoblot was probed with affinity purified anti-NR2A (1381-1394) (1µg/mL) yielding an immunoreactive band of M_r180000

Lane 1	Starting material (25µL)
Lane 2	Solubilised membranes (25µL)
Lane 3	Unsolubilised membranes (25µL)
Lane 4	Unbound protein (25µL)
Lane 5	Elution fraction 1 (100µL)
Lane 6	Elution fraction 2 (100µL)
Lane 7	Elution fraction 3 (100µL)
Lane 8	Elution fraction 4 (100µL)
Lane 9	Elution fraction 5 (100µL)

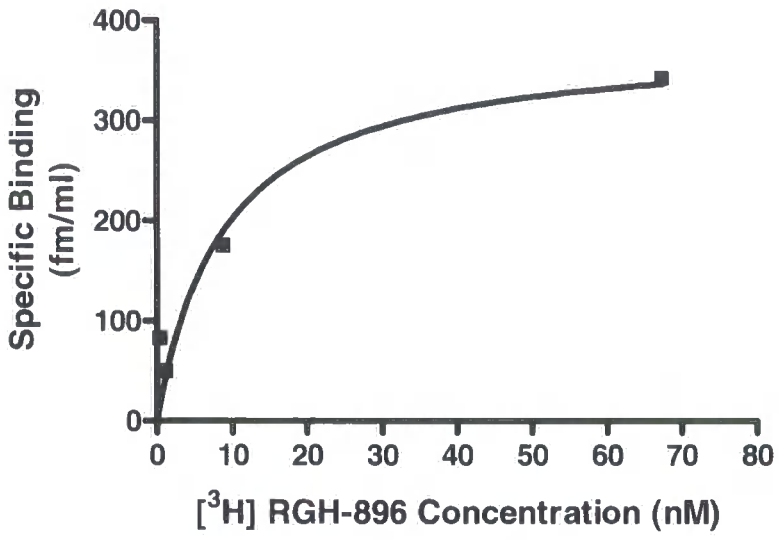

Figure 3.11: Representative graph of saturation binding analysis of NR1/NR2A/NR2B immunopurified material using [^{3}H] RGH-896 (1.25nM-60nM), defining non-specific binding with Ro 25,6981 (10^{-5}M). Representative results shown are best-fit to a one-site binding hyperbola. Analysis of the saturation binding data using non-linear least square regression showed that [^{3}H] RGH-896 bound with a K_D of 7.2 ± 8.1 nM, and a B_{max} of 257 ± 67 fmole/ml of protein. This immmunopurification experiment was repeated with similar results.

3.4 Discussion

This chapter has described the production of a panel of polyclonal antibodies raised in rabbits, through to characterising the antibody in immunoblotting studies and the generation of a new anti-NR2A (1381-1394) immunoaffinity column. The conjugated peptide-protein carrier was emulsified with Freund's complete for inoculation into the rabbit. The use of an adjuvant is required to nonspecifically stimulate antibody production. The use of the adjuvant is to form a deposit protecting the antigen from rapid catabolism and allows for slow release. The first injection of the conjugated peptide-protein was performed using complete Freund's adjuvant (CFA), which is a mixture that contains killed *Mycobacterium Tuberculosis.* This substance works by raising the level of a large set of soluble peptide growth factors known as lymphokines. These lymphokines stimulate the activity of antigen-processing cells directly and cause a local inflammatory reaction at the site of injection, which explains a large immune response to the first inoculation. Subsequent booster inoculations were performed using incomplete Freund's adjuvant (IFA), which does not contain killed *Mycobacterium Tuberculosis.* This methodology has been used to produce a range of successful NMDA receptor antibodies (Chazot *et al.,* 1992, 1993, 1994, 1995 1997a & b; Hawkins *et al.*, 1999).

The production of a peptide affinity column was designed to imitate the coupling of the peptide to the carrier protein. When using a peptide-carrier protein conjugate to raise an antibody, high non-specific binding can cause a problem. It was therefore essential to carry out affinity purification of the anti-peptide antibodies from the resultant antiserum to remove the anti-carrier protein antibodies. Following affinity purification of the anti-NR2A antibody, it was necessary to test the antibody using forebrain membranes by immunoblotting to verify that the antibody recognised the

native NR2A subunit. The resultant immunoblot, showed a specific immunoreactive protein species with a molecular weight of M_r 180000 ± 8000 (mean ± SD, n=4) which was coincident with that previously identified in the literature (Hawkins *et al.*, 1999).

To examine the specificity of the anti-NR2A antibody, native forebrain preparations and individual recombinant NMDA subunits expressed in HEK 293 cells were used. The immunoblot was probed with affinity-purified anti-NR2A receptor antibody in the presence and absence of the respective peptide. The resultant immunoblot probed with anti-NR2A receptor antibody identified a single immunoreactive species (M_r 180000) with NR2A transfected HEK 293 cells and forebrain membranes (Hawkins *et al.*, 1999). All bands were abolished by prior incubation of the anti-NR2A receptor antibody with NR2A peptide (1381-1394). Anti-NR2A antibody displayed no immunocross-reactivity with other NMDA receptor subunits when analysed against NR1/NR2B transfected HEK 293, thus indicating this antibody is specific only to NR2A subunits. Both the peptide blockade and lack of immunocross-reactivity with NR1 and NR2B functioned as a sound control measure to conclude the anti-NR2A antibody was specific for NR2A-subunit only. The resultant panel of anti-NR2A antibodies was used to generate an anti-NR2A immunoaffinity column (ImmunoPure® rProtein A IgG Plus Orientation Kit, Pierce, Rockford, UK). The binding efficiency of the anti-NR2A (1381-1394) antibody to the novel immunoaffinity column was very high (94.1%) compared to that of Hawkins *et al.*, (1999), where only 67 ± 18% of the anti-NR2A antibody immunnoreactivity was retained. Following validation of the ability and efficiency of this column to bind NR2A containing receptors, it was used to further characterise the NR2B-selective compound RGH-896.

Ro 25,6981, an ifenprodil analog, is selective for NR2B containing NMDA receptors with an approximate 5000-fold higher affinity for heteromeric NR1/NR2B receptors than NR1/NR2A receptors, showing the selectivity for NR2B subunit (Mutel *et al.*, 1998). Studies by Brimebcome *et al.*, (1997) and Chazot (2000) have indicated CP-101,606 may be influenced by the presence of other NR2-subunit types within the NMDA receptor complex. These two NR2B-selective ligands, [^{3}H] Ro 25, 6981 (Hawkins *et al.*, 1999) and [^{3}H] CP-101,606 (Chazot *et al.*, 2002), show the presence of different NR2 subunits in receptor complexes can effect the binding of related radioligands. [^{3}H] Ro 25,6981 binds to both NR1/NR2B and NR1/NR2A/NR2B subtype receptors with similar high affinities suggesting Ro 25,6981 is selective for all NMDA receptors containing the NR2B subunit. Conversely, [^{3}H] CP 101,606 appears to bind only to NR1/NR2B subtype receptors and not to NR1/NR2A or NR1/NR2A/NR2B subtype receptors. This suggests that CP 101,606 is selective for dimeric NR1/NR2B-subtype.

In this chapter we have investigated the selectivity of the novel NR2B-selective antagonist RGH-896, using the novel immunopurification approach described by Chazot *et al.*, 2002, to assess whether RGH-896 behaves like Ro 25,6981 or CP-101,606. Co-transfection of mammalian cells with pCISNR1, NR2A and NR2B cDNA produces a heterogeneous mix of NR1, NR2A, NR2B, NR1/NR2A, NR1/NR2B and NR1/NR2A/NR2B subtype receptors (Brimecombe *et al.*, 1997). To isolate the NR1/NR2A/NR2B from NR1/NR2B receptors following triple subunit-transfection, we utilised an immunopurification strategy with the novel anti-NR2A (1381-1394) immunoaffinity column produced in this project. The immunopurified material was subjected to immunoblotting and radioligand binding saturation analysis to further characterise [^{3}H] RGH-896 binding properties. The pooled fractions when

analysed in radioligand saturation binding showed that [^{3}H] RGH-896 bound with a K_D of 7.2 ± 8.1 nM. The NR2B radioligand is therefore binding to forebrain membranes (K_D 6.5 ± 4.6 nM, Chapter 2), NR1/NR2B cell homogenates (K_i 9.5 nM, Chapter 2) and immunopurified material (K_D of 7.2 ± 8.1 nM) with a similar high affinity. Following solubilisation and immunopurification of the transfected material, subunits NR1, NR2A and NR2B were all present in immunopurified material (not shown) by using immunoblotting procedure. All immunoreactive bands detected were consistent with the predicted molecular size of the NR1, NR2A and NR2B subunit, respectively (Brose *et al.*, 1993; Chazot *et al.*, 1994; Blahos and Wenthold, 1996).

In conclusion, the novel finding from this chapter indicates RGH-896 binds with a similar high affinity to forebrain membranes, NR1/NR2B and NR1/NR2A/NR2B containing receptors. Therefore, RGH-896 binds to NR2B-containing receptors irrespective of the NR2 subunit composition (partners) similar to Ro 25,6981. The determination of the binding properties of the novel NR2B-selective NMDA antagonist RGH-896 is important as previous studies have shown CP 101,606 can be influenced by the presence of other NR2-subunit types within the NMDA receptor complex. The data generated in this chapter indicates RGH-896 is showing a binding profile similar to Ro 25, 6981. A number of NR2B-selective compounds have been developed to target specific areas of the brain depending upon the affected brain region. This chapter adds to the information relating to the pharmacological profile of these compounds; RGH-896 and Ro 25,6981 being distinct from CP 101,606. It still remains to be determined which of these two classes will be most useful to target for therapeutic benefit. Now that subtype selectivity of RGH-896 has been defined, the next chapter will use [^{3}H] RGH-896 to quantify NR2B-containing receptors in the

rodent and human brain using ligand autoradiography. The next chapter addresses whether levels of NR2B-containing receptors (defined using [^{3}H] RGH-896) in the anterior cingulate cortex correlate with specific psychotic symptoms in human dementia with Lewy bodies (DLB). A comparison will also be made with [^{3}H] Ro 25,6981 and [^{3}H] CP 101,606, in order to provide further evidence for NR2B receptor heterogeneity in the human brain.

Chapter 4

Ligand Autoradiographical Analysis of Rodent and Human Brain Tissue using a Novel NR2B-selective Antagonist, RGH-896 Focusing on the Anterior Cingulate Cortex

4.1 Introduction

In different CNS disease states, many similar adverse effects are seen in affected patients. Schizophrenics can show hallucinations, delusions, depression and cognitive deficits if not treated. In comparison, Alzheimer's disease patients can show cognitive deficits, dementias and depression but this disease will be treated with alternative therapies. This is due to the distinct brain region involved as there is an assortment of excitatory and inhibitory pathways afferent and efferent to the target region (Lewis and Liebermann, 2000). There are two hypothesis that are believed to be involved in schizophrenia and psychosis, these been the glutamate hypothesis and the dopamine hypothesis (see 1.10.6.7). Researchers follow their own thoughts to which theory to investigate but it is possible that both the dopamine and the glutamate hypotheses interlink due to the various connecting pathways involved between brain regions. For this thesis it is the glutamate hypothesis that will be investigated. NMDA receptor channel blockers, ketamine and phencyclidine (PCP) are capable of inducing a number of schizophrenic-like symptoms, including positive, negative and cognitive abnormalities in normal humans as well as exacerbating existing symptoms in

schizophrenic patients (Steinpreis, 1996). In rodents, NMDA receptor channel blockers induce behavioural, cognitive and neurochemical changes mimicking those observed in schizophrenic patients (Jentsch and Roth, 1999), therefore supporting an NMDA receptor hypofunction hypothesis of schizophrenia (Olney *et al.,* 1999). There is increasing evidence studying the NMDA receptor, to suggest a deficiency in glutamatergic neurotransmission may underlie the pathology of psychosis (Rujescu *et al.*, 2005). This NMDA hypofunction theory of schizophrenia is indirectly supported by new genetic findings. Several of the recently discovered putative schizophrenia genes may function by interacting with the glutamate activity through different effects on the NMDA receptor mediated transmission (Harrison and Weinberger, 2005). NMDA receptors have been implicated as a mediator of neuronal injury associated with many neurological disorders and consequently, compounds that enhance NMDA receptor-mediated transmission may be therapeutically beneficial (Kemp and McKernan, 2002). Gao *et al.,* (2000) and Grimwood *et al.,* (1999) have suggested that NR2B has a role to play in schizophrenia, where NMDA NR2B-subunit mRNA and NR1/NR2B-subtype binding sites have been shown to be selectively increased in hippocampal and cortical regions in schizophrenia (reviewed in Chazot, 2004).

A French neurologist, Paul Broca (1878) noted on the medial surface of the cerebrum, there was a group of cortical areas that were distinctly different from the surrounding cortex. Broca named this collection the "limbic lobe" as it formed a border around the brain stem. Papez (1937) proposed there was an "emotional system" lying on the medial wall of the brain that links the cortex with the hypothalamus, which became known as the Papez circuit. In the circuit, the cingulate cortex affects the hypothalamus via the hippocampus and fornix (a large bundle of axons leaving the

hippocampus), whereas the hypothalamus affects the cingulate cortex via the anterior thalamus. The correlation between Broca's limbic lobe and Papez's circuit gave rise to the limbic system which are anatomically interconnected and are involved in emotion, learning and memory.

The cingulate cortex is situated roughly in the middle of the cortex (Figure 4.1). Cingulate cortex can also be differentiated based on its thalamic connections (Vogt *et al.*, 1979). In addition, the anterior cingulate cortex (ACC) can be differentiated from the posterior cingulate cortex on the basis of cytoarchitecture and patterns of projection (Vogt *et al.*, 1992). The ACC receives signals primarily from the mid-line and intra-laminar nuclei and posterior cingulate cortex receives signals mainly from the anterior thalamic nuclei. ACC is the frontal part of the cingulate cortex and includes Brodmann's area 24 (ventral ACC) and 32 (dorsal ACC). The anterior cingulate cortex forms a collar around the corpus callosum, which relays neural signals between the right and left hemispheres (Vogt *et al*, 1995). Neuroimaging studies have identified the ACC's involvement in transient mood changes (Mayberg *et al.*, 1999), depression and anxiety disorders (Mayberg *et al.*, 2000; Brody *et al.*, 2001) and the perception of pain (Rainville *et al.*, 1997). It is thought that the dorsal ACC is primarily related to rational cognition while the ventral is more related to emotional cognition (Bush *et al.*, 2000). The cingulate cortex is a key brain region involved in functional psychosis, for example, depression (George *et al.*, 1997), delusions (Blackwood *et al.*, 2000), bipolar disorder (Blumberg, 2000) and hallucinations (Shergill *et al.*, 2000). Psychotic symptoms including impaired consciousness, delusions, auditory and visual hallucinations occur frequently in dementia with Lewy bodies (DLB) patients.

Ligand autoradiographical studies will be performed for the first time using the novel radioligand [^{3}H] RGH-896 in rodent brain. Conditions will be optimised and compared to other NMDA receptor NR2B-selective radioligands. Based on these optimised studies, human ligand autoradiography studies will be used to quantify levels and delineate the binding expression pattern of NR2B-selective antagonist radioligand [^{3}H] RGH-896, focusing on the ACC area of the brain and the psychotic clinical features of the individual DLB cases.

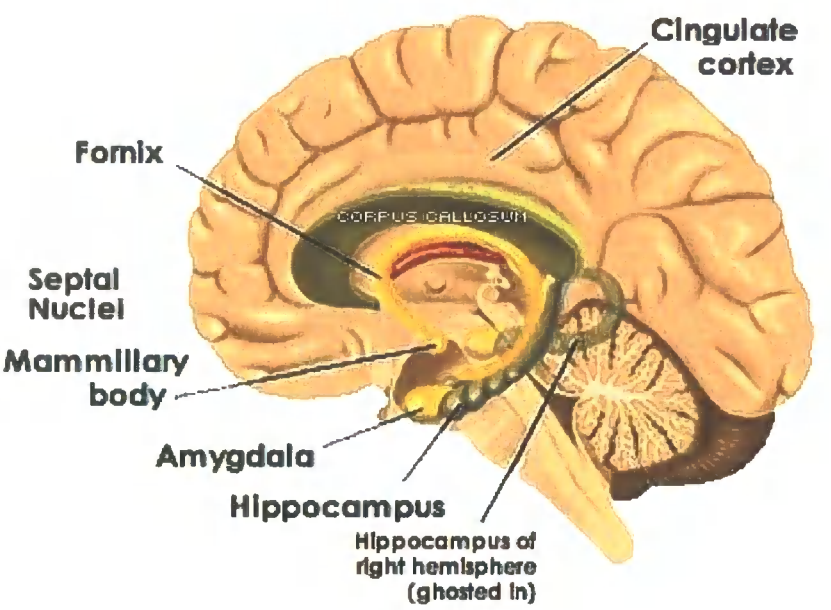

Figure 4.1: Major structures of the limbic system of the brain showing the cingulate cortex (Le Moyne College, New York)

5.2 Methods

5.2.1 Rodent Autoradiography

5.2.1.1 Tissue Isolation and Sectioning

An adult male wild-type Sprague Dawley rat (250-300g) was deeply anaesthetised with phenobarbital. To ensure no pain to the animal, the pinching and reflex of the hind paw was tested as well as the eye blinking reflex. Once these reflexes were abolished, the animal was pinned out on the dorsal surface, with the ribcage exposed and retracted. A cannula was inserted into the left ventricle of the heart to perfuse ice-cold 0.1M sodium phosphate buffer, pH 7.4, containing 0.1% (v/v) sodium nitrite via a peristaltic pump. An incision was made to the right atrium of the heart where the animal was exsanguinated in this way for 5 minutes. The perfusate was switched to the fixative of ice-cold 4% (w/v) paraformaldehyde in 0.1M sodium phosphate buffer, pH 7.4 for 20 minutes. The rodent brain was removed from the skull and immersed in the same fixative overnight at 4°C and later stored in PBS (< 7 days). Prior to sectioning of the tissue, the brain was incubated in 10% (w/v) sucrose in PBS for 48 hours. The sucrose infiltrated brain was frozen in isopentane over liquid nitrogen for 1 minute at -70°C, and was placed into the cryostat to equilibrate to -24°C. The whole brain was sectioned at 16μ, thaw-mounted onto poly-D-lysine coated slides and stored at -20°C. Various levels of the brain was analysed in the rodent autoradiography study to verify NR2B expression compared to the published literature.

4.2.1.2 Receptor Autoradiography

The method used was originally described by Mutel *et al.*, (1998) with modifications made specific to the radioligand. Sections were left to equilibrate to room temperature from -20°C for at least 1 hour prior to the experiment. The same method was repeated without 0.1% (w/v) BSA throughout, with 0.1% (w/v) BSA post-radioligand incubation and 0.1% (w/v) BSA throughout the whole experiment. The sections were pre-incubated for 2 x 10 minutes in 50mM Tris-HCl buffer, pH 7.4 containing 10mM EDTA at room temperature to remove endogenous ligands. Using pre-incubation buffer supplemented with 10nM [^{3}H] RGH-896 (approximate K_D value) (specific activity = 23Ci/mmol, stored at -20°C), the sections were incubated for 90 minutes at 4°C to achieve equilibrium. Non-specific binding was defined in the presence of spermidine (10^{-3}M) or Ro 25,6981 (10^{-5}M). Following incubation in radioligand, sections were washed in 50mM Tris-HCl buffer, pH 7.4 containing 10mM EDTA, for a total of 25 minutes (2 x 5 minutes, 1 x 15 minutes) at 4°C, and dipped in ice cold dH_2O. Sections were left to air dry under a stream of cold air until completely dry at room temperature. The dried slides were opposed to [^{3}H]-Hyperfilm for 4 or 6 weeks alongside [^{3}H]-autoradiography standards at room temperature. Following development in D-19 developer (Kodak) at room temperature and fixation in Unifix (Kodak) at room temperature, the autoradiographic data was quantified using image analysis.

4.2.1.3 Image Analysis

The developed brain images were scanned onto a flat-bed scanner and analysed using Image J imaging program, by capturing 5 areas (2mm x 2mm) of the region to be analysed from various autoradiograms. The [^{3}H]-autoradiography standards were utilised to produce a standard curve for each autoradiogram. The density of binding was calculated in fentomole per milligram of tissue (fm/mg), which was based on the comparison of optical density of sections with that of the autoradiographic standards. Adjustments were made according to the specific activity of the radioligand. Non-specific slides were adjacent sections from the total binding slides. Specific binding was calculated by subtracting the average of non-specific binding from the average in total binding. Brain structures to be analysed were identified from each autoradiogram. Five areas (2mm x 2mm) from a particular structure were captured in Image J, and the mean and standard deviation of the 5 areas for each brain region (hippocampus (subfields CA1, CA3 and dentate gyrus), cortical laminae and cerebellum) were calculated. Graphs corresponding to where the radioligand was binding were constructed using Microsoft Excel.

4.2.2 Human Autoradiography

All DLB cases were autopsy confirmed DLB patients who had been assessed during life as part of the Newcastle Dementia Case Register series. Diagnosis at autopsy was in accordance to the Consensus criteria for clinical and neuropathological diagnosis of DLB. Written consent was received from the next of kin to use the tissue in the study.

The studies were approved by Newcastle and North Tyneside Local Research Ethics Committee. Tissue was obtained from the Brain Bank in Newcastle General Hospital, Tyne & Wear. Sections chosen to be analysed contained cingulate cortex in control cases, dementia with Lewy bodies (DLB) cases, and Parkinson's Disease with dementia (PD + DLB) cases using the Coronal Map of Brodmann Areas in the Human Brain (Perry *et al.*, 1993). Five control cases with no evidence of neurological or psychiatric disease (4 male and 1 female) with age ranging from 67-78 were compared to eight pooled DLB and PD+DLB cases (5 male and 3 female) with age ranging from 72-87. The demographic data are shown in Table 4.1. At the time of this preliminary investigation, human tissue was limited and hence the variation of the demographics of the chosen cases, where ranges vary from a MMSE score of 6 to an MMSE score of 22, as a MMSE score over 24 out of a possible 30 is classed as effectively normal.

Assessments including a standardised psychiatric history (Dewey *et al.*, 1992) and assessment of cognitive function (Roth *et al.*, 1986) were completed. Neuropsychiatric evaluation was measured using the Columbia University Scale for Psychopathology in Alzheimer's Disease (CUSPAD) to evaluate psychotic features (Devanand *et al.*, 1992). The Mini Mental State Examination (MMSE) (Folstein *et al.*, 1975) explores the orientation, short-term memory, attention, concentration, calculating ability and motor activities. The assessments and evaluations were repeated at least annually until death and symptoms were classified as persistent if they were present continuously for at least six months at some stage of the dementia.

Table 4.1: Demographic data of DLB and DLB (PD+dem) cases

Case Number	Gender	Age (Years)	Post-Mortem Delay (Hours)	Diagnosis	MMSE	Impaired Consciousness	Delusions	Auditory Hallucinations	Visual Hallucinations
1	F	77	48	DLB	16	1	1	0	1
2	M	79	16	DLB	N/A	1	0	0	0
3	F	72	24	DLB (PD+dem)	6	1	1	1	1
4	M	87	4	DLB	10	0	1	0	1
5	M	77	60	DLB (PD+dem)	15	0	1	1	1
6	M	77	33	DLB (PD+dem)	N/A	0	1	1	1
7	F	79	64	DLB (PD+dem)	22	1	0	0	1
8	M	76	85	DLB (PD+dem)	N/A	0	0	0	0

MMSE: Mini Mental State Examination; PD: Parkinson's Disease; dem: dementia

4.2.2.1 Tissue Isolation

The brain was divided into two hemispheres at autopsy, where the right hemisphere was fixed in formalin for neuropathological analysis and the left hemisphere was sliced coronally into 1cm slices. The 1cm slices were sealed in airtight polythene, rapidly frozen in Arcton at -70°C, further cooled over liquid nitrogen and stored at -80°C. Prior to sectioning the tissue was sub-dissected to provide blocks containing cingulate cortex (Perry *et al.*, 1993). The 1cm slices of tissue were allowed to warm to 15°C. Tissue was mounted onto cryostat blocks with 8% carboxymethylcellulose. Coronal sections were cut at 20 microns from snap-frozen tissue and thaw mounted onto Vectabond coated slides (Vector Laboratories, UK). Sections were left to air dry for 1-2 hours and were stored at -80°C until use for receptor autoradiography.

4.2.2.2 Receptor Autoradiography

The method used was originally described by Mutel *et al.*,(1998) with modifications made specific to the radioligand. Sections were left to equilibrate to room temperature from -80°C for at least 1 hour prior to the experiment. The sections were pre-incubated for 2 x 10 minutes in 50mM Tris-HCl buffer, pH 7.4 containing 10mM EDTA and 0.1% BSA at room temperature to remove endogenous ligands. Using pre-incubation buffer supplemented with 5nM [^{3}H] RGH-896 (specific activity = 23Ci/mmol, stored at -20°C), the sections were incubated for 90 minutes at 4°C to achieve equilibrium. Non-specific binding was defined in the presence of Ro 25,6981 (10^{-5}M) (See Chapter 2). Following incubation in radioligand, sections were washed

in 50mM Tris-HCl buffer, pH 7.4 containing 0.1% BSA, for a total of 25 minutes (2 x 5 minutes, 1 x 15 minutes) at 4°C, and dipped in ice cold dH_2O. Sections were left to air dry under a stream of cold air until completely dry at room temperature. The dried slides were opposed to [^{3}H]-Hyperfilm for 4 weeks alongside [^{3}H]-autoradiography standards at 4°C. Following development in Devalex (Patterson Scientific) for 5 minutes at room temperature, rinse in cold water for 1 minute and fixation in Black and White Amfix (Patterson Scientific) for 6 minutes at room temperature, the autoradiographic data was quantified using image analysis.

4.2.2.3 Image Analysis

The developed brain images were captured using a Dage 72 MTI CCD72S video camera and were quantitatively analysed by computer-assisted densitometry using Microcomputer Imaging Device (MCID Elite) Version 7.0 software from Imaging Research Inc., Ontario, Canada. The [^{3}H]-autoradiography standards were utilised to produce a standard curve for each autoradiogram. The density of binding was calculated in fentomole per milligram of tissue (fm/mg), which was based on the comparison of optical density of sections with that of the autoradiographic standards. Adjustments were made according to the specific activity of the radioligand. Non-specific slides were adjacent sections from the total binding slides. Specific binding was calculated by subtracting the average of non-specific binding from the average in total binding. Brain structures were identified using the Atlas of the Human Brain (Mai *et al.*, 2004). The mean and standard deviation for the various dissections of the anterior cingulate cortex were calculated. Statistical analysis incorporated correlation

analysis where statistical significance was deemed at $p<0.05$, students't-test and unpaired t-test where statistical significance was deemed at $p<0.05$, using Microsoft Excel. Graphs were constructed using Microsoft Excel.

4.3 Results

4.3.1 Optimisation of Rodent Autoradiography

Previous work in the laboratory has successfully used 1mM spermidine to define non-specific binding of two NR2B selective radioligands ([^{3}H] Ro 25,6981 and [^{3}H] CP-101,606) for both rodent and human ligand autoradiography (Sheahan and Chazot, manuscripts in preparation) (Figure 4.3), in agreement with the autoradiography protocol used by Mutel *et al.*, (1998).

In this study, [^{3}H] RGH-896 binding was poorly displaced by 1mM spermidine compared to other radioligands (Figure 4.2 and Figure 4.3), [^{3}H] Ro 25,6981 and [^{3}H] CP 101,606, where there was little difference in specific and non-specific binding in all regions of the brain. The second surprising observation to note is the labelling in the cerebellum using [^{3}H] RGH-896 where there is a distinct labelling pattern compared to very low/zero binding levels using [^{3}H] Ro 25,6981 and [^{3}H] CP 101,606 (Sheahan *et al*, unpublished) (Figure 4.3). The use of 0.1% (w/v) BSA was introduced to the protocol to reduce the high level of apparent non-specific binding. In order to reduce this apparent non-specific binding and insensitivity to spermidine, the protocol was repeated twice, firstly with 0.1% (w/v) BSA in the post-incubation buffer and, secondly with 0.1% (w/v) BSA present throughout the procedure, with non-specific binding defined in both cases in the presence of Ro 25,6981 (10^{-5}M). The addition of 0.1% (w/v) BSA greatly reduced the apparent non-specific binding of [^{3}H] RGH-896 (Figure 4.4). The use of Ro 25,6981 greatly improved the specific:non-specific ratio.

4.3.2 Analysis of Rodent Autoradiography

The areas of the rodent brain analysed were hippocampus (subfields CA1, CA3 and dentate gyrus), cortical laminae and cerebellum (Figure 4.5). Analysis shows there are higher binding levels of [^{3}H] RGH-896 in the CA1 region and the dentate gyrus of the hippocampus compared to the binding levels in the CA3 region of the hippocampus and the cortical laminae. A significantly lower level of specific binding is seen in the cerebellum (Figure 4.6).

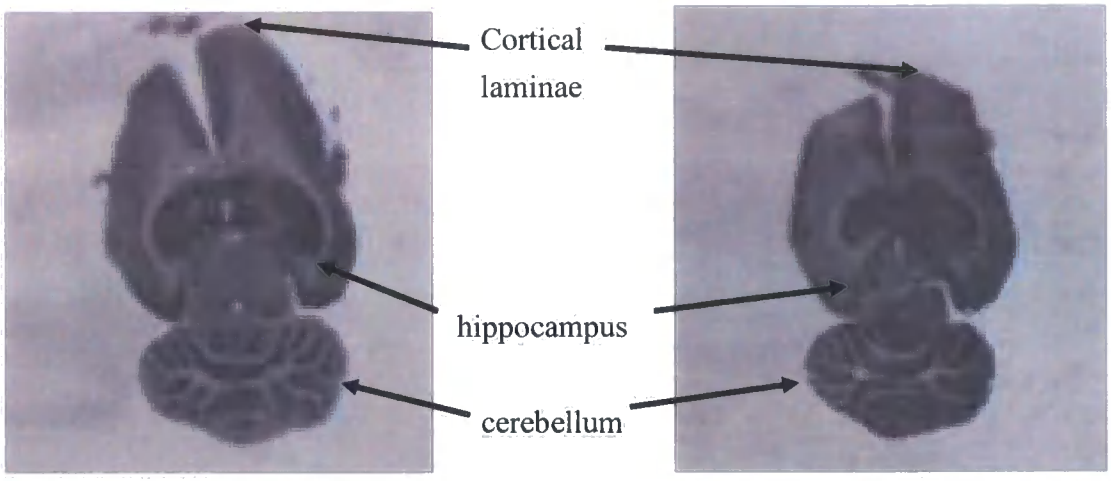

Total Binding **Non-Specific**

Figure 4.2: Representative ligand autoradiographical image of a rat horizontal ventral brain slice using [^{3}H] RGH-896 defining non-specific binding using spermidine (10^{-3}M).

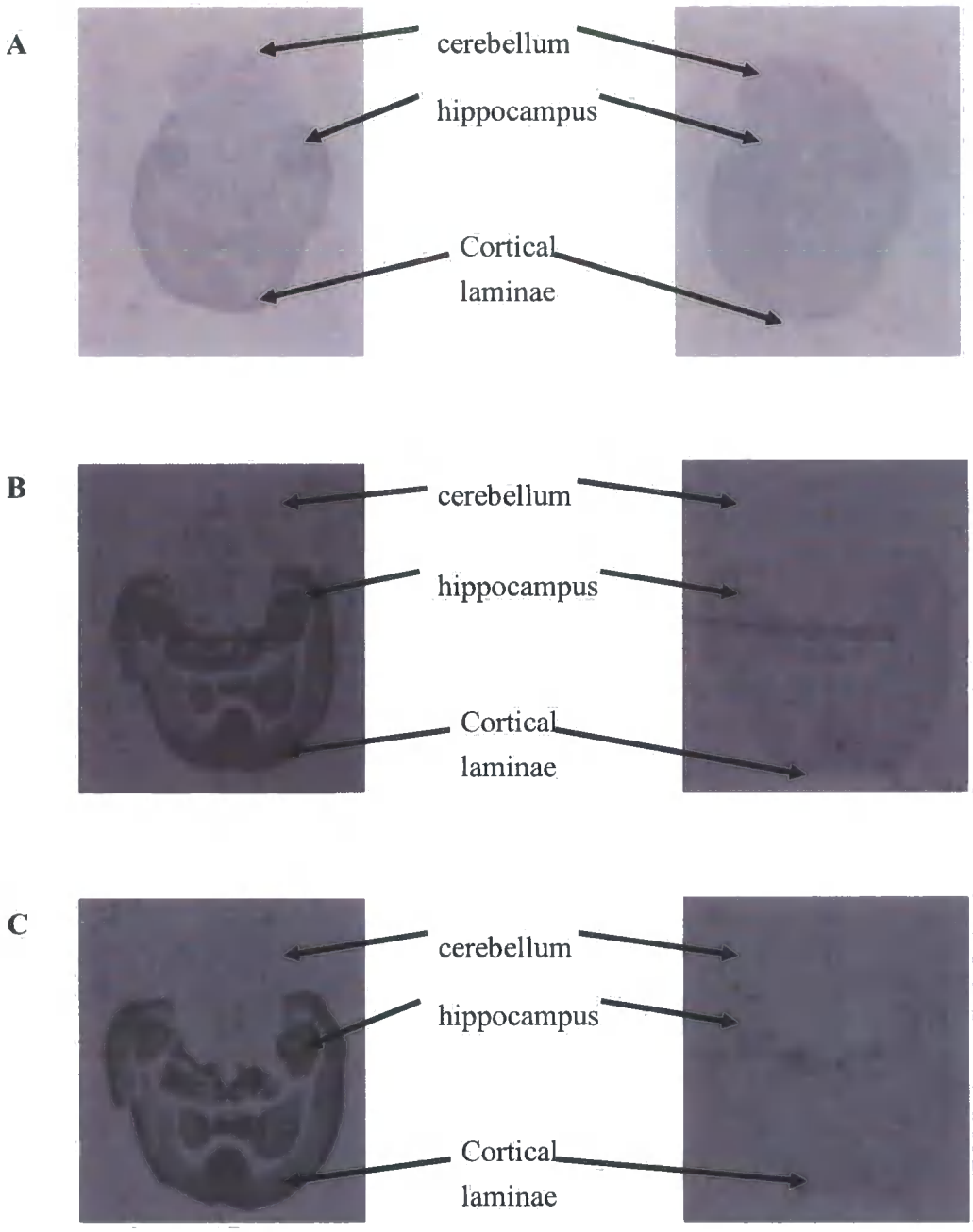

Figure 4.3: Representative comparative autoradiograms of (**A**) [^{3}H] RGH-896, (**B**) [^{3}H] Ro 25,6981, and (**C**) [^{3}H] CP-101,606 carried out under identical conditions, defining non-specific binding using spermidine (10^{-3}M) (**B** & **C**) and Ro 25,6981 (10^{-5}M) (**A**), respectively showing higher binding levels in the cerebellum using [^{3}H] RGH-896 compared to binding levels using [^{3}H] Ro 25,6981 and [^{3}H] CP-101,606 (Sheahan *et al*, unpublished).

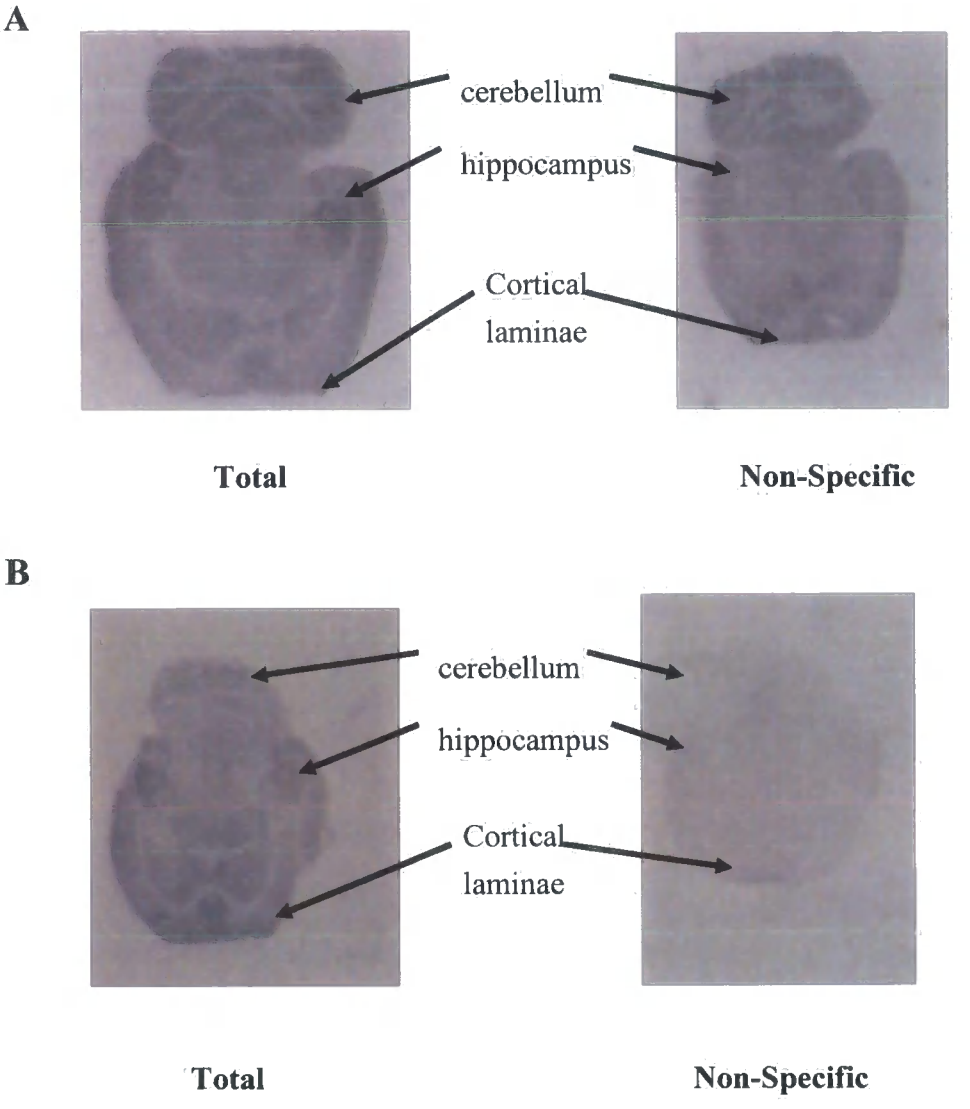

Figure 4.4: Representative autoradiogram of comparative analysis of the experimental procedure with the addition of 0.1% (w/v) BSA defining non-specific binding using Ro 25,6981 (10^{-5}M).

(A) Experimental procedure with 0.1 % (w/v) BSA in post-radioligand incubation buffers

(B) Experimental procedure with 0.1% (w/v) BSA present throughout the protocol

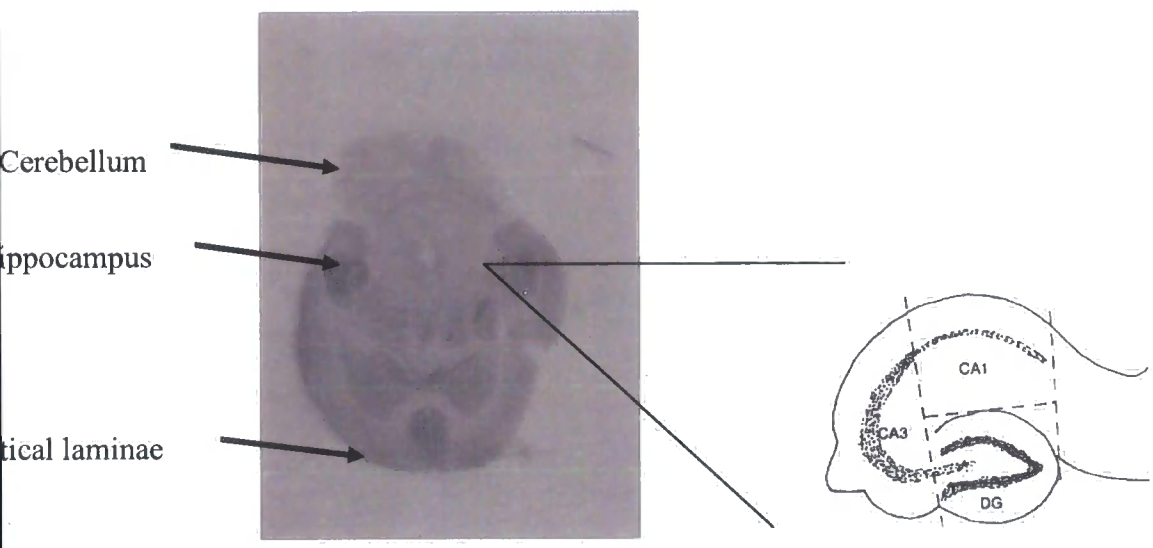

Figure 4.5: Representative sample of regions of the rodent brain analysed including hippocampus (subfields CA1, CA3 and dentate gyrus), cortical laminae and cerebellum

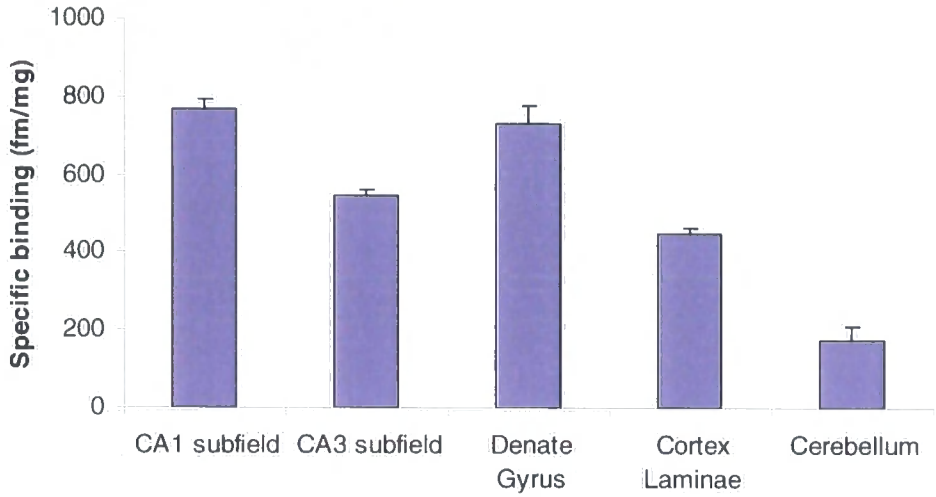

Figure 4.6: Comparison of various structures analysed in rodent ligand autoradiographical study showing [^{3}H] RGH-896 binding levels with the addition of 0.1% (w/v) BSA and defining non-specific binding using Ro 25,6981 (10^{-5}M)

(n = 6-12 randomly selected sections from the same rat brain)

4.3.3 Analysis of Human Autoradiography

Following on from the image analysis, the density of binding (fmoles/mg) was determined for various sections of the ACC, including the cingulate cortex as a whole, the inner and outer areas, the inferior cingulate and the superior cingulate (Figure 4.7). Representative autoradiograms of [^{3}H] RGH-896 binding defining non-specific binding using Ro 25,6981 (10^{-5}M) are shown in Figure 4.8 as observed images, but it is important to note that these observed images were magnified for analysis.

The range of areas analysed were compared to matched control data. Although no significance was established, a trend was observed with a small reduction in specific binding in all DLB cases compared to control cases in the various areas of the cingulate cortex analysed (Figure 4.9). The levels of binding compared well with those seen with [^{3}H] Ro 25,6981 (i.e. approx 200 fmol/mg), which are significantly higher than those seen with [^{3}H] CP-101,606. Furthermore, the overall preservation of binding sites was also consistent with studies performed with [^{3}H] Ro 25,6981 (Sheahan, unpublished).

A range of psychotic symptoms occur frequently in DLB patients, which include impaired consciousness, delusions, auditory and visual hallucinations. To evaluate these symptoms and their potential relationship to NR2B receptors, specific [^{3}H] RGH-896 binding was determined in conjunction with the clinical data as not all cases experienced the same symptoms. With the exception of the superior cingulate data, there was little change in specific binding levels when analysing the patients that had experienced delusions compared to those which had not (Figure 4.10). All areas analysed of the cingulate cortex show significantly higher [^{3}H] RGH-896 binding in cases that had endured auditory hallucinations in comparison to those who had not

(Figure 4.11). In contrast, no such significant differences were seen with respect in patients with visual hallucinations (Figure 4.12) or impaired consciousness (Figure 4.13), although there was a trend in the superior cingulate cortex in Figure 4.13.

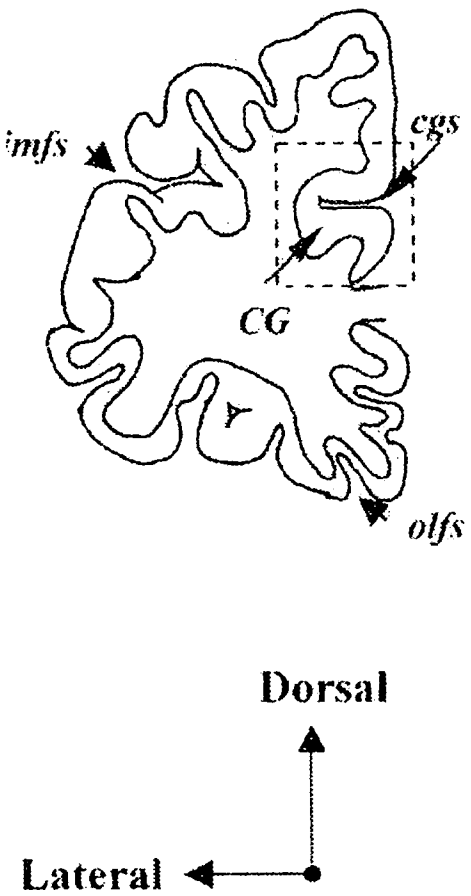

Figure 4.7: The various regions of the ACC analysed (CG – cingulate gyrus; cgs – cingulate sulcus)

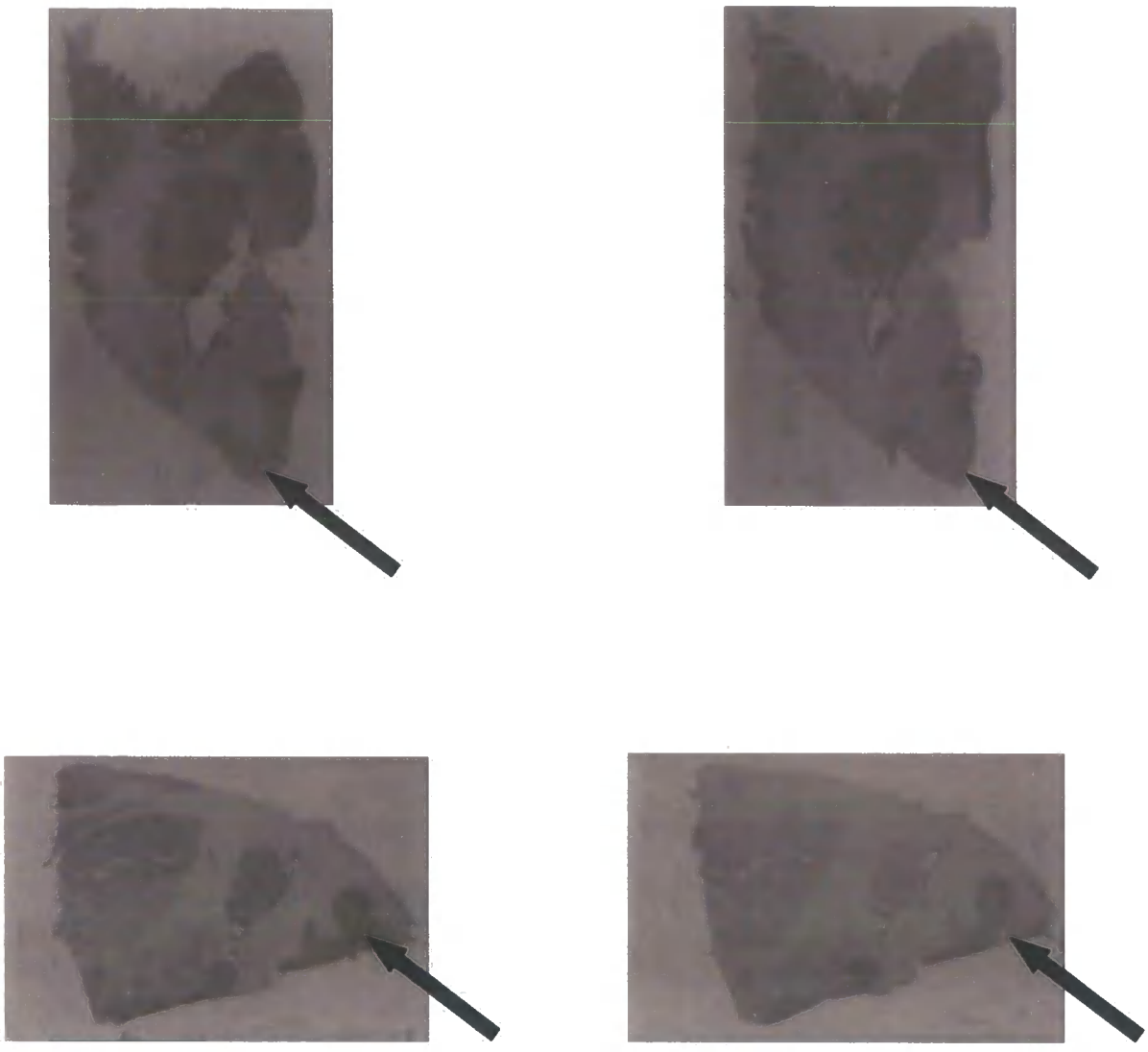

Figure 4.8: Representative autoradiogram of [^{3}H] RGH-896 binding levels in the presence of 0.1% (w/v) BSA and defining non-specific binding using Ro 25,6981 (10^{-5}M)/ Arrow marks the position of the anterior cingulate cortex.

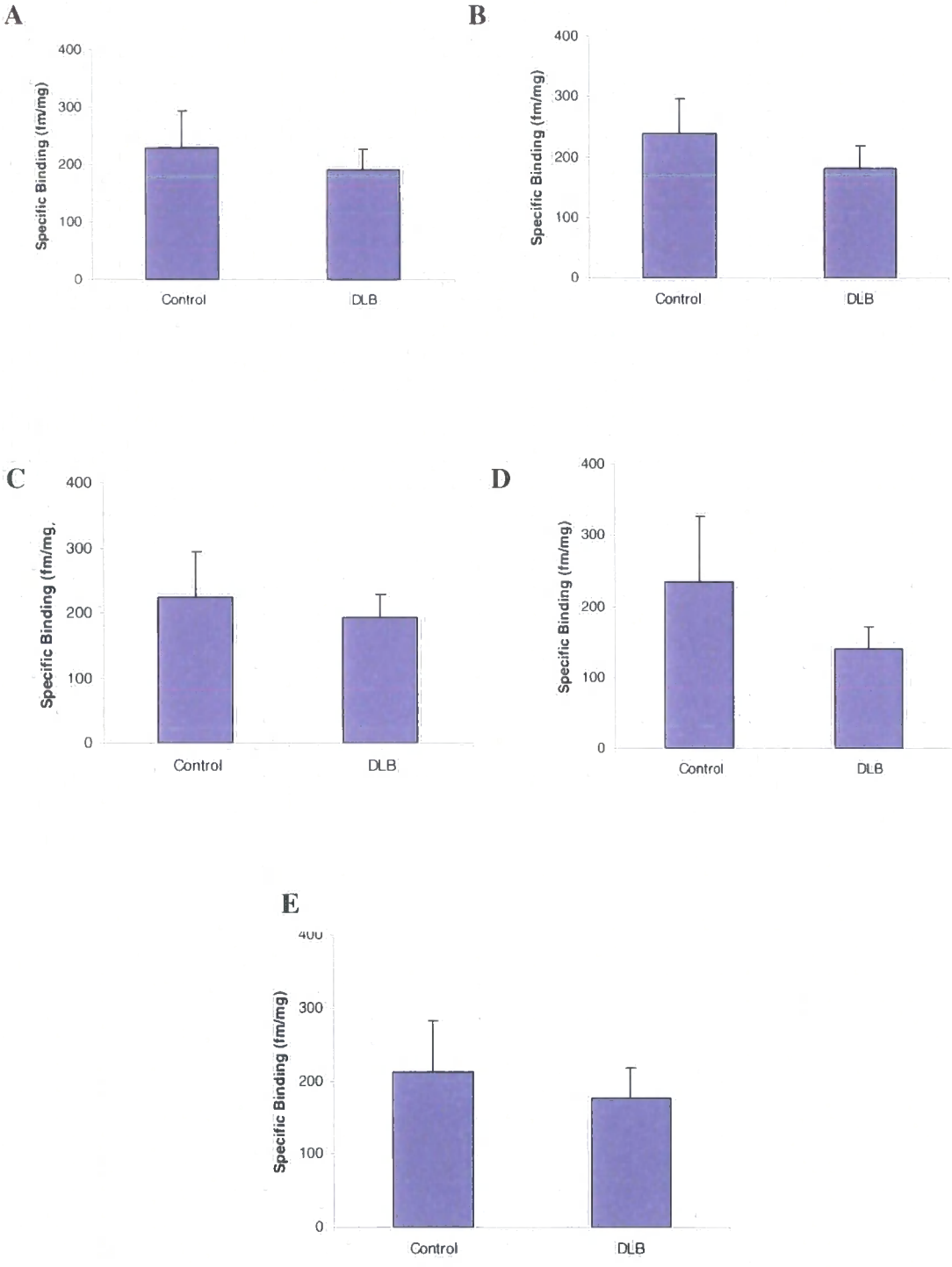

Figure 4.9: Comparison of control and DLB data in (**A**) Whole Cingulate Cortex, (**B**) Outer Cingulate Cortex, (**C**) Inner Cingulate cortex, (**D**) Inferior Cingulate, (**E**) Superior Cingulate (n = 4-8 cases)

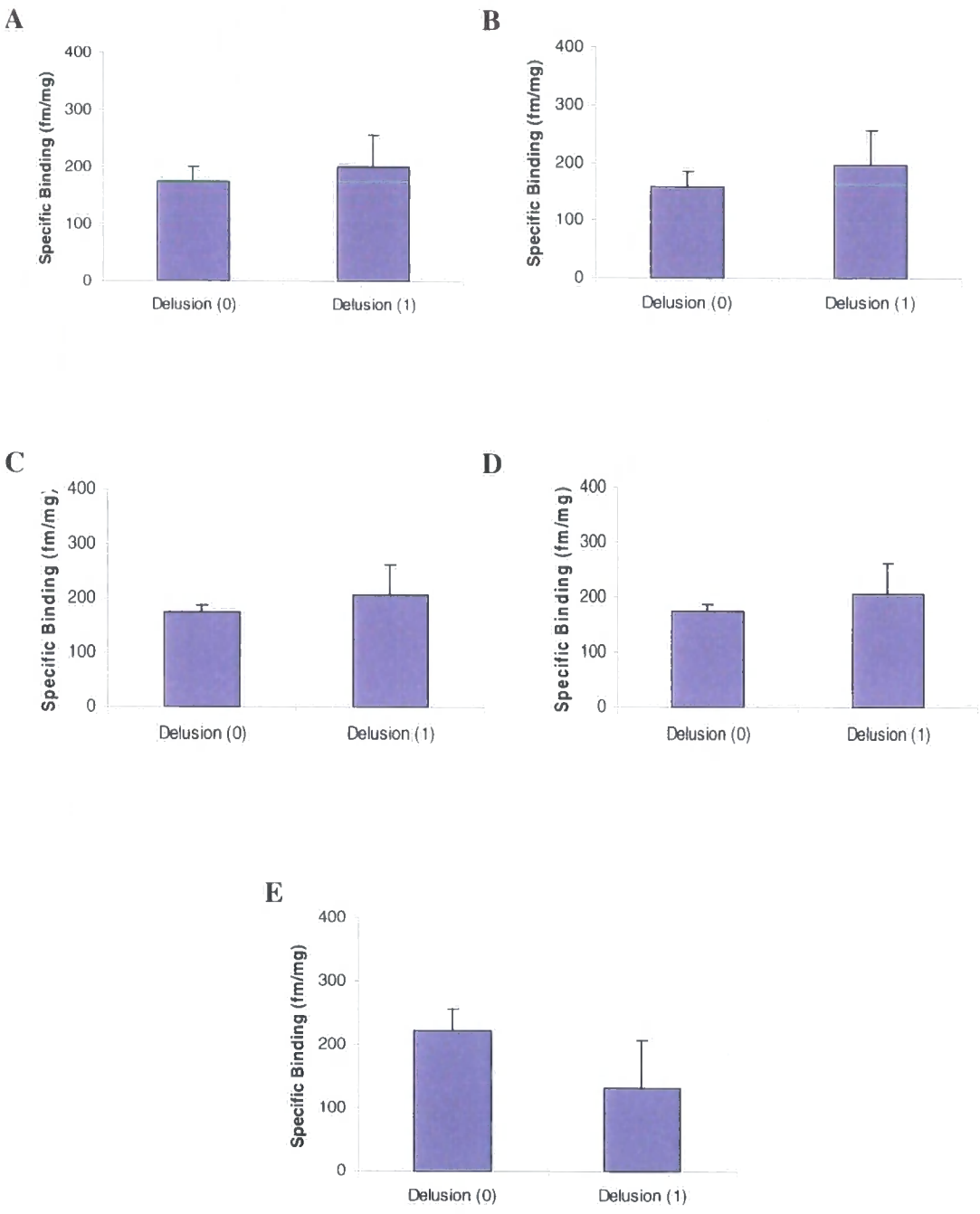

Figure 4.10: Comparison of control and DLB data in (**A**) Whole Cingulate Cortex, (**B**) Outer Cingulate Cortex, (**C**) Inner Cingulate cortex, (**D**) Inferior Cingulate, (**E**) Superior Cingulate where Delusion (0) indicates no delusions and Delusion (1) indicates the patient had experienced delusions (n = 5-8 cases)

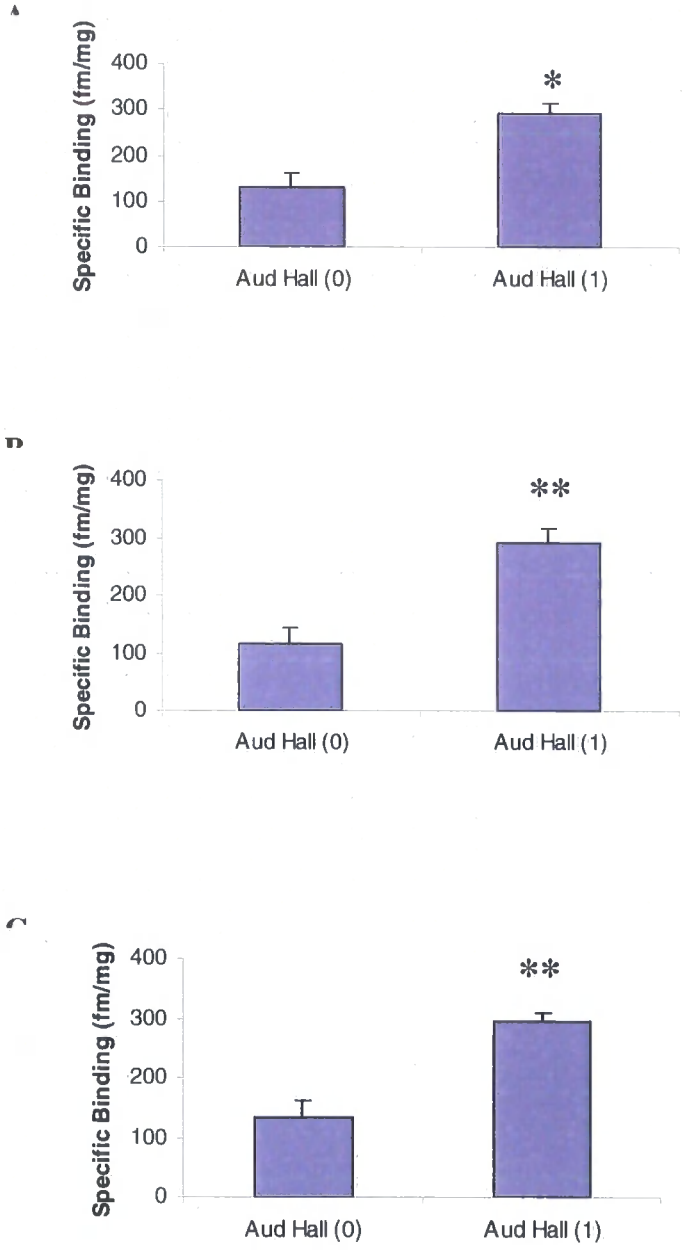

Figure 4.11: Comparison of auditory hallucinations data in (**A**) Whole Cingulate Cortex, (**B**) Outer Cingulate Cortex, (**C**) Inner Cingulate Cortex where *$p<0.05$, **$p<0.001$ (n = 3-5 cases), where Aud Hall (0) indicates no auditory hallucinations and Aud Hall (1) indicates the patient had experienced auditory hallucinations

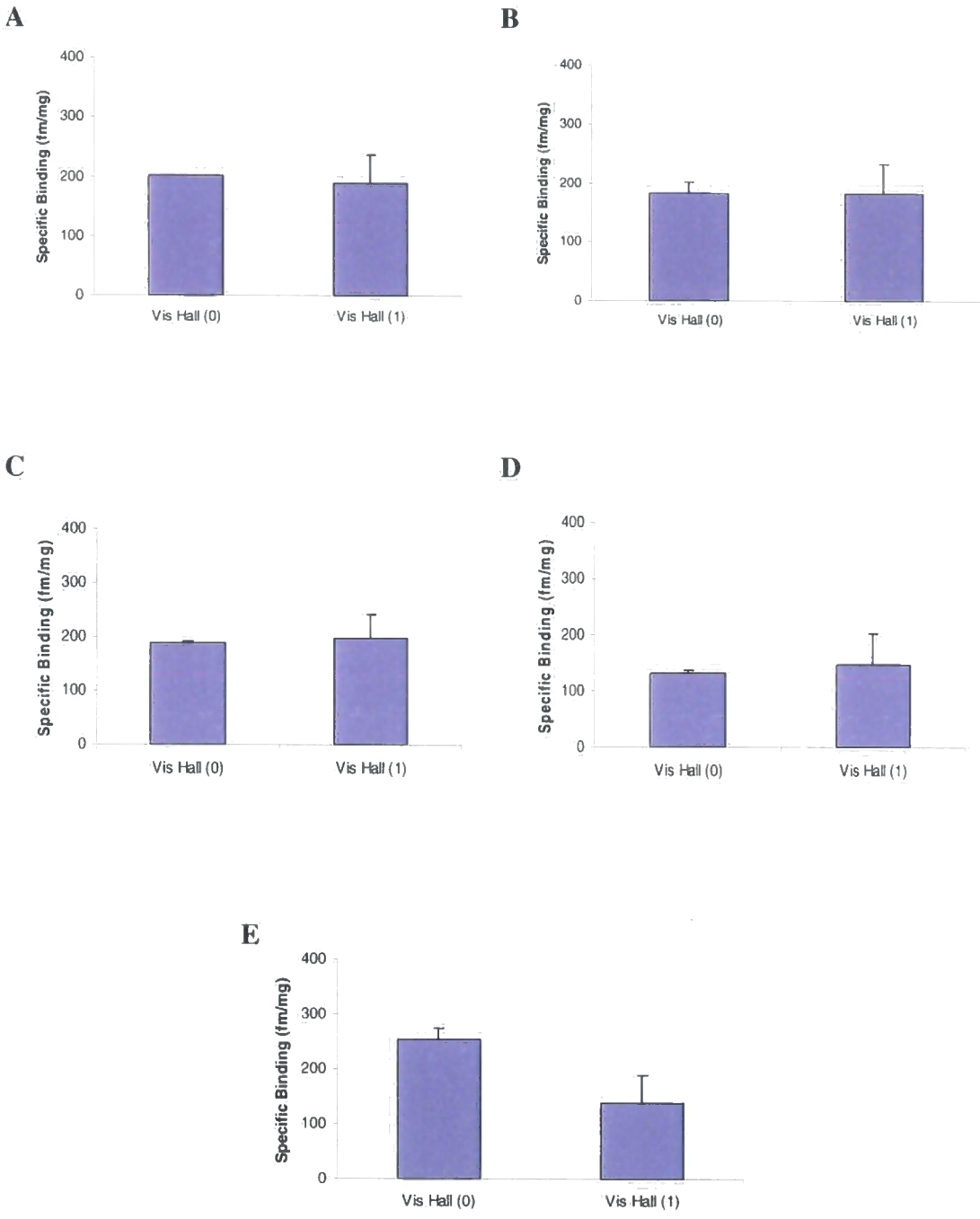

Figure 4.12: Comparison of visual hallucinations data in (**A**) Whole Cingulate Cortex, (**B**) Outer Cingulate Cortex, (**C**) Inner Cingulate Cortex, (**D**) Inferior Cingulate, (**E**) Superior Cingulate (n = 2-5 cases), where Vis Hall (0) indicates no visual hallucinations and Vis Hall (1) indicates the patient had experienced visual hallucinations

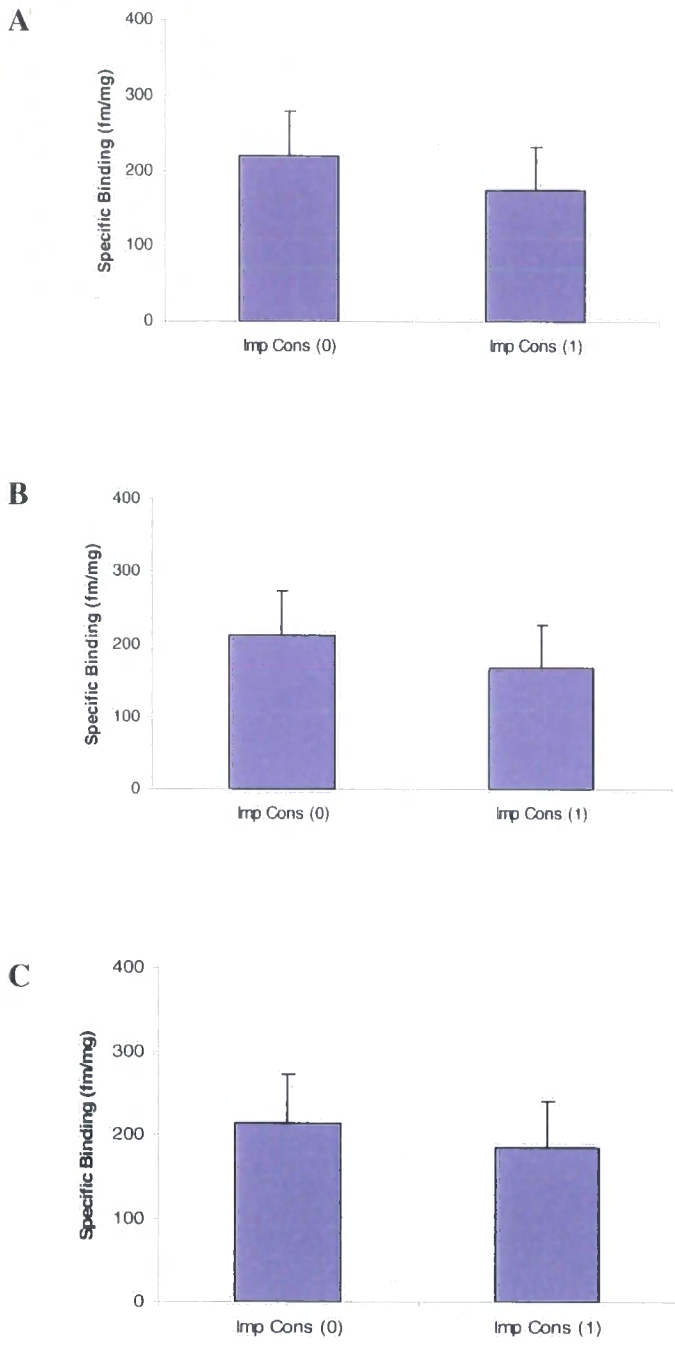

Figure 4.13: Comparison of impaired consciousness data in (**A**) Whole Cingulate Cortex, (**B**) Outer Cingulate Cortex, (**C**) Inner Cingulate Cortex (n =3–4 cases) where Imp Cons (0) indicates no impaired consciousness and Imp Cons (1) indicates the patient had experienced impaired consciousness

4.4 Discussion

The use of ligand autoradiography can determine the mapping of cellular components of the brain that have been radioactively labelled. Previous studies in the laboratory and published data have successfully utilised polyamines to define non-specific binding of NR2B radioligands (Sheahan and Chazot, unpublished; Mutel *et al.*, 1998). The marked difference of [^{3}H] RGH-896 binding sensitivity to spermidine (10^{-3}M) compared to other radioligands, [^{3}H] Ro 25,6981 and [^{3}H] CP 101,606 was followed up with a series of investigative radioligand binding experiments (See Chapter 2). Using male adult rat forebrain membranes, competition binding studies confirmed that spermidine displays a significantly lower (42-fold) affinity for [^{3}H] RGH-896 than [^{3}H] Ro 25, 6981 (Chapter 2, Figure 2.1). This explained the lack of apparent specific [^{3}H] RGH-896 binding when spermidine was used to define non-specific binding in the initial rodent ligand autoradiographical studies.

The next series of ligand autoradiography were performed using Ro 25, 6981 (10^{-5}M) to define non-specific binding. This was selected as Ro 25,6981 displaced [^{3}H] RGH-896 with an affinity close to the value previously determined using direct [^{3}H] Ro 25,6981 binding studies in rat forebrain membranes and NR1/NR2B transfected HEK 293 cells (Chazot *et al.*, 2002) (Chapter 2, Figure 2.2). Furthermore, the K_D value for [^{3}H] RGH-896 in male adult rat forebrain membranes using Ro 25,6981 (10^{-5}M) to define specific binding, was in close agreement with previous unpublished Gedeon Richter studies (Chapter 2, Figure 2.3). The amendment to the ligand autoradiography protocol with the addition of 0.1% (w/v) BSA, successfully defined specific binding of [^{3}H] RGH-896 to many forebrain structures, consistent with both [^{3}H] Ro 25,6981 and [^{3}H] CP 101,606 (Figure 4.4) (Sheahan and Chazot,

unpublished). The areas of the rodent brain analysed in this study were the hippocampus (CA1, CA3 and dentate gyrus), cortical laminae and cerebellum (Figure 4.5). The hippocampus is split up into these three sub-regions as there appears to be significant differences in the mechanism by which LTP is expressed (Schulz *et al.*, 1999; Song *et al.*, 2001). Furthermore, neurons in the CA1, CA3 and denate gyrus are differentially sensitive to excitotoxic cell death (Ben-Ari *et al.*, 1980; Golarai *et al.*, 2001; Grady *et al.*, 2003; Olsson *et al.*, 2003). Autoradiography analysis showed higher binding levels of [^{3}H] RGH-896 in the CA1 region and the dentate gyrus of the hippocampus compared to the binding levels in the CA3 region of the hippocampus and the cortical laminae. Previous studies using a semi-quantitative Western blotting technique have shown expression levels of NR2B has been found to differ among the CA1, CA3 and dentate gyrus of the hippocampus. This study demonstrated a greater expression of NR2B levels in the CA1 region relative to the CA3 and dentate gyrus of the hippocampus (Coultrap *et al.*, 2005), following a similar trend with the binding levels of [^{3}H] RGH-896. The outer laminae appeared more heavily labelled than the inner laminae of the cortex consistent with other labelling observed with both [^{3}H] Ro 25,6981 and [^{3}H] CP 101,606. The differences in specific binding levels of [^{3}H] RGH-896 in the hippocampus are due to differential expression of NR2B subunits. A lower level of specific binding was seen in the cerebellum (Figure 4.6) which was expected as the NR2B subunit is predominantly found in the hippocampus, cerebral cortex, striatum and the olfactory bulbs (Luo *et al.*, 1997; Charton *et al.*, 1999) and not the cerebellum. The apparent binding in the cerebellum using [^{3}H] RGH-896 requires further investigation, and may represent an additional binding site for this ligand, not detected with [^{3}H] Ro 25,6981 or [^{3}H] CP 101,606. Previous reports from the laboratory have shown that the NR2B is expressed in small amounts in the

cerebellum, although no functional support has thus far surfaced (Thompson *et al.*, 2000). Following the amendments in the rodent studies, the improved conditions with the addition of 0.1% (w/v) BSA to reduce the high level of apparent non-specific binding, were adopted for the human autoradiography study. A point to note is due to the use of human tissue in the next section, the rodent and the human autoradiography were conducted in two separate establishments and hence there are differences in the resolutions of the rodent autoradiography compared to the human autoradiography.

The focus of the human autoradiography study was to look at the anterior cingulate cortex (ACC) in relation to psychotic symptoms experienced in DLB patients (McKeith *et al.*, 2004). There is growing evidence that limbic cortical abnormalities exist in psychosis (Shapiro, 1993; Tamminga, 1997, 1998; Weinberger, 1996). The hippocampal and parahippocampal cortices, alongside the cingulate cortices were defined by Broca as the limbic lobe (Vogt *et al.*, 1997). The cingulate cortex can be divided into anterior (Brodmann's Area 24, BA24) and posterior domains where the anterior lacks a granular layer IV but has a prominent layer Va, while the posterior cingulate is granular (Vogt *et al.*, 1995). The ACC is associated with attentional, emotional and cognitive functions. The ACC has significant reciprocal connections particularly from the inner layers to the amygdala (Vogt *et al.*, 1992), a brain structure thought to be central to emotional processing, whereas the outer layers receive projections from the hippocampus (Vogt *et al.*, 1979; Tamminga *et al.*, 2000). The psychosis associated with DLB patients can include schizophrenic-like episodes (McKeith *et al.*, 2004). Abnormalities in glutamatergic neurotransmission have been reported in the ACC in schizophrenia (Benes, 2000; see review Tamminga *et al.*, 2000). In addition, there is also evidence indicating abnormalities in other neurotransmitter systems in the ACC in schizophrenia including dopamine, GABA

and serotonin, which could all influence abnormal excitatory activity in the ACC (Benes, 2000; Zavitsanou and Huang, 2002).

In this small pilot study, a trend was observed with a modest reduction in specific binding of [^{3}H] RGH-896 in all DLB cases compared to control cases in the various areas of the ACC analysed. When comparing [^{3}H] RGH-896 to a well defined NR2B-selective antagonist [^{3}H] Ro 25,6981, there was also a modest comparable decrease in specific binding in the ACC of DLB cases compared to age-matched controls lending weight that this may be significant (Sheahan *et al.*, unpublished). The predominant neurotransmitters in the limbic cortex are glutamate and GABA, where glutamate is present in pyramidal and granule cells (Ottersen *et al.*, 1989). Many studies have looked at the fluctuations of different neurotransmitter levels in neuropathological cases, but Deakin *et al.*, (1989) interestingly found a reduction in D-[^{3}H]-aspartate binding, which is a putative marker for glutamate terminals. An explanation of the reduction in [^{3}H] RGH-896 binding is a small decline in NR2B-containing receptors in the ACC in DLB cases. NR2B-containing receptor densities in the ACC were further measured in a prospectively assessed series of patients diagnosed as DLB and age matched controls. Comparisons were determined within the DLB cohort between groups with and without psychotic symptoms that occur frequently in DLB patients these include impaired consciousness, delusions, auditory and visual hallucinations. To evaluate these symptoms, specific binding was determined in conjunction with the clinical data since not all cases experienced the same symptoms. Delusions are frequently seen in DLB cases (Ballard *et al.*, 1999; Aarsland *et al.*, 2001; Ballard *et al.*, 2001; Marantz and Verghese, 2002). Our results, with the exception of the superior cingulate data, indicate there was an apparent modest increasing trend in specific binding levels in patients that had experienced delusions, although these did

not reach significance. Abnormalities in the ACC may be related to delusions. Research shows in Alzheimer's disease that patients, who have experience delusions, are reported to have a lower metabolic rate (Mentis *et al.*, 1995; Sultzer *et al.*, 2003) and lower regional blood perfusion in the ACC (Mega *et al.*, 2000). In contrast, schizophrenic patients experiencing hallucinations have a high metabolic rate of glucose in the ACC (Cleghorn *et al.*, 1990) and display high neuronal activity measured by fluorescence magnetic resonance imaging (fMRI) (Shergill *et al.*, 2000). Auditory hallucinations are elementary and do not appear to include command or single voice hallucinations. Examples of elementary auditory hallucinations include banging, knocking, sizzling, a doorbell, footsteps, muffled voices, sounds of many people talking in a room or rummaging sounds. Notably, all areas analysed of the ACC show a significant 2-fold increase in binding levels in cases that had endured auditory hallucinations compared to cases which did not. Auditory hallucinations have been measured in schizophrenic patients by functional magnetic resonance imaging (fMRI) and this study indicated the ACC is associated with the activation of auditory hallucinations (Shergill *et al.*, 2000). Cleghorn *et al.,* (1990) has analysed regional brain metabolism, which has demonstrated auditory hallucinations rates correlate with the changing metabolism in the ACC. These data represent the first evidence that a change in NR2B receptor may underlie auditory hallucinations observed in a subpopulation of DLB cases. Recurrent visual hallucinations are a core feature of DLB cases. Visual hallucinations are associated with greater deficits in cortical acetylcholine (Perry *et al.*, 1991). The analysis of visual hallucinations in the various areas of the ACC produced very similar levels of specific binding, and therefore no significant differences were seen, indicating there is no apparent change in NR2B-containing receptor levels. A supporting feature of DLB is impaired

consciousness. Although not significant, all areas analysed of the ACC displayed an apparent trend of a decrease in specific binding levels when examining patients that had experienced impaired consciousness.

In conclusion, both radioligand binding (Chapter 2) and rodent autoradiography (Chapter 4), showed a marked difference in [^{3}H] RGH-896 binding sensitivity to spermidine (10^{-3}M) compared to [^{3}H] Ro 25,6981 and [^{3}H] CP 101,606. Thus indicating [^{3}H] RGH-896 is binding to a distinct but overlapping binding site to [^{3}H] Ro 25,6981 and [^{3}H] CP 101,606. Using rodent autoradiography, the binding profile of [^{3}H] RGH-896 was similar to published expression profile of NR2B subunit containing receptors (Coultrap *et al.,* 2005), indicating NR2B-subunit specificity of [^{3}H] RGH-896. Hence this compound can be used as a useful tool in the future to probe for NR2B expression. The expression of NR2B subunits using human ligand autoradiography was established in the ACC (at levels comparable to [^{3}H] Ro 25,6981 and significantly higher than [^{3}H] CP 101,606) which is associated with psychosis in DLB patients. This small pilot study indicates that along with clinical data of affected patients, this ligand autoradiography method is able to quantify and map the cellular components of the brain that are related certain symptoms by the use of a specific radioligand. Herein, this chapter provides the first preliminary evidence of cases which had experienced auditory hallucinations displaying a significant increase in NR2B-containing receptors in the ACC. In addition, a general overall preservation of NR2B receptors were observed in DLB patients compared to age matched controls in the ACC, which correlates with parallel studies using [^{3}H] Ro 25,6981 and [^{3}H] CP 101,606 (unpublished observations), indicating that this subtype remains a viable target for therapeutic manipulation in patients suffering from DLB.

Overall Discussion and Future Direction

Pharmacological and functional properties of the NMDA receptor are highly dependent on the constitution of the receptor complex. The main aim of this project was to investigate NMDA receptor subtype selectivity of a novel NR2B receptor antagonist, RGH-896, the most advanced clinical drug of this class, currently in Phase II trials. Herein, native, recombinant and immunopurified preparations have been utilised to determine the pharmacological properties of RGH-896 using radioligand binding techniques. Further characterisation of this ligand was employed to delineate the level of NR2B receptors and the regional distribution of these receptors in rodent and human tissue using a novel radioligand, [^{3}H] RGH-896 and an optimised ligand autoradiographical protocol.

Routinely, spermidine is utilised to define non-specific binding of NR2B-subunit containing receptors (Hawkins, 1999; Chazot *et al.*, 2002). A series of radioligand binding studies showed spermidine displayed a significantly lower affinity for [^{3}H] RGH-896 binding site compared to the [^{3}H] Ro 25,6981 binding site, indicating [^{3}H] RGH-896 binds to a distinct binding site other than the usual NR2B binding domain for [^{3}H] Ro 25,6981 and [^{3}H] CP-101,606. Radioligand binding competition studies indicated [^{3}H] Ro 25,6981 was highly sensitive to RGH-896, whereas [^{3}H] MK-801 was insensitive to RGH-896. In contrast, competition binding studies showed comparable displacement by ifenprodil of both [^{3}H] MK-801 and [^{3}H] Ro 25,6981 binding. This contrasting allosteric coupling to the MK-801 binding site displayed by ifenprodil and RGH-896 indicate further evidence for a fundamental difference in the binding sites of NR2B-selective ligands. Recombinant studies in the thesis suggested

RGH-896 will bind to NR2B-containing receptors irrespective of NMDA receptor subunit combinations. To directly demonstrate this pharmacological profile proposed, a novel immunopurification procedure was employed.

A new panel of polyclonal antibodies was produced and used to generate a novel anti-NR2A immunoaffinity column. To examine the specificity of the anti-NR2A antibody, native forebrain and recombinant NMDA subunits were transfected into HEK 293 cells. The anti-NR2A antibody displayed no immunological cross-reactivity with other NMDA receptor subunits when analysed against various NMDA receptor subunits transfected into HEK 293, thus indicating this antibody is specific only to the NR2A subunit. Following validation of the efficiency of the resultant immunoaffinity column, it was used to further confirm the selectivity of the novel NR2B-selective compound RGH-896. Following detergent-extraction and immunopurification of the transfected material, all subunits NR1, NR2A and NR2B were shown to be present in immunopurified material consistent with previous studies (Brose *et al.*, 1993; Chazot *et al.*, 1994; Blahos and Wenthold, 1996; Chazot *et al.*, 2002). The NR2B antagonists, Ro 25,6981 and CP-101,606, show subtype selectivity. Ro 25,6981 binds to NR1/NR2B and NR1/NR2A/NR2B subtype receptors with similar high affinities, indicating Ro 25,6981 to be selective for all NR2B-containing subtype receptors (Hawkins *et al.*, 1999). In contrast, CP-101,606 shows further selectivity as it can distinguish between NR1/NR2A, NR1/NR2B and NR1/NR2A/NR2B subtype receptors with higher apparent selectivity for NR1/NR2B as has been shown in single channel recordings (Brimecombe *et al.*, 1997), cytotoxicity (Boeckmann and Aizenman, 1996) and immunobiochemical studies (Chazot *et al.*, 2002). In this thesis, the first evidence is provided that RGH-896 has a similar pharmacological profile to Ro 25,6981, based on the direct measurement of the affinity of RGH-896 for

NR1/NR2A/NR2B subtype using an immunopurification approach. RGH-896 binds with a similar high affinity to forebrain membrane NMDA receptors, NR1/NR2B and immunoisolated NR1/NR2A/NR2B receptors. Therefore, this thesis provides strong evidence that RGH-896 binds to NR2B-containing receptors irrespective of the NR2 subunit composition (partners) analagous to Ro 25,6981.

Following the definition of the subtype selectivity of RGH-896, the ligand autoradiography approach was employed to quantify NR2B-containing receptors in the rodent and human brain. To compare the binding expression topology of [^{3}H] RGH-896 to [^{3}H] Ro 25,6981 and [^{3}H] CP-101,606, various areas of the rodent brain were quantified. The analysis showed higher binding levels of [^{3}H] RGH-896 in the CA1 region and the dentate gyrus of the hippocampus compared to the binding levels in the CA3 region of the hippocampus and the cortical laminae. In addition, the outer laminae appeared more heavily labelled than the inner laminae of the cortex. The expression profile of [^{3}H] RGH-896 was consistent with other labelling patterns observed with both [^{3}H] Ro 25,6981 and [^{3}H] CP-101,606 (Sheahan *et al.*, unpublished). A lower level of specific binding was seen in the cerebellum which was to be expected as the NR2B subunit is predominantly found in the hippocampus, cerebral cortex, striatum and the olfactory bulbs (Luo *et al.*, 1997; Charton *et al.*, 1999), and not the cerebellum. The apparent significant binding in the cerebellum using [^{3}H] RGH-896 compared to background levels using [^{3}H] Ro 25,6981 or [^{3}H] CP-101,606 requires further investigation as this may represent an additional binding site for this ligand which is not detected with [^{3}H] Ro 25,6981 or [^{3}H] CP-101,606.

Following rodent autoradiography analysis, a series of ligand autoradiography experiments were conducted using human brain tissue from patients that had suffered DLB, to investigate the specific binding profile of [^{3}H] RGH-896, in particular, in the

anterior cingulate cortex (ACC). The ACC was chosen for this investigation as it is a key brain region involved in functional psychosis, a common but heterogeneous set of symptoms observed in DLB. The clinical information for the human autoradiography study was gathered throughout illness as these cases were assessed as part of the Newcastle Dementia Case Register series. Autopsy analysis confirmed DLB cases in accordance to the Consensus criteria and studies using human tissue were approved by Newcastle and North Tyneside Local Research Ethics Committee. Control tissue used showed no evidence of neurological or psychiatric disease, whereas diseased tissue was obtained from patients with a history of DLB. Clinical evaluation accumulated throughout the assessment process included effects that are common with patients. These psychotic symptoms included impaired consciousness, delusions, auditory hallucinations and visual hallucinations. For evaluation of these symptoms, specific [^{3}H] RGH-896 binding was determined in conjunction with the clinical data as not all cases experienced the same symptoms.

The analysis of [^{3}H] RGH-896 binding showed a surprising overall preservation of NR2B subunits in DLB patients, compared to age-matched controls, including the ACC. Analysis with other NR2B-specific ligands, [^{3}H] Ro 25,6981 and [^{3}H] CP-101,606, replicated this finding of an overall preservation of NR2B receptors in the ACC (and many other brain structures). [^{3}H] RGH-896 produced a similar binding expression profile to [^{3}H] Ro 25,6981 and [^{3}H] CP-101,606. The levels of [^{3}H] CP-101,606 binding were generally lower than both [^{3}H] RGH-896 and [^{3}H] Ro 25,6981 (comparable levels), consistent again with the proposed relative selectivity of CP-101,606 for a subpopulation of NR2B receptors. Furthermore, this thesis provides the first evidence for a correlation between higher NR2B receptors in the ACC of DLB cases with the presence of auditory hallucinations. Such as, correlation was not seen

with other psychotic symptoms.

To achieve additional information about RGH-896 pharmacology may other experiments could be proposed. Here, only NR1/NR2A/NR2B combination of NMDA subunit complexes has been investigated. It would be very useful to look at other subunit combinations known to exist in the CNS (for example, NR1/NR2B/NR2D) as this would confirm the overall subunit selectivity of this novel ligand. Competition curves in Chapter 2 for RGH-896 binding to HEK 293 cell homogenates revealed the presence of an apparent low-affinity binding site. The binding of RGH-896 to the low affinity site requires further investigation as preliminary results indicate RGH-896 is not binding to the σ-site, being insensitive to 1,3-di-o-tolylguanidine (DTG) (unpublished observations). Regarding the rodent autoradiographical study, although RGH-896 is highly selective for structures of the brain that contain predominantly NR2B-containing receptors, the identity of the RGH-896 binding site in the cerebellum remains unclear. There may still be the possibility that this ligand is binding additional binding sites other than the NR1/NR2B and NR1/NR2A/NR2B combination. A more detailed human autoradiography study would provide additional information as the number of cases in this pilot study was modest; a larger cohort of cases and investigating more anatomical regions of the brain which are linked to psychosis and other DLB symptoms would be beneficial. To determine the exact binding site for RGH-896, site-directed mutagenesis studies could be considered as these studies determine the residues which are absolutely required for high-affinity binding (See Gallagher *et al.*, 1996). As the data in this thesis is *in vitro* and *ex vivo*, there is a huge potential for *in vivo* models to help acquire more information. *In vivo* models could potentially be utilised to investigate the effects of RGH-896, in particular, its effects upon in

emotional and cognitive behaviours (both are known to involve the ACC and are common symptoms in DLB). The ACC seems to be especially involved when effort is required to conduct a task involving early memory and problem solving (Allman *et al.*, 2001). NMDA receptors are critical for learning and memory as non-selective and uncompetitive NMDA receptor antagonists disrupt learning and memory in animals and humans. Novel all-in-one animal behavioural models developed in our laboratory may prove very useful to assess the effects of RGH-896 upon emotional and cognitive behaviours (Ennaceur *et al.*, 2006a,b, unpublished manuscripts). Initial studies showed ifenprodil and eliprodil to be effective in seizure and stroke models at doses which do not disrupt learning and memory (Sanger and Joly, 1991; Clissold *et al.*, 1992; Patat *et al.*, 1994; Doyle *et al.*, 1998). More recently, Guscott *et al* (2002) showed pre-treatment of CP-101,606 had no effect on acquisition training in the Morris watermaze task, signifying the selective NR2B receptor antagonist does not impair spatial memory in rats. These studies indicate RGH-896, an overall NR1/NR2B selective receptor antagonist, ought to provide therapeutic effects without unwanted cognitive deficits. Several major pharmaceutical companies have reported news of NR2B receptor antagonists in Phase I and Phase II clinical trials for various CNS pathologies, most notably chronic pain (ACC plays a role in this process) (Brown and Krupp, 2006; Chizh and Headley, 2005; Muir, 2006; McCauley, 2005). To date, any further work of the NR2B receptor antagonists have been deferred until Phase II results of RGH-896 are published by Gedeon Richter. This Phase II clinical trial for RGH-896 is investigating its role for the treatment of neuropathic pain. RGH-896 and its related compounds from the company can potentially block pain signalling without interacting with other NMDA receptor subtypes thus have the ability to improve the therapeutic index and the side effect profile of this class of compound. If

this class of compound is successful for treating pain states, then companies will test the potential for this compound in many other disease areas, including psychosis, where glutamate transmission plays a key role. This thesis forms the basis of novel methodologies and investigations into the molecular pharmacology of RGH-896. The findings presented in this thesis should form a solid foundation for the commencement of additional projects in the future.

References

A

Aarsland, D., Ballard, C., Larsen, J.P. & McKeith, I. (2001). A comparative study of psychiatric symptoms in dementia with Lewy bodies and Parkinson's disease with and without dementia. *International Journal of Geriatric Psychiatry*, **16**, 528-536.

Adeagbo, A.S. (1984). Vascular relaxation by ifenprodil in the isolated perfused rat mesenteric artery. *Journal of Cardiovascular Pharmacology*, **6**, 1142-1147.

Akazawa, S., Shigemoto, R., Bessho, Y., Nakanishi, S. & Mizuno, N. (1994). Differential expression of five *N*-methyl-D-aspartate receptor subunit mRNAs in the cerebellum of developing and adult rats. *Journal of Comparative Neurology*, **347**, 150-160.

Albert, M. S. & Funkenstein, H.H. (1992). The effects of age: normal variation and its relation to disease. In: Ashbury, A.K., McKhann, G.M. & McDonald, W.I, editors. *Diseases of the nervous system: clinical neurobiology*. Philadelphia: Saunders; p598-611.

Alder, C.M., Malhotra, A.K., Elman, I., Goldberg, T., Egan, M., Pickar, D. & Breier, A. (1999). Comparison of ketamine-induced thought disorder in healthy volunteers and thought disorder in schizophrenia. *American Journal of Psychiatry*, **156**, 1646-1649.

Allman, J.M., Hakeem, A., Erwin, J.M., Nimchinsky, E. & Hof, P. (2001). The anterior cingulate cortex: The evolution of an interface between emotion and cognition. *Annals New York Academy of Sciences*, **935**, 107-117.

Anson, L.C., Chen, P.E., Wyllie, D.J.A., Colquhoun, D. & Schoepfer, R. (1998). Identification of amino acid residues of the NR2A subunit that control glutamate potency in recombinant NR1/NR2A NMDA receptors. *Journal of Neuroscience*, **18**, 581-589.

Angrist, B., Sathananthan, G., Wilk, S. & Gershon, S. (1974). Amphetamine psychosis: behavioural and biochemical aspects. *Journal of Psychiatry Research*, **11**, 13-23.

Avenet, P., Leonardon, J., Besnard, F., Graham, D., Depoortere, H. & Scatton, B. (1997). Antagonist properties of eliprodil and other NMDA receptor antagonists at rat NR1A/NR2A and NR1A/NR2B receptors expressed in Xenopus oocytes. *Neuroscience Letters*, **223**, 133-136.

B

Bai, L., Ontl, T., Xing, Y., Scruggs, B., Anderson, K., Aniya, J. *et al.* (2002). Relationships between NMDA receptor expression in prefrontal cortex and spatial reference and working memory during aging. *Society of Neuroscience Abstracts*, **28**, 94.4

Bai, L., Hof, P.R., Standaert, D.G., Xing, Y., Nelson, S.E., Young, A.B. & Magnusson, K.R. (2004). Changes in expression of the NR2B subunit during aging in macaque monkeys. *Neurobiology of aging*, **25**, 201-208.

Ballard, C., Holmes, C., McKeith, I., Neill, D., O'Brien, J., Cairns, N. *et al*, (1999). Psychiatric morbidity in dementia with Lewy bodies: a prospective clinical and neuropathological comparative study with Alzheimer's disease. *American Journal of Psychiatry*, **156**, 1039-1045.

Ballard, C.G., O'Brien, J.T., Swann, A.G., Thompson, P., Neill, D. & McKeith, I.G. (2001). The natural history of psychosis and depression in dementia with Lewy bodies and Alzheimer's disease: persistence and new cases over 1 year follow-up. *Journal of Clinical Psychiatry*, **62**, 46-49.

Barton, M.E. & White, H.S. (2004). The effect of CGX-1007 and CI-1041, novel NMDA receptor antagonists, on kindling acquisition and expression. *Epilepsy Research*, **59**, 1-12.

Barton, M.E., White H.S. & Wilcox, K.S. (2004). The effect of CGX-1007 and CI-1041, novel NMDA receptor antagonists, on NMDA receptor-mediated EPSCs. *Epilepsy Research*, **59**, 13-24.

Bear, M.F., Connors, B.W. & Paradiso, M.A. (1996). Neuroscience: Exploring the brain, p26, *Williams & Wilkins, London, UK.*

Ben-Ari, Y., Tremblay, E. & Ottersen, O.P. (1980). Injections of kainic acid into the amygdaloid complex of the rat: an electographic, clinical and histological study in relation to the pathology of epilepsy. *Neuroscience*, **5**, 515-528.

Benes, F.M. (2000). Emerging principles of altered neural circuitry in schizophrenia. *Brain Research Reviews*, **31**, 342-349.

Benke, D., Wenzel, A., Scheurer, L., Fritschy, J.M. & Möhler, H. (1995). Immunobiochemical characterization of the NMDA-receptor subunit NR1 in the developing and adult rat brain. *Journal of Receptor Signal Transduction Research*, **15**, 393-411.

Bennett J. A. & Dingledine, R.(1995). Topology profile for a glutamate receptor: three transmembrane domains and a channel-lining reentrant membrane loop. *Neuron*, **14**, 373-384.

Benetello, P. (1995). New antiepileptic drugs. *Pharmacological Research*, **31**, 155-162.

Bettler, B., Boulter, J., Hermans-Borgmeyer, I., O'Shea-Greenfield, A., Deneris, E.S., Moll, C., Borgmeyer, U., Hollmann, M. & Heinemann, S. (1990). Cloning of a novel glutamate receptor subunit, GluR5: expression in the nervous system during development. *Neuron*, **5**, 583-595.

Bi,X., Rong,Y., Chen,J., Dang,S., Wang, Z. & Baudry, M. (1998). Calpain-mediated regulation of NMDA receptor structure and function. *Brain Research*, **790**, 245-253.

Birch, P.J., Grossman, C.J. & Hayes, A.G. (1988). 6, 7-Dinitro-quinoxaline-2,3-dion and 6-nitro,7-cyano-quinoxaline-2,3-dion antagonise responses to NMDA in the rat spinal cord via an action at the strychnine-insensitive glycine receptor. *European Journal of Pharmacology*, **156**, 177-180

Biton, B., Granger, P., Depoortere, H., Scatton, B. & Avenet, P. (1995). Block of P-type Ca^{2+} channels by the NMDA receptor antagonist eliprodil in acutely dissociated rat Purkinje cells. *European Journal of Pharmacology*, **294**, 91-100.

Blackwood, N.J., Howard, R.J., ffytche, D.H., Simmons, A., Bentall, R.P. & Murray, R.M. (2000). Imaging attentional and attributional bias: an fMRI approach to the paranoid delusion. *Psychological Medicine*, **30**, 873-883.

Blahos, J. 2nd & Wenthold, R.J. (1996). Relationship between N-methyl-D-aspartate receptor NR1 splice variants and NR2 subunits. *Journal of Biological Chemistry*, **271**, 15669-15674.

Bleakman, D. & Lodge, D. (1998). Neuropharmacology of AMPA and kainite receptors. *Neuropharmacology*, **37**, 1187-1204.

Bleuler, E. (1911). Dementia Praecox. The Group of Schizophrenias, (trans J.Zinkin, 1950). New York: International Universities Press.

Bliss. T.V.P. & Lømo, T. (1973). Long-lasting potentiation of synaptic transmission in the denate area of the anaesthetised rabbit following stimulation of the perforant path. *Journal of Physiology*, **232**, 331-356.

Bliss, T.V.P. & Collingridge, G.L. (1993). A synaptic model of memory: long-term potentiation in the hippocampus. *Nature*, **1**, 623-634.

Blumberg, H.P., Stern, E., Martinez, D., Ricketts, S., de Asis, J., White, T., Epstein, J., McBride, P.A., Eidelberg, D., Kocsis, J.H. & Silbersweig, D.A. (2000). Increased anterior cingulate and caudate activity in bipolar mania. *Biological Psychiatry*, **48**, 1045-1052.

Boeckman, F.A. & Aizenman, E. (1996). Pharmacological properties of acquired excitotoxicity in Chinese hamster ovary cells transfected with N-methyl-D-aspartate receptor subunits. *Journal of Pharmacology and Experimental Therapeutics*, **279**, 515-523.

Bochet, P., Audinat, E., Lambolez, B., Crepel, F., Rossier, J., Iino, M., Tsuzuki, K. & Ozawa, S. (1994). Subunit composition at the single-cell level explains functional properties of a glutamate-gated channel. *Neuron,* **12**, 383-388.

Bordi, F., Pietra, C., Ziviani, L. & Reggiani, A. (1997). The glycine antagonist GV150526 protects somatosensory evoked potentials and reduced the infarct area in the MCAo model of focal ischemia in the rat. *Experimental Neurobiology*, **145**, 425-433.

Boyce, S., Wyatt, A., Webb, J.K., O'Donnell, R., Mason, G., Rigby, M., Sirinathsinghji, D., Hill, R.G., & Rupniak, N.M. (1999). Selective NMDA NR2B antagonists induce antinociception without motor dysfunction: correlation with restricted localisation of NR2B subunit in dorsal horn. *Neuropharmacology,* **38**, 611-623.

Brimcombe, J.C., Boeckman, F.A. & Aizenman, E. (1997). Functional consequences of NR2 subunit composition in single recombinant N-methyl-D-aspartate receptors. *Proceedings of the National Academy of Sciences USA,* **94,** 11019-11024.

Brimecombe, J.C., Gallagher, M.J., Lynch, D.R. & Aizenman, E. (1998). An NR2B point mutation affecting haloperidol and CP101,606 sensitivity of single recombinant *N*-methyl-D-aspartate receptors. *Journal of Pharmacology and Experimental Therapeutics,* **286**, 627-634.

Broca, P. (1878). Anatomie comparé de circonvolutions cérébrales. Le grand lobe limbique et la scissure limbique dans le série des mammiféres. *Revue d'Anthropologie,* **1**, 385-498.

Brody, A.L., Saxena, S., Mandelkern, M.A., Fairbanks, L.A., Ho, M.L. & Baxter, L.R. (2001). Brain metabolic changes associated with symptom factor improvement in major depressive disorder. *Biological Psychiatry*, **50**, 171-178.

Brose, N., Gasi,c G.P., Vetter, D.E., Sullivan, J.M. & Heinemann, S.F. (1993). Protein chemical characterization and immunocytochemical localization of the NMDA receptor subunit NMDA R1. *Journal of Biological Chemistry,* **268**, 22663-71.

Brown, D.G. & Krupp, J.J. (2006). N-methyl-D-aspartate receptor (NMDA) antagonists as potential pain therapeutics. *Current Topics in Medicinal Chemistry*, **6**, 749-770.

Buchan, A.M., Li, H., Cho, S. & Pulsinelli, W.A. (1991). Blockade of AMPA receptor prevents CA1 hippocampal injury following severe transient forebrain ischemia in adult rats. *Neuroscience Letters*, **132**, 255-258.

Buller, A.L., Larson, H.C., Schneider, B.E., Beaton, J.A., Morrisett, R.A. & Monaghan, D.T. (1994). The molecular basis of NMDA receptor subtypes: native receptor diversity is predicted by subunit composition. *Journal of Neuroscience*, **14**, 5471-5484.

Bush, G., Luu, P. & Posner, M.I. (2000). Cognitive and emotional influences in the anterior cingulate cortex. *Trends in Cognitive Sciences*, **4**, 215-222.

Byrne, E., Lennox, G., Lowe, J. & Godwin-Austin, R.B. (1989). Diffuse Lewy body disease: clinical features in 15 cases. *Journal of Neurological and Neurosurgical Psychiatry*, **52**, 709-717.

C

Carlsson, A. & Lindqvist, M. (1963). Effect of chlorpromazine of halperidol on formation of 3'-methyoxytyramine and normetanephrine in mouse brain. *Acta Pharmacological Toxicology*, **20**, 140–144.

Carlsson, M. & Carlsson, A. (1990). Interactions between glutamatergic and monoaminergic systems within the basal ganglia: implications for schizophrenia and Parkinson's disease. *Trends in Neurosciences*, **13**, 272-276.

Carter, C., Benavides, J., Legendre, P., Vincent, J.D., Noel, F., Thuret, F., Lloyd, K.G., Arbilla, S., Zivkovic, B., MacKenzie, E.T., Scatton, B. & Langer, S.Z. (1988). Ifenprodil and SL 82.0715 as cerebral anti-ischemic agents. II: Evidence for N-methyl-D-aspartate antagonist properties. *Journal of Pharmacology and Experimental Therapeutics*, **247**, 1222-1232.

Carter, C.S., MacDonald III, A.W., Ross, L.L. & Stenger, V.A. (2001). Anterior cingulate cortex activity and impaired self-monitoring of performance in patients with schizophrenia: an event-related fMRI study. *American Journal of Psychiatry*, **158**, 1423-1428.

Charton, J.P., Herkert, M., Becker, C.M. & Schroder, H. (1999). Cellular and subcellular localization of the 2B-subunit of the NMDA receptor in the adult rat telencephalon. *Brain Research*, **816**, 609-617.

Chatterton, J.E., Awobuluyi, M., Premkumar, L.S., Takahashi, H., Talantova, M. (2002). Excitatory glycine receptors containing the NR3 family of NMDA receptor subunits. *Nature*, **415**, 79398.

Chazot, P.L., Cik, M. & Stephenson, F.A. (1992). Immunological detection of the NMDAR1 glutamate receptor subunit expressed in human embryonic kidney 293 cells and in rat brain. *Journal of Neurochemistry*, **59**, 1176-1178.

Chazot, P.L., Fotherby, A. & Stephenson, F.A. (1993). Evidence of the involvement of a carboxyl group in the vicinity of the MK801 and magnesium ion binding site of the N-methyl-D-aspartate receptor. *Biochemical Pharmacology*, **45**, 605-610.

Chazot, P.L., Coleman, S.K., Cik, M. & Stephenson, F.A. (1994). Molecular characterisation of NMDA receptors expressed in mammalian cells yields evidence for the coexsistence of three subunit types within a discrete receptor molecule. *Journal of Biological Chemistry*, **269**, 24403-24409.

Chazot, P.L., Cik, M. & Stephenson, F.A. (1995). An investiagation into the role of N-Glycosylation in the functional expression of a recombinant heteromeric NMDA receptor. *Molecular Membrane Biology,* **12,** 331-337.

Chazot, P.L. & Stephenson, F.A. (1997a). Biochemical evidence for the existence of a pool of unassembled C2 Exon-containing NR1 subunits of the mammalian forebrain NMDA receptor. *Journal of Neurochemistry,* **68**, 507-516.

Chazot, P.L. & Stephenson, F.A. (1997b). Molecular dissection of native mammalian forebrain NMDA receptors containing the NR1 C2 exon: direct demonstration of NMDA receptors comprising NR1, NR2A, and NR2B subunits within the same complex. Journal *of Neurochemistry*, **69**, 2138-2144.

Chazot, P.L., Pollard, S. & Stephenson, F.A. (1998). Immunoprecipitation of receptors: In: Boulton, A.A., Baker, G.B. & Bateson, A.N. (Eds.), *Neuromethods*, 34, Humana Press Inc., Towowa, NJ.

Chazot, P.L., Cik, M., Stephenson, F.A. (1999). Transient expression of functional NMDA receptors in mammalian cells. *Methods in Molecular Biology*, **128**, 33-42.

Chazot, P.L. (2000). CP-101,606. *Current Opinion in Investigational Drugs,* **1**, 370-374.

Chazot, P.L., Lawrence, S. & Thompson, C.L. (2002). Studies on the subtype selectivity of CP-101,606: evidence for two classes of NR2B-selective NMDA receptor antagonists. *Neuropharmacology*, **42**, 319-324.

Chazot, P.L. (2004). The NMDA receptor NR2B Subunit: A Valid Therapeutic Target for Multiple CNS Pathologies. *Current Medicinal Chemistry*, **11,** 389-396.

Chenard, B.L., Bordner, J., Butler, T.W., Chambers, L.K., Collins, M.A., De Costa, D.L., Ducat, M.F., Dumont, M.L., Fox, C.B., Mena, E.E., Menniti, F.S., Nielson, J., Pagnozzi, M.J., Richter, K.E.G., Ronau, R.T., Shalaby, I.A., Stemple, J.Z. & White, W.F. (1995). (1*S*,2*S*)-1-(4-Hydroxyphenyl)-2-(4-hydroxy-4-phenylpiperidino)-1-propanol: A potent new neuroprotectant which blocks *N*-methyl-D-aspartate responses. *Journal of Medicinal Chemistry,* **38,** 3138-3145.

Cheng, Y. & Prusoff, W.H. (1973). Relationship between the inhibition constant (K_I) and the concentration of inhibitor which causes 50 per cent inhibition (I_{50}) of an enzymatic reaction. *Biochemical Pharmacology*, **22**, 3099-3108.

Chiodo, L.A. & Bunney, S.B. (1983). Typical and atypical neuroleptics: differential effects of chronic administration on the activity of A9 and A10 midbrain dopamingeric neurons. *Journal of Neuroscience,* **3**, 1607-1619.

Chizh, B.A., Headley, P.M. & Tzschentke, T.M. (2001). NMDA receptor antagonists as analgesics: focus on the NR2B subtype. *Trends in Pharmacological Sciences*, **22**, 636-642.

Chizh, B.A. & Headley, P.M. (2005). NMDA antagonist and neuropathic pain – multiple drug targets and multiple uses. *Current Pharmaceutical Design*, **11**, 2977-2994.

Choi, D.W. (1988). Glutamate Neurotoxicity and Diseases of the Nervous System. *Neuron*, **1**, 623-634.

Choi, D.W. & Rothman, S.M. (1990). The role of glutamate neurotoxicity in hypoxic-isochemic neuronal death. *Annual Review of Neuroscience*, **13**, 171-182.

Ciabarra, A. M., Sullivan, J.M., Gahn, L.G., Pecht, G., Heinemann, S. & Sevarino, K.A. (1995). Cloning and characterization of chi-1: a developmentally regulated member of a novel class of the ionotropic glutamate receptor family. *Journal of Neuroscience*, **15**, 6498–6508

Cik, M., Chazot, P.L. & Stephenson, F.A. (1993). Optimal expression of cloned NMDAR1/NMDAR2A heteromeric glutamate receptors: a biochemical characterization. *Biochemical Journal*, **296**, 877-883.

Cleghorn, J., Garnett, E., Nahmais, C., Brown, G., Kaplan, R., Szechtman, H., *et al* (1990). Regional brain metabolism during auditory hallucinations in chronic schizophrenia. *British Journal of Psychiatry*, **157**, 562-570.

Clissold, D.B., Karbon, E.W., Ferkany, J.W., Hartmann, T. & Pontecorvo, M.J. (1992). Effects of strychnine-insensitive glycine receptor antagonists and sigma agents on working memory performance: comparison with dizocilpine and scopolamine. *Behavioural Pharmacology*, **3**, 393-402.

Collingridge, G.L. & Singer,W. (1990). Excitatory amino acid receptors and synaptic plasticity. *Trends in Pharmacological Sciences*, **11**, 290-296.

Collingridge, G.L. & Watkins, J.C. (1994). The NMDA Receptor, 2nd Ed, Oxford University Press, Oxford, UK.

Conn, P.J. (2003). Physiological roles and therapeutic potential of metabotropic glutamate receptors. *Annals of the New York Academy of Sciences*, **1003**, 12–21.

Conn, P.J. & Pin, J-P. (1997). Pharmacology and functions of metabotropic glutamate receptors. *Annual Review of Pharmacology and Toxicology*, **37**, 205–237.

Contreras, P.C., Bremer, M.E. & Gray, N.M. (1990). Ifenprodil and SL 82.0715 potently inhibit binding of [^{3}H]-(+)-3-PPP to binding sites in rat brain. *Neuroscience Letters*, **116**, 190-193.

Cotzias, G., Papavasilliou, P & Gellene, R. (1969). Modification of parkinsonism – chronic treatment with L-Dopa. *New England Journal of Medicine*, **28**, 337-345.

Coughenour, L.L. & Cordon, J.J. (1997). Characterization of haloperidol and trifluperidol as subtype-selective N-methyl-D-aspartate (NMDA) receptor antagonists using [^{3}H]TCP and [^{3}H]ifenprodil binding in rat brain membranes. *Journal of Pharmacology and Experimental Therapeutics*, **280**, 584-592.

Coultrap, S.J., Nixon, K.M., Alvestad, R.M., Valenzuela, C.F. & Browning, M.D. (2005). Differential expression of NMDA receptor subunits and splice variants among the CA1, CA3 and denate gyrus of the adult rat. *Molecular Brain Research*, **135**, 104-111.

Curtis, D.R., Phillis, I.W. & Watkins, J.C. (1959). Chemical excitation of spinal neurons. *Nature*, **183**, 611-612.

D

Dagert, M. & Ehrlich, S.D. (1979). Prolonged incubation in calcium chloride improves the competence of Escherichia coli cells. *Gene*, **6**, 23-28.

D'Amato, R.J., Zweig, R.M., Whitehouse, P.J., Wenk, G.L., Singer, H.S., Mayeux, R., Price, D.L. & Snyder, S.H. (1987). Aminergic system in Alzheimer's Disease and Parkinson's Disease. *Annals of Neurology*, **22**, 229-236.

Danysz, W., Zajaczkowski, W. & Parsons, C.G. (1995). Modulation of learning processes by ionotropic glutamate receptor ligands. *Behavioural Pharmacology*, **6**, 455-474.

Das, S., Sasaki, Y.F., Rothe, T., Premkumar, L. S., Takasu, M., Crandall, J. E., Dikkes, P., Conner, D. A., Rayudu, P. V., Cheung, W., Chen, H. S., Lipton, S. A. & Nakanishi, N. (1998). Increased NMDA current and spine density in mice lacking the NMDA receptor subunit NR3A. *Nature*, **393**, 377-381.

Davies, S.N. & Lodge, D. (1987). Evidence for involvement of N-methylaspartate receptors in "wind-up" of class 2 neurons in the dorsal horn of the rat. *Brain Research*, **424**, 402-406.

Deakin, J.F.W., Slater, P., Simpson, M.D.C., Gilchrist, A.C., Skan, W.J., Royston, M.C., Reynolds, G.P. & Cross, A.J. (1989). Frontal cortical and left temporal glutamatergic dysfunction in schizophrenia. *Journal of Neurochemistry*, **52**, 1781-1786.

Del Dotto, P., Pavese, N., Gambaccini, G., Bernardini, S., Metman, L.V., Chase, T.N. & Bonuccelli, U. (2001). Intravenous amantadine improves levadopa-induced dyskinesias: an acute double-blind placebo-controlled study. *Movement Disorders*, **16**, 515-520.

Devanand, D.P., Miller, L., Richards, M., Marder, K., Bell, K., Mayeux, R., *et al* (1992). The Columbia University scale for psychopathology in Alzheimer's disease. *Archives of Neurology*, **49**, 371-376.

Dewey, M.E., Copeland, J.R.M., Lobo, A., Saz, P. & Dia, S.L. (1992). Computerised diagnosis from a standardized history schedule: a preliminary communication about the organic section of the HAS-AGECAT system. *International Journal of Geriatric Psychiatry*, **7**, 443-446.

Di, X., Bullock, R., Watson, J., Fatouros, P., Chenard, B., White, F. & Corwin, F. (1997). Effect of CP 101,606, a novel NR2B subunit antagonist of the N-methyl-D-asparate receptor, on the volume of ischemic brain damage of cytotoxic braib edema after middle cerebral artery occlusion in the feline brain. *Stroke*, **28**, 2244-2251.

Dickenson, A.H. & Sullivan, A.F. (1987). Evidence for the role of the NMDA receptor in the frequency dependent potentiation of deep rat dorsal horn nociceptive neurons following C fibre stimulation. *Neuropharmacology*, **26**, 1235-1238.

Dingledine, R., McBain, C.J. & McNamara, J.O. (1990). Excitatory amino acid receptors in epilepsy. *Trends in Pharmacological Science*, **11**, 334-338.

Doyle, K.M., Feerick, S., Kirkby, D.L., Eddleston, A., Higgins, G.A. (1998). Comparison of various N-methyl-D-aspartate receptor antagonists in a model of short-term memory and on overt behaviour. *Behavioural Pharmacology*, **9**, 671-681.

Drejer, J. & Honore, T. (1988). New quinoxalinediones show potent antagonism of quisqualate responses in cultured mouse cortical neurons. *Neuroscience Letters*, **87**, 104-108.

Dunah AW, Yasuda RP, Wolfe BB. (1998). Developmental regulation of tyrosine phosphorylation of the NR2D NMDA glutamate receptor subunit in rat central nervous system. *Journal of Neurochemistry, 71, 1926-1934.*

E

Egebjerg, J., Bettler, B., Hermans-Borgmeyer, I. & Heinemann, S. (1991). Cloning of a cDNA for a glutamate receptor subunit activated by kainate but not AMPA. *Nature*, **351**, 745-748.

F

Feldman, R.S. & Quenzer, L.F. (1984). Fundamentals of Neuropsychopharmacology. *Sinaueur Associates Incorporated.*

Feldman, R.S., Meyer, J.S. & Quenzer, L.F. (1997). Principles of Neuropsychopharmacology. *Sinaueur Associates Incorporated.*

Ferrer-Montiel, A.V. & Montal, M. (1996). Pentameric subunit stoichiometry of a neuronal glutamate receptor. *Proceedings of the National Academy of Sciences USA*, **93**, 2741-2744.

Fischer, G., Mutel, V., Trube, G., Malherbe, P., Kew, J.N., Mohacsi, E., Heitz, M.P. & Kemp, J.A. (1997). Ro-256981, a highly potent and selective blocker of N-methyl-D-aspartate receptors containing the NR2B subunit. Characterisation in vitro. *Journal of Pharmacology and Experimental Therapeutics*, **283,** 1285-1292.

Folstein M.F., Folstein, S.E. & McHugh, P.R. (1975). Mini Mental State: a practical method for grading the state pf patients for the clinician. *Psychiatry Research*, **12**, 189-198.

Forrest, D., Yuzaki, M., Soares, H.D., Ng, L., Luk, D.C., Sheng, M., Stewart, C.L., Morgan, J.I., Connor, J.A. & Curran, T. (1994). Targeted disruption of NMDA receptor 1 gene abolishes NMDA response and results in neonatal death. *Neuron*, **13**, 325-38.

Foster, A.C. & Fagg, G.E. (1984). Acidic amino acid binding in mammalian neuronal membranes: their characteristics and relationship to synaptic receptors. *Brain Research Reviews*, **7**, 103-164.

Foster, A.C. & Wong, E.H.F. (1987). The novel anticonvulsant MK-801 binds to the activated state of the N-methyl-D-aspartate receptor in rat brain. *British Journal of Pharmacology*, **91,** 403-409.

Foster, A.C., Kemp, J.A., Leeson, P.D., Grimwood, S., Donald, A.E., Marshall, G.R., Priestley, T., Smith, J.D., & Carling, R.W. (1992). Kynurenic acid analogues with improved affinity and selectivity for the glycine site on the *N*-methyl-D-aspartate receptor from rat brain. *Molecular Pharmacology*, **41,** 914-922.

Franklin, S.O., Elliott, K., Zhu, Y-S., Wahlestedt, C. & Inturrisi, C.E. (1993). Quantitation of NMDA receptor (NMDA-R1) mRNA levels in the adult and developing rat CNS. *Molecular Brain Research*, **19**, 93-100.

Fuster, J.M. (1999). Synopsis of function and dysfunction of the frontal lobe. *Acta Psychiatrica Scandinavica*, **395**, 51-57.

G

Gaiarsa, J.L., Caillard, O. & Ben-Ari, Y. (2002). Long-term plasticity at GABAergic and glycinergic synapses: mechanisms and functional significance. *Trends in Neurosciences*, **25**, 564-570.

Gallagher, M.J., Huang, H., Pritchett, D.B. & Lynch, D.R. (1996). Interactions between ifenprodil and the NR2B subunit of the N-methyl-D-aspartate receptor. *Journal of Biological Chemistry*, **271**, 9603-9611.

Gao, X.M., Sakai, K., Roberts, R.C., Conley, R.R., Dean, B. & Tamminga, C.A. (2000). Ionotropic Glutamate Receptors and Expression of *N*-Methyl-D-Aspartate Receptor Subunits in Subregions of Human Hippocampus: Effects of Schizophrenia. *American Journal of Psychiatry*, **157**, 1141-1149.

Geiger, J.R.P., Melcher, T., Koh, D-S., Sakmann, B., Seeburg, P. H., Jonas, P. & Monyer, H. (1995). Relative abundance of subunit mRNAs determines gating and Ca^{2+} permeability of AMPA receptors in principal neurons and interneurons in rat CNS. *Neuron,* **15,** 193-204.

George, M.S., Ketter, T.A., Parekh, P.I., Rosinsky, N., Ring, H.A., Pazzaglia, P.J., Marangell, L.B., Callahan, A.M. & Post, R.M. (1997). Blunted left cingulate activation in mood disorder subjects during a response interference task (the Stroop). *Journal of Neuropsychiatry and Clinical Neuroscience*, **9**, 55-63.

Gill, R., Alanine, A., Bourson, A., Buttelmann, B., Fischer, G., Heitz, M-P., Kew, J.N.C., Levet-Trafit, B., Lorez, H-P., Malherbe, P., Miss, M.T., Mutel, V., Pinard, E., Roever, S., Schmitt, M., Trube, G., Wybrecht, R., Wyler, R. & Kemp, J.A. (2002). Pharmacological characterisation of Ro 63,1908 (1-[2-(4-hydroxy-phenoxy)-ethyl]-4-(4-methyl-benzyl)-piperidin-4-01), a novel sinotype-selective N-methyl-D-aspartate antagonist. *Journal of Pharmacology and Experimental Therapeutics*, **302**, 940-948.

Goebel, D.J. & Poosch, M.S. (1999). NMDA receptor subunit gene expression in the rat brain: A quantitative analysis of endogenous mRNA levels of NR1Com, NR2A, NR2B, NR2C, NR2D and NR3A. *Molecular Brain Research,* **69,** 164-170.

Golarai, G., Greenwood, A.C., Fenney, D.M. & Conner, J.A. (2001). Physiological and structural evidence for hippocampal involvement in persistent seizure susceptibility after traumatic brain injury. *Journal of Neuroscience*, **21**, 8523-8537.

Gotti, B., Duverger, D., Bertin, J., Carter, C., Dupont, R., Frost, J., Gaudilliere, B., MacKenzie, E. T., Rousseau, J., Scatton, B. & Wick, A. (1988). Ifenprodil and SL 82.0715 as cerebral anti-ischemic agents. I. Evidence for efficacy in models of focal cerebral ischemia. *Journal of Pharmacology and Experimental Therapeutics*, **247,** 1211-1221.

Grady, M.S., Charleston, J.S., Maris, D., Witgen, B.M. & Lifshitz, J. (2003). Neuronal and glial cell number in the hippocampus after experimental traumatic brain injury: analysis by stereological estimation. *Journal of Neurotrauma,* **20**, 929-941.

Gray, D. (2000). American Chemical Society 219th National Meeting (Part II) Division of Medicinal Chemistry Symposia, San Francisco, CA, USA. *IDDB Meeting Report,* March 26-30.

Grimwood, S., Le Bourdelles, B., Atack, J.R., Barton, C., Cockett, W., Cook, S.M., Gilbert, E., Hutson, P.H., McKernan, R.M., Myers, J., Ragan, C.I., Wingrove, P.B. & Whiting, P.J. (1996). Generation and characterisation of stable cell lines expressing recombinant human N-methyl-D-aspartate receptor subtypes. *Journal of Neurochemistry*, **66**, 2239-2247.

Grimwood, S., Slater, P., Deakin, J.F. & Hutson, P.H. (1999). NR2B-containing NMDA receptors are up-regulated in temporal cortex in schizophrenia. *Neuroreport*, **10**, 461-465.

Gurwitz, D. & Weizman, A. (2002). The NR2B subunit of glutamate receptors as a potential target for relieving chrinic pain: prospects and concerns. *Drug Discovery Today,* **7**, 403-406.

Guscott, M., Clarke, H., Murray, F., Grimwood, S., Hutson, P.H. & Bristow, L. (2002). The effect of (±)-CP-101,606, an NMDA receptor NR2B subunit selective antagonist, in the Morris watermaze. *European Journal of Pharmacology,* **476**, 193-199.

H

Harding, A.J., Broe, G.A. & Halliday, G.M. (2002). Visual hallucinations in Lewy body disease related to Lewy bodies in the temporal lobe. *Brain*, **125**, 391-403.

Harrison, P.J. (1997). Schizophrenia: a disorder of neurodevelopment? *Current Opinion in Neurobiology*, **7**, 285-289.

Harrison, P.J. & Weinberger, D.R. (2005). Schizophrenia genes, gene expression and neuropathology: on the matter of their convergence. *Molecular Psychiatry,* **10**, 40-68.

Hawkins, L. M., Chazot, P.L. & Stephenson, F.A. (1999). Biochemical evidence for the co-association of three N-methyl-D-aspartate (NMDA) R2 subunits in recombinant NMDA receptors. *Journal of Biological Chemistry,* **274**, 27211-27218.

Heckers, S., Heinsen, H., Heinsen, Y. & Beckmann, H. (1991). Cortex, white matter, and basal ganglia in schizophrenia: a volumetric post-mortem study. *Biological Psychiatry*, **29**, 556-66.

Hempel, A., Hempel, E., Schonknecht, P., Stippich, C. & Schroder, J. (2003). Impairment in basal limbic function in schizophrenia during affect recognition. *Psychiatry Research*, **122**, 115-124.

Herb, A., Burnashev, N., Werner, P., Sakmann, B., Wisden, W. & Seeburg, P.H. (1992). The KA-2 subunit of excitatory amino acid receptors shows widespread expression in brain and forms ion channels with distantly related subunits. *Neuron*, **8,** 775-785.

Hess, S.D., Daggett, L.P., Deal, C., Lu, C.C., Johnson, E.C. & Velicelebi, G. (1998). Functional characterization of human N-methyl-D-aspartate subtype 1A/2D receptors. *Journal of Neurochemistry*, **70**, 1269-1279.

Hirai, H., Kirsch, J., Laube, B., Betz, H. & Kuhse, J. (1996). The glycine binding site of the *N*-methyl-D-aspartate receptor subunit NR1: identification of novel determinants of co-agonist potentiation in the extracellular M3-M4 loop region. *Proceedings of the National Academy of Sciences USA,* **93,** 6031-6036.

Hocking, G. & Cousins, M.J. (2003). Ketamine in chronic pain management: an evidence based review. *Anaesthesia and Analgesia,* **97**, 1730-1739.

Hollmann, M., O'Shea-Greenfield, A., Rogers, S.W. & Heinemann, S. (1989). Cloning and functional expression of a member of the glutamate receptor family. *Nature*, **342**, 643-648.

Hollmann, M., Boulter, J., Maron, C., Beasley, L., Sullivan, J., Pecht, G. & Heinemann, S. (1993). Zinc potentiates agonist-induced currents at certain splice variants of the NMDA receptor. *Neuron*, **10**, 943-954.

Hollmann, M. & Heinemann, S. (1994). Cloned glutamate receptors. *Annual Review of Neuroscience*, **17**, 31-108.

Huntley, G.W., Vickers, J.C. & Morrison, J.H. (1994). Cellular and synaptic localization of NMDA and non-NMDA receptor subunits in neocortex: organizational features related to cortical circuitry, function and disease. *Trends in Neuroscience*, **17**, 536-543.

I

Ilyin, V.I., Whittemore, E.R., Guastella, J., Weber, E. & Woodward, R.M. (1996). Subtype-selective inhibition of *N*-methyl-D-aspartate receptors by haloperidol. *Molecular Pharmacology*, **50,** 1541-1550.

J

Jarvitt, D.C. & Zukin, S.R. (1991). Recent advances in the phencyclidine model of schizophrenia. *American Journal of Psychiatry*, **148**, 1301-1308.

Jentsch, J.D. & Roth, R.H. (1999). The neuropsychopharmacology of phencyclidine: From NMDA receptor hypofunction to the dopamine hypothesis of schizophrenia. *Neuropsychopharmacology*, **20**, 201-225.

Jonas, P., Racca, C., Sakmann, B., Seeburg, P. H. & Monyer, H. (1994). Differences in Ca^{2+} permeability of AMPA-type glutamate receptor channels in neocortical neurons caused by differential GluR-B subunit expression. *Neuron*, **12**, 1281-1289.

K

Kamboj, R.K., Schoepp, D.D., Nutt, S., Shekter, L., Korczak, B., True, R.A., Rampersad, V., Zimmerman, D.M. & Wosnick, M.A. (1994). Molecular cloning, expression and pharmacological characteristion of human EAA1, a human kainite receptor. *Journal of Neurochemistry*, **62**, 1-9.

Kamenetz, F., Tomita, T., Hsieh, H., Seabrook, G., Borchelt, D., Iwatsubo, T., Sisodia, S. & Malinow, R. (2003). APP processing and synaptic function. *Neuron*, **37**, 925-937.

Keinänen, K., Wisden, M., Sommer, B., Werner, P., Herb, A., Verdoorn, T.A., Sakmann, B. & Seeburg, P.H. (1990). A family of AMPA-selective glutamate receptors. *Science*, **249**, 556-560.

Keinänen, K., Arvola, M., Kuusinen, A. & Johnson, M. (1997). Ligand recognition in glutamate receptors: Insights from mutagenesis of the soluble AMPA-binding domain of GluR-D. *Biochemical Society Transactions*, **25**, 835-838.

Kemp, J.A. & McKernan, R.M. (2002). NMDA receptor pathway as drug targets. *Nature Neuroscience*, **5**, 1039-1042.

Kemp, J.A., Kew, J.N.C. & Gill, R. *Handbook of Experimental Pharmacology*. Vol. 141 (eds. Jonas, P. & Monyer, H.) 495-527 (Springer, Berlin, 1999).

Kew, J.N.C. & Kemp, J.A. (1998). An allosteric interaction between the NMDA receptor polyamine and ifenprodil sites in rat cultured cortical neurons. *Journal of Physiology*, **512**, 17-28.

Kew, J.N.C., Koester, A., Moreau, J-L., Jenck, F., Ouagazzal, A-M., Mutel, V., Richards, J.G., Trube, G., Fischer, G., Montkowski, A., Hundt, W., Reinscheid, R.K., Pauly-Evers, M., Kemp, J.A. & Bluethmann, H. (2000). Functional consequences of reduction in NMDA receptor glycine affinity in mice carrying targeted point mutations in the glycine binding site. *Journal of Neuroscience*, **20,** 4037-4049.

Kim, J.S., Kornhuber, H.H., Schmid-Burgk, W. & Holzmuller, B. (1980). Low cerebrospinal fluid glutamate in schizophrenic patients and a new hypothesis on schizophrenia. *Neuroscience Letters*, **20**, 379-382.

Klockgether, T. & Turski, L. (1990). NMDA antagonists potentiate antiparkinsonian actions of L-dopa in monoamine-depleted rats. *Annals of Neurology*, 28, 539-546.

Koh, J., Yang, L.L & Cotman, C.W. (1990). B-amyloid protein increase the vulnerability of cultured cortical neurons to excitotoxic damage. *Brain Research*, **533**, 315-32.

Kotter, H. (1994). Postsynaptic integration of glutamatergic and dopaminergic signals in the striatum. *Progression in Neurobiology*, **44**, 163-196.

Kreapelin, E. (1919). Dementia Praecox, (trans R.Barclay). Edinburgh: Livingstone.

Kremer, B., Weber, B. & Hayden, M.R. (1992). New insights into the clinical features, pathogenesis and molecular genetics of Huntington disease. *Brain Pathology*, **2**, 321-335.

Krystal, J.H., Karper, L.P., Seibyl, J.P., Freeman, G.K., Delaney, R., Bremner, J.D., Heninger, G.R., Bowers, M.B. & Charney, D.S. (1994). Subanesthetic effects of the noncompetitive NMDA antagonist, ketamine, in humans-psychotomimetic, perceptual, cognitive and neuroendocrine responses. *Archives of General Psychiatry*, **51,** 199-214.

Kuryatov, A., Laube, B., Betz, H. & Kuhse, J. (1994). Mutational analysis of the glycine-binding site of the NMDA receptor: Structural similarity with bacterial amino acid-binding proteins. *Neuron*, **12**, 1291-1300.

L

Lang, A.P. & Lozano, A.E. (1998). Parkinson's disease. *New England Journal of Medicine*, **339**, 1044-1053.

Laube, B., Hirai, H., Sturgess, M., Betz, H. & Kuhse, J. (1997). Molecular determinants of agonist discrimination by NMDA receptor subunits: analysis of the glutamate binding site on the NR2B subunit. *Neuron*, **18**, 493-503.

Laube, B., Kuhse, J. & Betz, H. (1998). Evidence for a tetrameric structure of recombinant NMDA receptors. *Journal of Neuroscience*, **18**, 2954-61.

Le Peillet, E., Arvin, B., Moncada, C. & Meldrum, B.S. (1992). The non-NMDA antagonists, NBQX and GYKI52466, protect against cortical and striatal cell loss following transient global ischaemia in the rat. *Brain Research*, **571**, 115-120.

Legendre, P. & Westbrook, G.L. (1991). Ifenprodil blocks N-methyl-D-aspartate receptors by a two-component mechanism. *Molecular Pharmacology*, **40**, 289-298.

Lewis, D.A. & Liebermann, J.A. (2000). Catching up on Schizophrenia: Natural History and Neurobiology. *Neuron*, **28**, 325-334.

Li, L., Fan, M., Icton, C.D., Chen, N., Leavitt, B.R., Hayden, M.R., Murphy, T.H. & Raymond, L.A. (2003). Role of NR2B-type NMDA receptors in selective neurodegeneration in Huntington disease. *Neurobiology of Aging*, **24**, 1113-1121.

Li, L., Murphy, T.H., Hayden, M.R. & Raymond, L.A. (2004). Enhanced striatal NR2B-containing N-methyl-D-aspartate receptor-mediated synaptic currents in a mouse model of Huntington disease. *Journal of Neurophysiology*, **92**, 2738-2746.

Lomeli, H., Wisden, W., Köhler, M., Keinänen, K., Sommer, B. & Seeburg, P.H. (1992). High-affinity kainate and domoate receptors in rat brain. *FEBS Letters*, **307**,139–143.

Löschmann, P.A., De Croote, C., Smith, L., Wüllner, U., Fischer, G., Kemp, J.A., Jenner, P. & Klockgether, T. (2004). Antiparkinsonian activity of Ro 25-6981, a NR2B subunit specific NMDA receptor antagonist, in animal models of Parkinson's disease. *Experimental Neurology*, **187**, 86-93.

Low, C-M., Lyuboslavsky, P., French, A., Le, P., Wyatte, K., Theil, W.H., Marchan, E.M., Igarashi, K., Kashiwagi, K., Gernert, K., Williams, K., Traynelis, S.F. & Zheng, F. (2003). Molecular determinants of proton-sensitive N-methyl-D-aspartate receptor gating. *Molecular Pharmacology*, **63**, 1212-1222.

Lowry, O.H., Rosebrough, N.J., Farr, A.L. & Randall, R.J. (1951). Protein measurement with the Folin phenol reagent. *Journal of Biological Chemistry*, **193**, 265-275.

Luis, C.A., Barker, W.W., Gajaraj, K., Harwood, D., Petersen, R., Kashuba, A., Waters, C., Jimison, P., Pearl, G., Petito, C., Dickson, D. & Duara, R. (1999). Sensitivity and specificity of three clinical criteria for dementia with Lewy bodies in an autopsy-verified sample. *International of Geriatric Psychiatry,* **14**, 526-533.

Luo, J., Wang, Y., Yasuda, R.P., Dunah, A.W. & Wolfe, B,B. (1997). The majority of N-methyl-D-aspartate receptor complexes in adult rat cerebral cortex contain at least three different subunits (NR1/NR2A/NR2B). *Molecular Pharmacology,* **1**, 79-86.

Lynch, D. R., Lawrence, J. J., Lenz, S., Anegawa, N. J., Dichter, M. & Pritchett, D. B. (1995). Pharmacological characterization of heterodimeric NMDA receptors composed of NR 1a and 2B subunits: Differences with receptors formed from NR 1a and 2A. *Journal of Neurochemistry*, **64,** 1462-1468.

Lynch, D.R. & Gallagher, M.J. (1996). Inhibition of N-methyl-D-aspartate receptors by haloperidol: Developmental and pharmacological characterization in native and recombinant receptors. *Journal of Pharmacology and Experimental Therapeutics,* **279,** 154-161.

Lynch, D.R., Shim, S.S., Seifert, K.M., Kurapathi, S., Mutel, V., Gallagher, M.J. & Guttmann, R.P. (2001). Pharmacological characterization of interactions of Ro-256981 with the NR2B (epsilon2) subunit. *European Journal of Pharmacology,* **416**, 185-195.

M

McBain, C. J. & Mayer, M. L. (1994). N-methyl-D-aspartic acid receptor structure and function. *Physiological Reviews,* **74**, 723-760.

McCauley, J.A. (2005). NR2B subtype-selective NMDA receptor antagonists: 2001-2004. *Expert Opinion in Therapeutic Patents,* **15**, 389-407.

McKeith, I.G., Galasko, D., Wilcock, G. & Byrne, J.E. (1995). Lewy body dementia: diagnosis and treatment. *British Journal of Psychiatry*, **167**, 709-717.

McKeith, I.G., Galasko, D., Kosaka, K., Perry, E.K., Dickson, D.W., Hansen, L.A., Salmon, D.P., Lowe, J., Mirra, S.S., Byrne, E.J., Lennox, G., Quinn, N.P., Edwardson, J.A., Ince, P.G., Bergeron, C., Burns, A., Miller, B.L., Lovestone, S., Collerton, D., Jansen, E.N., Ballard, C., De Vos, R.A., Wilcock, G.K., Jellinger, K.A. & Perry, R.H. (1996). Consensus guidelines for the clinical and pathologic diagnosis of dementia with Lewy bodies (DLB): report of the consortium on DLB International Workshop. *Neurology*, **47**, 1113-1124.

Madden, D.R. (2002). The structure and function of the glutamate receptor ion channels. *Nature Reviews Neuroscience*, **3**, 91-101.

Magnusson, K.R., Scanga, C., Wagner, A.E. & Dunlop, C. (2000). Changes in anesthetic sensitivity and glutamate receptors in the aging canine brain. *Journal of Gerontology in Biological Science*, **55A**, B448-54.

Magnusson, K.R. (2001). Influence of diet restriction on NMDA receptor subunits and learning during aging. *Neurobiology of Aging*, **22**, 613-627.

Mai, J.K., Paxinos, G., & Assheuer, J.K. (2004). Atlas of the Human Brain, Second Edition (Spiral-bound), *Elsevier Academic Press*, London, UK.

Malhotra, A.K., Pinals, D.A., Weingartner, H., Sirocco, K., Missar, C.D., Pickar, D. & Breier, A. (1996). NMDA receptor function and human cognition:the effects of ketamine in healthy volunteers. Neuropsychopharmacology, 14, 301-307.

Mano, I. & Teichberg, V.I. (1998). A tetrameric subunit stoichiometry for a glutamate receptors channel complex. *Neuroreport*, **9**, 327-331.

Marantz, A.G. & Verghese, J. (2002). Capgras' syndrome in dementia with Lewy bodies. *Journal of Geriatric Psychiatry and Neurology*, **15**, 239-241.

Marino, M.J., Valenti, O. & Conn, P.J. (2003). Glutamate receptors and Parkinson's disease: opportunities for intervention. *Drugs Aging*, **20**, 377-397.

Matsuda, K., Kamiya, Y., Matsuda, S. & Yuzaki, M. (2002). Cloning and characterization of a novel NMDA receptor subunit NR3B: a dominant subunit that reduces calcium permeability. *Molecular Brain Research,* **100,** 43-52.

Mattson, M.P., Guo, Z.H. & Geiger J.D. (1999). A secreted form of amyloid precursor protein enhances basal glucose and glutamate transport and protects against oxidative impairment of glucose and glutamate transport in synaptosome by cyclic GMP-mediated mechanism. *Journal of Neurochemistry*, **73**, 532-537.

Mayberg, H.S., Liotti, M., Brannan, S.K., McGinnis, S., Mahurin, R.K., Jerabek, P.A., Silva, J.A., Tekell, J.L., Martin, C.C., Lancaster, J.L. & Fox, P.T. (1999). Reciprocal limbic-cortical function as negative mood: converging PET findings in depression and normal sadness. *American Journal of Psychiatry*, **156**, 675-682.

Mayberg, H.S., Brannan, S.K., Tekell, J.L., Silva, J.A., Mahurin, R.K., McGinnis, S., Jarabek, P.A. (2000). Regional metabolic effects of fluoxetine in major depression: serial changes and relationship to clinical response. *Biological Psychaitry*, **48**, 830-843.

Mega, M.S., Lee, L., Dinov, I.D., Mishkin, F., Toga, A.W. & Cummings, J.L. (2000). Cerebral correlates of psychotic symptoms of Alzheimer's disease. *Journal of Neurology, Neurosurgery & Psychiatry*, **69**, 167-171.

Menniti, F., Chenard, B., Collins, M., Ducat, M., Shalaby, I. & White, F. (1997). CP 101,606, a potent neuroprotectant selective for forebrain neurons. *European Journal of Pharmacology*, **331**, 117-126.

Mentis, M.J., Weinstein, E.A., Horwitz, B., McIntosh, A.R., Pietrini, P., Alexander, G.E. *et al* (1995). Abnormal brain glucose metabolism in the delusional misidentification syndromes: a positron emission tomography study in Alzheimer's disease. *Biological Psychiatry*, **38**, 438-449.

Molina, J.A., Gomez, P., Vargas, C., Ortiz, S., Perez-Rial, S., Uriguen, L., Oliva, J.M., Villanueva, C. & Manzanares, J. (2005). Neurotransmitter amino acid in cerebrospinal fluid of patients with dementia with Lewy bodies. *Journal of Neural Transmission,* **112**, 557-563.

Monaghan, D.T., Yao, D. & Cotman, C.W. (1984). Distribution of [^{3}H]AMPA binding sites in rat brain as determined by quantitative autoradiography. *Brain Research*, **324**, 160164.

Montastruc, J.L., Rascol, O., Senard, J.M. & Rascol, A. (1992). A pilot study of N-methyl-D-aspartate (NMDA) antagonist in Parkinson's disease. *Journal of Neurological and Neurosurgical Psychiatry,* **55,** 630-631.

Monyer, H., Sprengel, R., Schoepfer, R., Herb, A., Higuchi, M,. Lomeli, H., Burnashev, N., Sakmann, B. & Seeburg, P.H. (1992). Heteromeric NMDA receptors: Molecular and functional distinction of subtypes. *Science*, **256**, 1217-1221.

Mori, H. & Mishina, M. (1995). Structure and function of the NMDA receptor channel. *Neuropharmacology,* **34**, 1219-1237.

Mott, D.D., Doherty, J.J., Zhang, S., Washburn, M.S., Fendley, M.J., Lyuboslavsky, P., Traynelis, S.F. & Dingledine, R. (1998). Phenylethanolamines inhibit NMDA receptors by enhancing proton inhibition. *Nature Neuroscience,* **1**, 659-667.

Muir, K.W. (2006). Glutamate-basesd therapeutic approaches: Clinical trials with NMDA antagonists. *Current Opinion in Pharmacology*, **6**, 53-60.

Mutel, V., Buchy, D., Klingelschmidt, A., Messer, J., Bleuel, Z., Kemp, J.A. & Richards J.G. (1998). In vitro binding properties in rat brain of [^{3}H]Ro 25-6981, a potent and selective antagonist of NMDA receptors containing NR2B subunits. *Journal of Neurochemistry,* **70,** 2147–2155.

N

Naito, S. & Ueda, T. (1983). Adenosine triphosphate-dependent uptake of glutamate into protein I-associated vesicles. *Journal of Biological Chemistry*, **258**, 696-699.

Nash, J.E., Hill, M.P. & Brotchie, J.M. (1999). Antiparkinsonian actions of blockade of NR2B-containing NMDA receptors in the reserpine-treated rat. *Experimental Neurology*, **155**, 42-48.

Nash, J.E., Fox, S.H., Henry, B., Hill, M.P., Peggs, D., McGuire, S., Maneuf, Y., Hille, C., Brotchie, J.M. & Crossman, A.R. (2000). Antiparkinsonian actions of ifenprodil in the MPTP-lesioned marmoset model of Parkinson's disease. *Experimental Neurology*, **165**, 136-142.

Nash, J.E. & Brotchie, J.M. (2002). Characterisation of striatal NMDA receptors involved in the generation of parkinsonian symptoms: intrastriatal microinjection studies in the 6-OHDA-lesioned rat. *Movement Disorders*, **17**, 455-466.

Nishi, M., Hinds, H., Lu, H.-P., Kawata, M. & Hayashi, Y. (2001). Motoneuron-specific expression of NR3B, a novel NMDA-type glutamate receptor subunit that works in a dominant-negative manner. *Journal of Neuroscience*, **21**, RC185.

Nowicka, D. & Kaczmarek, L. (1996). Spatio-temporal pattern of N-methyl-D-aspartate receptor NR1 mRNA expression during postnatal development of visual structures of the rat brain. *Journal of Neuroscience Research*, **44**, 471-477.

O

Obeso, J.A., Olanow, C.W. & Nutt, J.C. (2000). Levadopa motor complications in Parkinson's disease. *Trends in Neuroscience*, **23**, 52-57.

Ohmori, J., Sakamoto, S., Kubota, H., Shimizu-Sasamata, M., Okada, M., Kawasaki, S., Hidaka, K., Togami, J., Furuya, T. & Murase, K. (1994). 6-(1*H*-Imidazol-1-yl)-7-nitro-2,3(1*H*,4*H*)-quinoxalinedione hydrochloride (YM90K) and related compounds: structure-activity relationships for the AMPA-type non-NMDA receptor. *Journal of Medicinal Chemistry*, **37**, 467-475.

Ohtani, K., Tanaka, H., Yoneda, Y., Yasuda, H., Ito, A., Nagata, R. & Nakamura, M. (2002). In vitro and in vivo antagonistic activities of SM-31900 for the NMDA receptor gylcine-binding site. *Brain Research*, **944**, 165-173.

Ohtani, K., Tanaka, H. & Ohno, Y. (2003). SM-31900, a novel NMDA receptor glycine-binding site antagonist, reduces infarct volume induced by permanent middle cerebral artery occlusion in spontaneously hypertensive rats. *Neurochemistry International*, **42**, 375-384.

Olney, J.W. & Farber, M.D. (1995). NMDA receptor antagonists as neurotherapeutic drugs, psychotogens, neurotoxins and research tools for studying schizophrenia. *Neuropsychopharmacology*, **3**, 335-345.

Olney, J.W., Newcomer, J.W. & Farber, N.B. (1999). NMDA receptor hypofunction model of schizophrenia. *Journal of Psychiatric Research*, **33**, 523-533.

Olsson, T., Wieloch, T. & Smith, M.L. (2003). Brain damage in a mouse model of global cerebral ischemia: effect of NMDA receptor blockade. *Brain research*, **982**, 260-269.

Ottersen, O.P. & Storm-Mathisen, J. (1989). Excitatory and inhibitory amino acids in the hippocampus, in: Chan-Palay, V., Kohler, C. (Eds.), The Hippocampus-New Vistas, Alan R. Liss, pp. 97-117.

P

Papa, S.M. & Chase, T.N. (1996). Levodopa-induced dyskinesias improved by a glutamate antagonist in parkinsonian monkeys. *Annuals of Neurology*, **39**, 574-578.

Papez, J.W. (1937). A proposed mechanism of emotion. *Archives of Neurology and Psychiatry*, **38**, 725-743.

Parsons, C.G. (2001). NMDA receptors as targets for drug action in neuropathic pain. *European Journal of Pharmacology*, **429**, 71-78.

Patat, A., Molinier, P., Herguetta, T., Brohier, S., Zieleniuk, I., Danjou, P., Warot, D. & Puech, A. (1994). Lack of amnestic, psychotomimetic or impairing effect on psychomotor performance of eliprodil, a new NMDA antagonist. *International Clinical Psychopharmacology*, **9**, 155-162.

Perry, E.K., McKeith, I., Thompson, P. *et al* (1991). Topography, extent, and clinical relevance of neurochemical deficits in dementia of Lewy body type, Parkinson's disease and Alzheimer's disease. *Annals of the New York Academy of Sciences*, **640**, 197-202.

Perry, E.K., Court, J.A., Johnson, M., Smith, C.J., James, V., Cheng, A.V., Kerwin, J.M., Morris, C.M., Piggott, M.A., Edwardson. J.A. (1993). Autoradiographic comparison of cholinergic and other transmitter receptors in the normal human hippocampus. *Hippocampus*, **3**, 307-315.

Petralia, R.S. & Wenthold, R.J. (1992). Light and electron immunocytochemical localization of AMPA-selective glutamate receptors in the rat brain. *Journal of Comparative Neurology*, **318**, 329-354.

Petralia, R. S., Yokotani, N. & Wenthold, R. J (1994). Light and electron microscope distribution of the NMDA receptor subunit NMDAR1 in the rat nervous system using a selective anti-peptide antibody. *Journal of Neuroscience*, **14**, 667-696.

Piggott, M.A., Perry, E.K., Perry, R.H. & Court, J.A. (1992). [^{3}H]MK-801 binding to the NMDA receptor complex, and its modulation in human frontal cortex during development and aging. *Brain Research*, **588**, 277-286.

Pin, J-P. & Duvoisin, R. (1995). Neurotransmitter receptors I: The metabotropic glutamate receptors: structure and functions. *Neuropharmacology*, **34**, 1-26.

Priestley, T., Laughton, P., Myers, J., Le Bourdelles, B., Kerby, J. & Whiting, P.J. (1995). Pharmacological properties of recombinant human N-methyl-D-aspartate receptors comprising NR1a/NR2A and NR1a/NR2B subunit assemblies expressed in permanently transfected mouse fibroblast cells. *Molecular Pharmacology*, **48**, 841-848.

Premkumar, L. S. & Auerbach, A. (1997). Stoichiometry of recombinant N-methyl-D-aspartate receptor channels inferred from single-channel current patterns. *Journal of General Physiology*, **110**, 485-502.

Pujic, Z., Matsumoto, I. & Wilce, P.A. (1993). Expression of the gene coding for the NR1 subunit of the NMDA receptor during rat brain development. *Neuroscience Letters*, **162**, 67-70.

R

Rafiki, A., Chevassus-au-Louis, N., Ben-Ari, Y., Khrestchatisky, M. & Represa, A. (1998). Glutamate receptors in dysplasic cortex: an in situ hybridization and immunohistochemistry study in rats with prenatal treatment with methylazoxymethanol. *Brain Research*, **782**, 142–152.

Rainville, P., Duncan, G.H., Price D.D., Carrier, B. & Bushnell, M.C. (1997). Pain affect encoded in human anterior cingulate but not somatosensory cortex. *Science*, **277**, 968-970.

Reggiani, A., Pietra, C., Arban, R., Marzola, P., Guerrini, U., Ziviani, L., Boicelli, A., Sbarbati, A. & Osculati, F. (2001). The neuroprotective activity of the glycine receptor antagonist GV150526: an in vivo study by magnetic resonance imaging. *European Journal of Pharmacology*, **419**, 147-153.

Reynolds, I.J. & Miller, R.J. (1989). Ifenprodil is a novel type of N-methyl-D-aspartate receptor antagonist: interaction with polyamines. *Molecular Pharmacology*, **36**, 758-765.

Riva, M.A., Tascedda, F., Molteni, R. & Racagni, G. (1994). Regulation of NMDA receptor subunit mRNA expression in the rat brain during postnatal development. *Molecular Brain Research*, **25**, 209-216.

Rock, D.M. & MacDonald, R.L. (1992a). The polyamine spermine has multiple actions on N-methyl-D-aspartate receptor single-channel currents in cultured cortical neurons. *Molecular Pharmacology*, **41**, 83-88.

Rock, D.M. & MacDonald, R.L. (1992b). Spermine and related polyamines produce a voltage-dependent reduction of N-methyl-D-aspartate receptor single-channel conductance. *Molecular Pharmacology*, **42**, 157-164.

Rosenmund, C., Stern-Bach, Y., & Stevens, C.F. (1998). The tetrameric structure of a glutamate receptor channel. *Science*, **280**, 1596-1599.

Rossi, D.J., Oshima, T. & Attwell, D. (2000). Glutamate release in sever brain ischaemic is mainly by reversed uptake. *Nature*, **403**, 316-321.

Roth, M., Tym, E., Mountjoy, C.Q., Huppert, F.A., Hendrie, H., Verma, S. *et al* (1986). CAMDEX-A standardized instrument for the diagnosis of mental disorder in the elderly with special reference to the early detection of dementia. *British Journal of Psychiatry*, **149**, 698-709.

Rothman, S.M. & Olney, J.W. (1986). Glutamate and pathophysiology of hypoxic-ischemic brain damage. *Annuals of Neurology*, **19**, 105-111.

Rujescu, D., Bender, A., Keck, M., Hartmann, A.M., Ohl, F., Raeder, H., Giegling, I., Genius, J., McCarley, R.W., Moller, H.J. & Grunze, H. (2005). A pharmacologyical model for psychosis based on N-methyl-D-aspartate receptor hypofunction: molecular, cellular, functional and behavioural abnormalities. *Biological Psychiatry*, **59**, 721-729.

S

Sacaan, A.I. & Johnson, K.M. (1989). Spermine enhances binding to the glycine site associated with the N- methyl-D-aspartate receptor complex *Molecular Pharmacology*, 36, 836-839.

Salgado-Pineda, P., Baeza, I., Perez-Gomez, M., Vendrell, P., Junque, C., Bargallo, H. *et al.* (2003). Sustained attention impairment correlates to gray matter decreases in first episode neuroleptic-naive schizophrenic patients. *Neuroimage*, **19**, 365-375.

Sambrook. J., Fritsch, E.F. & Maniatis, T. (1989). Molecular Cloning: a laboratory manual. *Cold Spring Harbor Laboratory Press.* Cold Spring Harbor, New York.

Sandkuhler, J. (2000). Learning and memory in pain pathways. *Pain*, **88**, 113-118.

Sanger, D.J. & Joly, D. (1991). Effects of NMDA receptor antagonists and sigma ligands on the acquisition of conditioned fear in mice. *Psychopharmacology*, **104**, 27-34.

Sasaki, Y.F., Rothe, T., Premkumar, L.S., Das, S., Cui, J., Talantova, M.V., Wong, H-K., Gong, X., Chan, X.F., Zhang, D., Nakanishi, N., Sucher, N.J. & Lipton, S.A. (2002). Characterization and Comparison of the NR3A Subunit of the NMDA Receptor in Recombinant Systems and Primary Cortical Neurons. *Journal of Neurophysiology*, **87**, 2052-2063.

Schulz, S., Siemer, H., Krug, M. & Hollt, V. (1999). Direct evidence for biphasic cAMP responsive element-binding protein phosphorylation during long-term potentiation in the rat denate gyrus in vivo. *Journal of Neuroscience*, **19**, 5683-5692.

Schwarcz, R., Whetsell, W.O. & Mangano, R.M. (1983). Quinolinic acid: an endogenous metabolite that produces axon-sparing lesions in the rat brain. *Science*, **219**, 316-318.

Seeburg, P.H. (1993). The molecular biology of mammalian glutamate receptor channels. *Trends in Neuroscience*, **16**, 359-365.

Selemon, L.D. & Goldman-Rakic, P.S. (1999). The reduced neuropil hypothesis: a circuit based model of schizophrenia. *Biological Psychiatry*, **45**, 17-25.

Selkoe, D.J. (1991). The molecular pathology of Alzheimer's Disease. *Neuron*, **6**, 487-198.

Shapiro, R.M. (1993). Regional neuropathology in schizophrenia: Where are we? Where are we going? *Schizophrenia Research*, **10**, 187-239.

Sheardown, M.J., Nielsen, E.O., Hansen, A.J., Jacobsen, P. & Honore, T. (1990). 2,3-Dihydroxy-6-nitro-7-sulfamoyl-benzo(F)quinoxaline: a neuroprotectant for cerebral ischemia. *Science (Wash DC)*, **247**, 571-574.

Sheng, M., Cummings, J., Roldan, L.A., Jan, Y.N. & Jan, L.Y. (1994). Changing subunit composition of heteromeric NMDA receptors during development of rat cortex. *Nature*, **368**, 144-147.

Shergill, S.S., Brammer, M.J., Williams, S.C., Murray, R.M. & McGuire, P.K. (2000). Mapping auditory hallucinations in schizophrenia using functional magnetic resonance imaging. *Archives of General Psychiatry*, **57**, 1033-1038.

Sloviter, R.S. (1991). Permanently altered hippocampal structure, excitability, and inhibition after experimental status epilepticus in the rat: the "dormant basket cell" hypothesis and its possible relevance to temporal lobe epilepsy. *Hippocampus*, **1**, 41-66.

Song, D., Xie, X., Wang, Z. & Berger, T.W. (2001). Differential effect of TEA on long-term synaptic modification in hippocampal CA1 and denate gyrus in vitro. *Neurobiology of Learning and Memory*, **76**, 375-387.

Steece-Collier, K., Chambers, L.K., Jaw-Tsai, S.S., Menniti, F.S. & Greenamyre, J.T. (2000). Antiparkinsonian actions of CP 101,606, an antagonist of NR2B subunit-containing N-methylD-aspartate receptors. *Experimental Neurology*, **163**, 239-243.

Steinpreis, R.E. (1996). The behavioural and neurochemical effects of phencyclidine in humans and animals: some implications for modeling psychosis. *Behavioural Brain Research*, **74**, 45-55.

Stensbol, T.B., Madsen, U. & Krogsgaard-Larsen, P. (2002). The AMPA receptor binding site: focus on agonists and competitive antagonists. *Current Pharmaceutical Design*, **8**, 857-72.

Stevens, J.R. (1973). An anatomy of schizophrenia? *Archives of General Psychiatry*, **29**, 177-190.

Storm-Mathisen, J., Otterson, O.P., FuLong, T., Gundersen, V., Laake, J.H. & Nordbo, G. (1986). Metabolism and transport of amino acids studied by immunocytochemistry. *Medicinal Biology*, **64**, 127-132

Sucher, N.J., Akbarian, S., Chi, C.L., Lecler, c.C.L., Awobuluyi, M., Deitcher, D.L., Wu, M.K., Yuan, J.P., Jones, E.G. & Lipton, S.A. (1995). Developmental and regional expression pattern of a novel NMDA receptor-like subunit (NMDA-L) in the rodent brain. *Journal of Neuroscience,* **15**, 6509-6520.

Sultzer, D.L., Brown, C.V., Mandelkern, M.A., Mahler, M.E., Mendez, M.F., Chen, S.T. *et al* (2003). Delusional thoughts and regional frontal/temporal cortex metabolism in Alzheimer's disease. *American Journal of Psychiatry*, **160**, 341-349.

Sun, L., Margolis, F.L., Shipley, M.T. & Lidow, M.S. (1998). Identification of a long variant of mRNA encoding the NR3 subunit of the NMDA receptor: its regional distribution and developmental expression in the rat brain. *FEBS Letters*, **441**, 392-396.

Sutcliffe, M.J., Wo, Z.G. & Oswald, R.E. (1996). Three-dimensional models of non-NMDA glutamate receptors. *Biophysical Journal,* **70**, 1575-1589.

Szatkowski, M. & Attwell, D. (1994). Triggering and execution of neuronal death in brain ischemia: two phases of glutamate release by different mechanisms. *Trends in Neuroscience*, **17**, 359-365.

Szydlowska, K., Kaminska, B., Baude, A., Parsons, C.G. & Danysz, W. (2007). Neuroprotective activity of selective mGlu1 and mGlu5 antagonists in vitro and in vivo. *European Journal of Pharmacology*, **554**, 18-29.

T

Takai, H., Katayama, K., Uetsuka, K., Nakayama, H. & Doi, K. (2003). Distribution of N-methyl-D-aspartate receptors (NMDARs) in the developing rat brain. *Experimental and Molecular Pathology,* **75**, 89-94.

Takano, K., Tatlisumak, T., Formato, J.E., Carano, R.A., Bergmann, A.G., Pullan, L.M., Bare, T.M., Sotak, C.H. & Fisher, M. (1997). Glycine site antagonists attenuates infarct size in experimental ischemia: postmortem and diffusion mapping studies. *Stroke*, **28**, 1255-1263.

Takaoka, S., Bart, R.D., Pearlstein, R., Brinkhous, A. & Warner, D.S. (1997). Neuroprotective effect of NMDA receptor glycine recognition site antagonism persists when brain temperature is controlled. *Journal of Cerebral Blood Flow Metabolism,* **17**, 161-167.

Tamaru, M., Yoneda, Y., Ogita, K., Shimizu, J. & Nagata, Y. (1991). Age-related decreases of the NMDA receptor complex in the rat cerebral cortex and hippocampus. *Brain Research*, **542**, 83-90.

Tamiz, A.P., Whittemore, E.R., Zhou, Z.L., Huang, J.C., Drewe, J.A., Chen, J.C., Cai, S.X., Webe,r E., Woodward, R.M. & Keana, J.F. (1998). Structure-activity relationships for a series of bis(phenylalkyl)amines: potent subtype-selective inhibitors of *N*-methyl-D-aspartate receptors. *Journal of Medicinal Chemistry,* **41,** 3499–3506.

Tamminga, C.A. (1997). Neuropsychiatric aspects of schizophrenia, in: Yudofsky, S.C., Hales, R.E. (Eds.), Neuropsychiatry, Third Edition, American Psychiatric Press, Washington, DC., pp. 855-882.

Tamminga, C.A. (1998a). Schizophrenia and glutamatergic transmission. *Critical Reviews in Neuroscience*, **12**, 21-36.

Tamminga, C.A. (1998b). Serotonin and schizophrenia. *Biological Psychiatry*, **44**, 1079-1080.

Tamminga, C.A., Vogel, M., Gao, X-M., Lahti, A.C. & Holcomb H.H. (2000). The limbic cortex in schizophrenia: focus on the anterior cingulate. *Brain Research Reviews*, **31**, 364-370.

Tanaka, H., Yasuda, H., Kato, T., Maruoka, Y., Kawabe, A., Kawasima, C., Ohtani, K. & Nakamura, M. (1995). Neuroprotective and anticonvulsant action of SM-18400, a novel strychnine-insenstive glycine site antagonists. *Journal of Cerebral Blood Flow Metabolism,* **15**, (Suppl.1) S431.

Tang, Y.P., Shimizu, E., Dube, G.R., Kerchner, G.A., Zhuo, M., Liu, G. & Tsien, J.Z. (1999). Genetic enhancement of learning and memory in mice. *Nature,* **401**, 63-69.

Tansey, E.M. (1991). Chemical neurotransmission in the autonomic nervous system: Sir Henry Dale and acetylcholine. *Clinical Autonomic Research*, **1**, 63-72.

Thompson, C.L., Drewery, D.L., Atkins, H.D., Stephenson, F.A. & Chazot, P.L. (2000). Immunohistochemical localization of N-methyl-D-aspartate receptor NR1, NR2A, NR2B and NR2C/D subunits in the adult mammalian cerebellum. *Neuroscience Letters*, **283**, 85-88.

Thompson, C.L., Drewy, D.L., Atkins, H.D., Stephenson, F.A. & Chazot, P.L. (2002). Immunohistochemical localization of NMDA receptor subunits in the adult murine hippocampal formation: evidence for a unique role of the NR2D subunit. *Molecular Brain Research,* **102**, 55-61.

Tsumoto, T. (1992). Long-term potentiation and long-term depression in the neocortex. *Progress in Neurobiology,* **39**, 209-228.

Turski, L., Bressler, K., Rettig, K.J., Loschmann, P.A. & Wachtel, H. (1991). Protection of the substania nigra from MPP+ neurotoxicity by N-methyl-D-aspartate antagonists. *Nature*, **349,** 414-418.

U

Ulas, J., Brunner, L.C., Geddes, J.W. Choe, W. & Cotman, C.W. (1992). N-methyl-D-aspartate receptor complex in the hippocampus of elderly, normal individuals and those with Alzheimer's disease. *Neuroscience*, **49**, 45-61.

V

Varney, M.A., Jachec, C., Deal, C., Hess, S.D., Daggett, L.P., Skvoretz, R., Urcan, M., Morrison, J.H., Moran, T., Johnson, E.C. & Velicelebi, G. (1996). Stable expression and characterization of recombinant human heteromeric N-methyl-D-aspartate receptor subtypes NMDAR1A/2A and NMDAR1A/2B in mammalian cells. *Journal of Pharmacology and Experimental Therapeutics*, **279**, 367-378.

Verdoorn, T.A., Burnashev, N., Monyer, H., Seeburg, P.H. & Sakmann, B. (1991). Structural determinants of ion flow through recombinant glutamate receptor channels. *Science*, **252**, 1715-1718.

Vincent, A., Palace, J. & Hilton-Jones, D. (2001). Myasthenia gravis. *Lancet*, **357**, 2122-2128.

Vogt, B.A., Rosene, D.L. & Pandya, D.N. (1979). Thalamic and cortical afferents differentiate anterior from posterior cingulate cortex in the monkey. *Science*, **204**, 205-207.

Vogt, B.A., Finch, D.M. & Olson, C.R. (1992). Functional heterogeneity in the cingulate cortex: The anterior executive and posterior evaluative regions. *Cerebral Cortex*, **2**, 435-443.

Vogt, B.A., Nimchinsky, E.A., Vogt, L.J. & Hof, P.R. (1995). Human cingulate cortex: surface features, flat maps, and cytoarchitecture. *The Journal of Comparative Neurology*, **359**, 490-506.

Vogt, B.A., Vogt, L.J., Nimchinsky, E.A. & Hof, P.R. (1997). Primate cingulate cortex chemoarchitecture and its disruption in Alzheimer's disease, in: Bloom, F.E., Bjorklund, A. & Hokfelt, T. (Eds.), Handbook of Chemical Neuroanatomy, 13: The Primate Nervous System, Part 1, Elsevier, pp. 453-488.

W

Wafford, K. A., Kathoria, M., Bain, C. J., Marshall, G., Le Bourdelles, B., Kemp, J. A. & Whiting, P. J. (1995). Identification of amino acids in the N-methyl-D-asparate receptor NR1 subunit that contribute to the glycine binding site. *Molecular Pharmacology*, **47**, 374-380.

Watanabe, M., Inoue, Y., Sakimura, K. & Mishina, M. (1993). Distinct spatio-temporal distributions of the NMDA receptor channel subunit mRNAs in the brain. *Annals of the New York Academy of Sciences,* **707**, 463-466.

Watanabe, M., Mishina, M. & Inoue, Y. (1994). Distinct distributions of five NMDA receptor channel subunit mRNAs in the brainstem. *Journal of Comparative Neurology,* **343,** 520-531.

Watkins, J. C. (1962). Synthesis of some acidic amino acids possessing neuropharmacological activity. *Journal of Medicinal & Pharmaceutical Chemistry,* **5**, 1187–1199

Watkins, J.C. & Evans, R.H. (1981). Excitatory amino acid transmitters. *Annual Review of Pharmacology and Toxicology,* **21**, 165-204.

Watkins, J.C. (1986) in *Excitatory Amino Acids* (Roberts, P.J., Storm-Mathisen, J. & Bradford, H.F. eds) pp1-39, MacMillan Press, London, UK.

Watkins, J.C. (1988) in *Frontiers of Excitatory Amino Acid Research* (Cavalheiro, E.A., Lehmann, J. & Turski, L. eds) pp3-10, Alan R Liss, New York, USA.

Waxman, E.A. & Lynch, D.R. (2005). N-methyl-D-aspartate Receptor Subtypes: Multiple Roles in Excitotoxicity and Neurological Disease. *Neuroscientist,* **11**, 37-49.

Wei, F., Wang, G.D., Kerchner, G.A., Kim, S.J., Xu, H.M., Chen, Z.F. & Zhuo, M. (2001). Genetic enhancement of inflammatory pain by brain NR2B overexpression. *Nature Neuroscience,* **4**, 164-169.

Weinberger, D. (1993). A connectionist approach to the prefrontal cortex. *Journal of Neuropsychiatry,* **5**, 241-253.

Weinberger, D.R. (1996). On the plausibility of 'The Neurodevelopmental Hypothesis' of schizophrenia. *Neuropsychopharmacology,* **14**, 1S-11S.

Wenk, G.L., Walker, L.C., Price, D.L. & Cork, L.C. (1991). Loss of NMDA, but not GABA-A, binding in the brains of aged rats and monkeys. *Neurobiology of Aging,* **12**, 93-98.

Wenthold, R.J., Yokotani, N., Doi, K. & Wada, K. (1992). Immunochemical characterization of the non-NMDA glutamate receptor using subunit-specific antibodies. *Journal of Biological Chemistry,* **267**, 501-507.

Wenzel, A., Scheurer, L., Kunzi, R., Fritschy, J. M., Mohler, H., & Benke, D. (1995). Distribution of NMDA receptor subunit proteins NR2A, 2B, 2C and 2D in rat brain. *Neuroreport,* **7,** 45-48.

Wenzel, A., Fritschy, J. M., Mohler, H. & Benke, D. (1997). NMDA receptor heterogeneity during postnatal development of the rat brain: differential expression of the NR2A, NR2B, and NR2C subunit proteins. *Journal of Neurochemistry,* **68**, 469-478.

Werner, P., Voigt, M., Keinänen, K., Wisden, W. & Seeburg, P. H. (1991). Cloning of a putative high-affinity kainate receptor expressed predominantly in hippocampal CA3 cells. *Nature,* **351**, 742-744.

Whetsell, W.O. & Shapira, N.A. (1993). Neuroexcitation, excitotoxicity, and human neurological disease. *Biological Disease*, **68**, 372-387.

Williams, K., Romano, C. & Molinoff, P.B. (1989). Effects of polyamines on the binding of [3H]MK-801 to the N-methyl-D-aspartate receptor: pharmacological evidence for the existence of a polyamine recognition site. *Molecular Pharmacology*, **36**, 575–581.

Williams, K., Dawson, V.L., Romano, C., Dichter, M.A. & Molinoff, P.B. (1990). Characterization of polyamines having agonist, antagonist, and inverse agonist effects at the polyamine recognition site of the NMDA receptor. *Neuron*, **5**, 199-208.

Williams, K. (1993). Ifenprodil discriminates subtypes of the *N*-methyl-D-aspartate receptor: selectivity and mechanisms at recombinant heteromeric receptors. *Molecular Pharmacology,* **44**, 851-859.

Williams, K., Zappia, A.M., Pritchett, D.B. Shen, Y.M. & Molinoff, P.B. (1994). Sensitivity of the N-methyl-D-aspartate receptor to polyamines is controlled by NR2 subunits. *Molecular Pharmacology*, **45**, 803-809.

Williams, K., Kashiwagi, K., Fukuchi, J.I. & Igarashi, K. (1995). An acidic amino acid in the *N*-methyl-D-aspartate receptor that is important for spermine stimulation. *Molecular Pharmacology*, **48**, 1087-1098.

Williams, K. (1997). Interactions of polyamines with ion channels. *Biochemical Journal,* **325**, 289-297.

Wisden, W. & Seeburg, P.H. (1993). A complex mosaic of high-affinity kainite receptors in rat brain. *Journal of Neuroscience*, **13**, 3582–3598.

Wo, Z.G. & R.E. Oswald. (1994). Transmembrane topology of two kainate receptor subunits revealed by N-glycosylation. *Proceedings of the National Academy of Sciences,* **91**, 7154-7158.

Wong, E.H.F., Knight, R. & Woodruff, G.N. (1988). [^{3}H]MK 801 labels a site on the N-methyl-D-aspartate receptor channel complex in rat brain membranes. *Journal of Neurochemistry,* **50,** 274-281.

Wong, H.K., Lui, X.B., Matos, M.F., Chan, S.F., Perez-Otano, I., Boysen, M., Cui, J., Nakanish, N., Trimmer, J.S., Jones, E.G., Lipton, S.A. & Sucher, N.J. (2002). Temporal and regional expression of the NMDA receptor subunit NR3A in the mammalian brain. *Journal of Comparative Neurology,* **450**, 303-317.

Z

Zavitsanou, K., Ward, P.B. & Huang, X-F. (2002). Selective Alterations in Ionotropic Glutamate Receptors in the Anterior Cingulate Cortex in Schizophenia. *Neuropsychopharmacology*, **27**, 826-833.

Zavitsanou, K. & Huang, X-F. (2002). Decreased [3H]spiperone binding in the anterior cingulate cortex in schizophrenia patients: an autoradiographical study. *Neuroscience*, **109**, 709-716.

Appendix 1

Sources of Materials

Amersham International, Aylesbury, Buckinghamshire, UK

Blotting Paper

HRP-linked secondary antibody, Mouse

HRP-linked secondary antibody, Rabbit

Hyperfilm™

Hybond Nitrocellulose

Cambrex Bio Science Verviers, Belgium

DMEM/F12 (1:1 mix) with 15mM HEPES and L-glutamine

Kodak Professional, UK

Polymax RT, developer and replenisher

Polymax RT, fixer and replenisher

National Diagnostics, UK

Ecoscint A

Patterson Scientific, UK

Devalex

Black and White Amfix

Pierce, Rockford, UK

Immunopure® rProtein A IgG Orientation Kit

Promega Ltd, Southampton, UK

HB101 Competent *E-coli* cells

Qiagen, Crawley, West Sussex, UK

Qiagen® Plasmid Maxi Kit

Semat International, Hertfordshire, UK

Radioligand filter paper

Sigma-Aldrich Company, Poole, Dorset, UK

Acrylamide/bis-acrylamide (30% solution)

Albumin, Bovine

Ammonium Persulfate

Ampicillin

β-actin

Bacterial agar

Brilliant Blue G (Coomassie Blue)

Bromophenol Blue

Butanol

Chloroform

p-Coumaric Acid

Cupric Sulfate, anhydrous

Dialysis tubing (visking size 11/4")

Diethylamine

Dimethyl Sulfoxide (DMSO)

Dithiothreitol (DTT)

N,N-Dimethylformamide

DMEM/F12 (1:1 mix) without L-glutamine

Dulbecco's Phosphate Buffered Saline

Ethanol

Ethylenediaminetetraacetic Acid (EDTA)

Ethylene Glycol-bis(β-aminoethyl ether)-N,N,N',N'-tetraacetic Acid (EGTA)

Folin & Ciocalteu's Phenol Reagent

Gentamycin Solution

Gluteraldehyde

Glycerol

Glycine

Glycine Ethyl Ester

Hydrochloric Acid

Hydrogen Peroxide (30% w/w solution)

Freund's Adjuvant Complete

Freund's Adjuvant Incomplete

Ifenprodil

Isopropanol

Lauryl Sulfate (SDS)

LB (Luria Bertani) Broth

Luminol

3-Maleimidobenzoic Acid N-hydroxysuccinimide Ester (MBS)

Methanol

Poly(ethyleneimine) solution

Ponceau S

Potassium Chloride

Potassium Phosphate, Monobasic

Potassium Sodium Tartrate

Prestained Molecular Weight Markers Kit

Protease inhibitor cocktail III

Sodium Azide

Sodium Bicarbonate Solution (7.5%)

Sodium Carbonate

Sodium Chloride

Sodium Deoxycholate

Sodium Hydrogen Carbonate

Sodium Hydroxide

Sodium Nitrite

Sodium Phosphate, Dibasic

Sodium Phosphate, Monobasic

Sucrose

N,N,N',N'-Tetramethylethylenediamine (TEMED)

Thyroglobulin, Bovine

Trizma Base

Trizma Hydrochloride

Trypsin-EDTA Solution

Tween-20

Vector Laboratories, UK

Vectabond coated slides

Miscellaneous

NR2A peptide from Sigma-Genosys Ltd, Cambridge, UK

Plasmid DNA from Dr Paul Chazot, Durham University, UK

Marvel, dried skimmed milk, <1% fat

[^{3}H]-compounds from Gedeon Richter Ltd, Hungary

Unlabelled compounds from Gedeon Richter Ltd, Hungary